THE ANTICIPATORY UNFOLDED PROTEIN RESPONSE AND ESTROGEN RECEPTOR MUTATIONS IN BREAST CANCER

BY

LIQUN YU

DISSERTATION

Submitted in partial fulfillment of the requirements
for the degree of Doctor of Philosophy in Biochemistry
in the Graduate College of the
University of Illinois at Urbana-Champaign, 2019

Urbana, Illinois

Doctoral Committee:

Professor David Shapiro, Chair
Professor Lin-Feng Chen
Assistant Professor Erik Nelson
Assistant Professor Kai Zhang

ABSTRACT

Estrogen, acting via estrogen receptor α (ERα), stimulates cancer cell proliferation and metastasis. Endocrine therapy targeting E_2:ERα activity often leads to development of antiestrogen resistance. Approximately 30% of patients who have metastatic endocrine therapy resistant breast cancer express ERα mutations. Two of the most common and therefore widely studied mutations are ERαY537S and ERαD538G. Patients whose metastatic breast tumors express Y537S or D538G mutations have 1 year and 6 months shorter median survival time than patients whose metastatic tumors express wild-type ERα.

To better characterized the aggressive phenotypes of the ERα mutations in breast cancer cells, we used CRISPR-Cas9 technology to replace wild-type ERα in T47D, human breast cancer cells, with the most common mutations, ERαY537S and ERαD538G. The mutant cells exhibit partially estrogen-independent and antiestrogen resistant gene expression and cell proliferation. A novel invasion-dissociation-rebinding (IDR) assay demonstrated that the mutant cells have a higher tendency to dissociate from invasion sites and rebind to a second site. Compared to wild type breast tumors, mutant tumors exhibited dramatic increases in lung metastasis. The ERαY537S mutation further enhanced the metastatic capability of the breast tumors. Gene set enrichment analysis (GSEA) showed Myc target pathways are highly induced in mutant cells. Moreover, chromatin immunoprecipitation showed constitutive, fulvestrant-resistant, recruitment of ERα mutants to the Myc enhancer region, resulting in estrogen-independent Myc overexpression in mutant cells and tumors. Knockdown and overexpression experiments showed Myc is necessary and sufficient for ligand-independent proliferation of the mutant cells but had no effect on metastasis-related phenotypes.

Other than gain-of-function mutations, breast cancer cells can develop therapy resistance via recently described pathways of hormone action. Our laboratory recently revealed that estrogen acting through ERα, rapidly phosphorylates and activates phospholipase C γ (PLCγ) resulting in transient calcium release from endoplasmic reticulum and mild activation of the unfolded protein response. I identified that this anticipatory UPR is a conserved pathway shared by different mitogenic hormones including epidermal growth factor, estrogen and progesterone. EGF rapidly induced a calcium increase in the cytosol and moderate activation of the IRE1α and ATF6α arms of the UPR, resulting in induction of BiP chaperone. Knockdown or inhibition of EGF receptor (EGFR), PLCγ or IP_3 receptor (IP_3R) blocks the increase in intracellular Ca^{2+}. While blocking the increase in intracellular Ca^{2+} by locking the IP_3R calcium channel with 2-APB had no effect on EGF activation of the ERK or AKT signaling pathways, it abolished EGF-mediated immediate early gene expression, suggesting EGF stimulated calcium efflux and signaling transduction are two independent pathways and are both essential for EGF regulated gene expression. Knockdown of ATF6α or XBP1, which regulate UPR-induced chaperone production, inhibited EGF stimulated cell proliferation. These data highlight the importance of anticipatory UPR pathway in the normal actions of mitogenic hormones.

Unlike EGFR which functions as a receptor tyrosine kinase, ERα cannot directly phosphorylate PLCγ. Using the small molecule ERα biomodulator, BHPI, which uses the same pathway as E_2 and induces toxic hyperactivation of the anticipatory UPR, we applied unbiased long-term-selection on ERα positive breast cancer cells and isolated T47D and MCF-7 cells that proliferate in the presence of a lethal concentration of BHPI.

We showed that 4 out of 11 T47D and almost all MCF-7 BHPI resistant clones have reduced Src expression. Src overexpression by virus transduction in resistant clones restored sensitivity to BHPI. Furthermore, in wild-type cells, several-fold knockdown of Src, but not of ERα, strongly blocked BHPI-mediated UPR activation and subsequent HMGB1 release and necrotic cell death. Supporting Src kinase linking estrogen and progesterone to activation of the anticipatory UPR, we identified extranuclear complexes of ERα:Src:PLCγ and progesterone receptor:Src:PLCγ. Thus, Src plays a previously undescribed pivotal role in activation of the tumor protective anticipatory UPR, thereby increasing the resilience of breast cancer cells.

ACKNOWLEDGEMENTS

I would like to thank all the scientists who have played an invaluable role in my career development as a scientist. First, I would like to thank my advisor, Dr. David Shapiro, for providing me with tremendous support on a daily basis in my pursuit of PhD training. Your patience and enthusiasm for science have been instrumental to my development as a scientist. I would like to express my appreciation to my doctoral committee members, Dr. Lin-Feng Chen for your diligent effort in guiding my thesis work, Dr. Erik Nelson for your invaluable feedback and support in both my research and career development and Dr. Kai Zhang for your insightful advice on my research.

Thank you to the former and current members of the Shapiro lab for the friendship and assistance. I would like to thank the research scientist Dr. Chengjian Mao for sharing your knowledge and techniques that help move my projects forward. To former members Dr. Neal Andruska, Dr. Lily Mahapatra, Dr. Mathew Cherian, Dr. Xiaobin Zheng and Dr. Mara Livezey for all the invaluable guidance and support in lab. To Ji, Lawrence, Darjan, Santa, Rui, Ciyang and Yu, this work would not have been possible without your contribution and assistance. I would also like to thank Dr. Sandra McMasters for providing media and support; Dr. Ben Ho Park of the Johns Hopkins Kimmel Cancer Center for providing the MCF-7 ERα mutant cell lines; Dr. William Helferich for generating the T47D breast cancer xenografts.

Above all else, I must thank my parents for their unwavering love and support. You have given up a lot of things so that I could pursue my dream in a different country. Nothing would be possible without your love, selflessness and support.

TABLE OF CONTENTS

LIST OF FIGURES

LIST OF TABLES

LIST OF ABBREVIATIONS

4-OHT, 4-hydroxy-tamxofien

ATF6α, activating transcription factor 6 α

AF, activating function

BHPI, 3,3-bis(4-hydroxyphenyl)-7-methyl-1,3,dihydro-2H-indol-2-one

BIK, BCL-2 interacting killer

BIM, BCL-2 interacting mediator of cell death

ChIP, chromatin immunoprecipitation

CHOP, CCAAT/enhancer-binding protein homologous protein

Co-IP, co-immunoprecipitation

Das, Dasatinib

DNA, deoxyribonucleic acid

DBD, DNA binding domain

E2, 17β-Estradiol

EGF, epidermal growth factor

EGFR, epidermal growth factor receptor

EGR1, early growth response 1

eIF2α, eukaryotic initiation factor 2α

EnR, endoplasmic reticulum

ER, estrogen receptor

ERα, estrogen receptor α

ERE, estrogen response element

ERK, extracellular receptor kinase

GREB1, growth regulation by estrogen in breast cancer 1

HMGB1, high mobility group box 1

ICI, ICI 182,780/Fulvestrant/Faslodex

IDR, invasion-dissociation-rebinding

IRE1α, inositol-requiring enzyme 1α

IVIS, *in vivo* imaging instruments

LBD, ligand binding domain

MDS, multidimensional scaling

NES, normalized enrichment score

P4, progesterone

PERK, protein kinase R (PKR)-like endoplasmic reticulum kinase

PGR, progesterone receptor gene

PR, progesterone receptor

PLCγ, phospholipase C γ

SERD, selective estrogen receptor degrader

SERM, selective estrogen receptor modulator

TCGA, The Cancer Genome Atlas

TDG, T47D-ERαY537S

THG, thapsigargin

TNBC, triple negative breast cancer

TUN, tunicamycin

TYS, T47D-ERαY537S

UPR, unfolded protein response

CHAPTER1

INTRODUCTION

ESTROGEN RECEPTOR

Naturally occurring estrogen, such as 17β estradiol (E2), plays a central role in the development and maintenance of the female reproductive system. Estrogen binds to estrogen receptor (ER), which belongs to the steroid nuclear receptor superfamily, initiates downstream gene expression regulation as well as signaling transduction (1). ER protein consists of six functional domains: 1) the N-terminal ligand-independent activation function-1 (AF-1) domain, functions as a transcriptional activation domain; 2) the DNA binding domain (DBD), directly interacts with DNA; 3) the hinge domain, contains nuclear localization signal and interacts with heat shock proteins; 4) the ligand binding domain (LBD), interacts with estrogen and overlaps with the 5) ligand-dependent AF-2 domain; 6) the c-terminal region which inhibits the receptor dimerization in the absence of estrogen (2). Even though original recognized as a transcription factor, estrogen receptor has been shown to promote various rapid, extranuclear signaling transductions that contribute to estrogen stimulated cell proliferation, migration and survival (3-5).

Although E2: ER has beneficial effects on reproductive, skeleton and cardiovascular system, aberrant expression of estrogen and abnormal ER function may cause initiation, promotion, and progression of breast cancer (6). Studies have shown the strong association between the risk of the breast cancer and the elevated estrogen levels in the blood (7, 8). At diagnosis, approximate 75% of the breast cancers express estrogen receptor α (ERα). Endocrine therapies for patients who have ERα positive breast cancer include aromatase inhibitor, which reduces estrogen production; selective estrogen

receptor modulators (SERM), which compete with estrogen binding with ERα; selective estrogen receptor degrader or down-regulator (SERD), which not only compete with estrogen but also degrade ERα after binding (9).

Although endocrine therapy is highly effective in blocking ERα activities, intrinsic and acquired resistance often develops. Multiple mechanisms that are responsible for endocrine therapy resistance have been proposed, including downregulation of ERα expression (10), dysregulation of cell cycle signaling molecules (11), alteration of cell survival pathways (12) as well as crosstalk between ERα and growth factor pathways (13). For patients who have metastatic breast cancer, therapies remain poor.

ESTROGEN RECEPTOR α MUTATIONS

Even though the mechanisms underlining endocrine therapy-resistance are complex, several studies have provided new insights into the pathogenesis of anti-estrogen resistance in breast cancer. About 20 years ago, pioneer work done by Karnik and Borg identified nucleotide changes within ERα gene (ESR1) in hormone-independent ER-positive breast tumors using single strand conformation polymorphism (14, 15). At the same time, the structure-function analysis of ERα done by Katzenellenbogen lab revealed that a single amino acid substitution on tyrosine 537 was able to confer estrogen-independent constitutive transcriptional activity and association with nuclear receptor coactivator on breast cancer cells (16). Very recently, with the advent of sensitive DNA sequencing technologies, several studies unveiled that approximate 30% of the advanced metastatic breast cancers harbor gain-of-function ERα mutations (17-21). Notably, the ERα mutations identified in these metastatic endocrine therapy-resistant tumors are clustered within the LBD of the ERα, especially residues L536, Y537 and D538 (22).

A recent biophysical and structural biology study revealed that mutant ERs bearing Y537S and D538G point mutations have reduced affinity to both agonist and antagonist (23). And the point mutations confer a stabilized agonist conformation on ERα which leads to antiestrogen resistance. Martin et al. demonstrated that ERαY537S had increased association with co-regulators GREB1 and FOXA1 than that seen for wild-type ERα using comparative RIME (rapid immunoprecipitation with tandem mass spectrometry of endogenous proteins) (24). A genome-wide study integrating RNAseq and ChIPseq data showed that ERα mutations lead to unique hormone-independent chromatin binding and distinct gene expression profiles (25). These studies provided mechanistic explanations for ligand-independent constitutive activities and anti-estrogen resistance seen in the ERα mutants.

While the ESR1 mutations were identified almost exclusively in the metastatic ER+ breast tumors (22), whether ERα mutations confer breast cancer cells with increased metastatic capability remains unclear. An orthotopic xenograft study done by Jeselsohn et al. revealed that MCF-7 tumors harboring ERαY537S mutation have much better metastatic capability than the tumors harboring ERαD538G mutation. Moreover, none of the mice bearing wild-type MCF-7 xenografts developed metastases in distant organs (25). This finding suggests ERα mutant cells have increased invasive and metastatic capability, however, the underlining mechanisms remain unknown.

EPIDERMAL GROWTH FACTOR

Epidermal growth factor (EGF) stimulates cell proliferation and promotes tumor growth by binding to epidermal growth factor receptor (EGFR). The EGF receptor tyrosine kinase family consists of four members: EGFR (ErbB1/HER1), ErbB2 (HER2), ErbB3 (HER3)

and ErbB4 (HER4) (26). The ErbB family receptors are single chain transmembrane proteins consisting of an extracellular ligand-biding domain, a transmembrane domain and an intracellular tyrosine kinase domain (27). Growth factors, such as EGF, activate ErbBs by inducing structural changes result in formation of homodimers and heterodimers. ErbB2 dimerizes with all other ErbB family members, yet cannot bind any ligands by itself; whereas ErbB3 has an inactive pseudo-kinase intracellular domain and can only function in heterodimeric complex (28). Receptor dimerization leads to phosphorylation and activation of the intracellular kinase domain, and phosphotyrosine residues then initiate downstream signaling pathways including Ras/MAPK, PI3 kinase/AKT, PLCγ/PKC and Jak/STAT pathways (29).

Overexpression and constitutive activation of EGFR have been associated with cancer cell proliferation, survival, angiogenesis and metastasis (30). Amplification of EGFR gene has been described in lung cancer, gastric cancer, glioblastoma as well as breast cancer (31, 32). EGFR is expressed in most breast cancers and is overexpressed in ~50% of the triple-negative breast cancer (TNBC, ERα-, PR- and HER2-) and in highly-aggressive invasive breast cancer (IBC) (32-34). Other mechanisms of EGFR dysregulation include missense gene mutations and cross-talk with other receptor tyrosine kinases (35, 36). Deregulated EGFR signaling reduces cells sensitivity of anticancer drugs, therefore therapies combining anti-EGFR drugs with chemotherapy have been tested for triple-negative breast tumors. Sustained erlotinib treatment increased TNBC’s sensitivity and cell death in response to doxorubicin (37).

SRC KINASE

The proto-oncogene cellular Src (c-Src) is a non-receptor tyrosine kinase protein which plays a critical role in mediating signal transduction through interacting with multiple proteins and protein complexes. It is important in regulating cell adhesion, proliferation, migration, differentiation, survival and angiogenesis (38-41). Dysregulated Src expression occurs in several tumor types and has been associated with malignant progression of cancer (42). Overexpression of Src are found in numerous human tumors, including breast, pancreatic, colon, lung and prostates cancers (43-45). In breast cancer, Src overexpression has been correlated with latent bone metastasis (46). Using genome-wide gene expression data from 615 breast tumors, Zhang et al. showed that expression of a Src response signature (SRS) in primary breast tumors is associated with latent bone metastasis. These data highlighted the critical role of Src in advanced tumors.

Src has been shown to interact with steroid hormone receptors, ERα and progesterone receptor (PRs), through either direct association or scaffold protein tethering (47-49). In breast cancers, Src is a crucial protein in a complex interaction network. Crosstalk between Src, EGFR and ERα contributes to tamoxifen resistance in breast cancer cells (50) and in patients (44). A very recent study revealed that loss of C-terminal Src kinase (CSK), a suppressor of Src family kinases, confers endocrine therapy resistance on ER+ breast cancer cells (51). Given the importance of Src in ER+ breast cancer cells, ongoing trials are exploring combination of Src inhibitors dasatinib and bosutinib with endocrine therapies (52).

Given its critical role in multiple signaling pathways that regulate several biological processes, Src expression is tightly controlled. Biochemical and structural studies have discerned the general mechanism by which Src activity is regulated (42). In normal cells,

activated Src undergoes reversible protein dephosphorylation and ubiquitin-mediated protein degradation (53, 54). Previous study indicates deregulation of the ubiquitin-proteasome pathway is responsible for Src activation in cancer cells (55). The transcription factor CULT1 reduces proteasome mediated Src protein degradation leading to increased tumor cell migration (56). ErbB2 increases Src protein stability through inhibiting calpain protease and promotes breast cancer metastasis (57). Efforts have been made to trigger Src protein instability and prevent maturation, therefore diminish Src activity. Src degradation was achieved using drugs that inhibit HSP90 activity or disrupt the association of HSP90 with c-Src (58, 59).

UNFOLDED PROTEIN RESPONSE

Endoplasmic reticulum (EnR) is the major organelle in the cell where the secreted and membrane proteins get folded and modified. The protein quality control and homeostasis within the EnR is monitored by a collection of conserved signaling pathways termed the unfolded protein response (UPR). Three arms of the UPR have been identified in the EnR, namely the inositol-requiring protein-1 (IRE1), activating transcription factor-6 (ATF6) and protein kinase RNA (PKR)-like ER kinase (PERK) (60, 61). Mild UPR activation increases lipid synthesis to expand EnR membrane and induces molecular chaperone production to boost the protein folding capacity in the cells (61). In the cancer cells, which are exposed to intrinsic and external insults that may trigger the EnR stress, the UPR is usually upregulated in comparison to cells in normal tissues (62). Recently, our laboratory and others discovered that mitogenic steroid and peptide hormones activate the anticipatory UPR and prepare cells for the future needs of increased protein folding capacity that may company cell proliferation (63, 64). Estrogen activates a rapid calcium

release from the EnR mediated by phosphorylated phospholipase C gamma (PLCγ). This mild calcium depletion within the EnR lumen result in activation of the protective anticipatory UPR and increased expression of molecular chaperones (63).

Under severe and irreversible EnR stresses, sustained reactive UPR activation induces pro-death pathways. There are multiple apoptosis mechanisms by which EnR could trigger and eventually elicit cell death, involving: (1) induction of the proapoptotic transcription factor CHOP and GADD34 by hyperactivating PERK-eIF2α (65), (2) tethering IRE1α to ASK-JNK cascade (66), (3) induction of calcium release from EnR lumen leading to mitochondria fission and cytochrome c release (67). How sustained anticipatory UPR activation kills cancer cells was recently revealed by our laboratory (68, 69). A small molecule anticancer drug, BHPI, acting through ERα, distorts anticipatory UPR resulting in persistent activation of PLCγ and sustained production of IP3, allowing continued calcium efflux from EnR lumen into the cytosol. To restore calcium homeostasis, cells activate ATP dependent sarco/endoplasmic reticulum Ca2+-ATPase (SERCA) pumps. Because the IP3R Ca2+ channel stays open, Ca2+ pumped back into the EnR by SERCA leaks back out. This futile cycle rapidly depletes ATP and eventually leads to necrotic cell death (69).

OVERVIEW OF THESIS

Here, using breast cancer cell lines bearing the ERαY537S and ERαD538G mutations (70), I characterized the aggressive phenotypes of the mutant cells. I used RNA sequencing analysis to demonstrate the unique gene expression patterns of the ERα mutants; showed that ERα mutation bearing cells have increased invasion ability using the newly developed invasion-dissociation-rebinding assay; validated that the mutations

confer breast cancer cells with increased metastatic capability. I also showed that hormone-independent constitutive overexpression of Myc pathway is responsible for anti-estrogen resistant cell proliferation observed in the mutant cells but had no effect in promoting invasiveness of the breast cancer cells.

Furthermore, I demonstrated that other mitogenic hormones including EGF and progesterone can activate the anticipatory UPR in breast cancer cells. EGF induced calcium release from the EnR lumen into the cytosol is required for EGF regulated immediate early gene expression and mild activation of the UPR increased molecular chaperones prepare cells for future cell proliferation. Using an unbiased long-term BHPI selection, we identified MCF-7 and T47D clones that can grow in the presence of lethal concentration BHPI. 4 out of 11 T47D and almost all MCF-7 BHPI-resistant clones have reduced expression of proto-oncogene c-Src. Knockdown Src in breast cancer cells rescued cells from BHPI induced necrotic cell death and restore Src expression in BHPI-resistant clones re-sensitized the cells to UPR hyperactivation. Src is not only the protein kinase couples activation of estrogen receptor to the anticipatory UPR activation but also the rate-limiting protein that regulates UPR hyperactivation.

REFERENCES

1. Nilsson S, Makela S, Treuter E, Tujague M, Thomsen J, Andersson Gr, et al. Mechanisms of estrogen action. Physiol Rev. 2001;81(4):1535-65.

2. Kumar V, Green S, Stack G, Berry M, Jin J-R, Chambon P. Functional domains of the human estrogen receptor. Cell. 1987;51(6):941-51.

3. Filardo EJ, Quinn JA, Bland KI, Frackelton Jr AR. Estrogen-induced activation of Erk-1 and Erk-2 requires the G protein-coupled receptor homolog, GPR30, and occurs via trans-activation of the epidermal growth factor receptor through release of HB-EGF. Mol Endocrinol. 2000;14(10):1649-60.

4. Kelly MJ, Levin ER. Rapid actions of plasma membrane estrogen receptors. Trends in Endocrinology & Metabolism. 2001;12(4):152-6.

5. Sun M, Paciga JE, Feldman RI, Yuan Z-q, Coppola D, Lu YY, et al. Phosphatidylinositol-3-OH kinase (PI3K)/AKT2, activated in breast cancer, regulates and is induced by estrogen receptor α (ERα) via interaction between ERα and PI3K. Cancer Res. 2001;61(16):5985-91.

6. Yager JD, Davidson NE. Estrogen carcinogenesis in breast cancer. New Engl J Med. 2006;354(3):270-82.

7. Wolff MS, Toniolo PG, Lee EW, Rivera M, Dubin N. Blood levels of organochlorine residues and risk of breast cancer. JNCI: Journal of the National Cancer Institute. 1993;85(8):648-52.

8. Wu AH, Pike MC, Stram DO. Meta-analysis: dietary fat intake, serum estrogen levels, and the risk of breast cancer. J Natl Cancer Inst. 1999;91(6):529-34.

9. Clarke R, Tyson JJ, Dixon JM. Endocrine resistance in breast cancer - An overview and update. Mol Cell Endocrinol. 2015.

10. Encarnación CA, Ciocca DR, McGuire WL, Clark GM, Fuqua SA, Osborne CK. Measurement of steroid hormone receptors in breast cancer patients on tamoxifen. Breast cancer research and treatment. 1993;26(3):237-46.

11. Span PN, Tjan-Heijnen VC, Manders P, Beex LV, Sweep CF. Cyclin-E is a strong predictor of endocrine therapy failure in human breast cancer. Oncogene. 2003;22(31):4898.

12. Riggins RB, Bouton AH, Liu MC, Clarke R. Antiestrogens, aromatase inhibitors, and apoptosis in breast cancer. Vitamins & Hormones. 2005;71:201-37.

13. Osborne CK, Shou J, Massarweh S, Schiff R. Crosstalk between estrogen receptor and growth factor receptor pathways as a cause for endocrine therapy resistance in breast cancer. Clin Cancer Res. 2005;11(2):865s-70s.

14. Karnik PS, Kulkarni S, Liu X-P, Budd GT, Bukowski RM. Estrogen receptor mutations in tamoxifen-resistant breast cancer. Cancer Res. 1994;54(2):349-53.

15. Zhang Q-X, Borg Å, Wolf DM, Oesterreich S, Fuqua SA. An estrogen receptor mutant with strong hormone-independent activity from a metastatic breast cancer. Cancer Res. 1997;57(7):1244-9.

16. Weis KE, Ekena K, Thomas JA, Lazennec G, Katzenellenbogen BS. Constitutively active human estrogen receptors containing amino acid substitutions for tyrosine 537 in the receptor protein. Mol Endocrinol. 1996;10(11):1388-98.

17. Jeselsohn R, Yelensky R, Buchwalter G, Frampton G, Meric-Bernstam F, Gonzalez-Angulo AM, et al. Emergence of constitutively active estrogen receptor-α mutations in

pretreated advanced estrogen receptor–positive breast cancer. Clin Cancer Res. 2014;20(7):1757-67.

18. Robinson DR, Wu Y-M, Vats P, Su F, Lonigro RJ, Cao X, et al. Activating ESR1 mutations in hormone-resistant metastatic breast cancer. Nat Genet. 2013;45(12):1446-51.

19. Toy W, Shen Y, Won H, Green B, Sakr RA, Will M, et al. ESR1 ligand-binding domain mutations in hormone-resistant breast cancer. Nat Genet. 2013;45(12):1439-45.

20. Merenbakh-Lamin K, Ben-Baruch N, Yeheskel A, Dvir A, Soussan-Gutman L, Jeselsohn R, et al. D538G mutation in estrogen receptor-α: a novel mechanism for acquired endocrine resistance in breast cancer. Cancer Res. 2013;73(23):6856-64.

21. Li S, Shen D, Shao J, Crowder R, Liu W, Prat A, et al. Endocrine-therapy-resistant ESR1 variants revealed by genomic characterization of breast-cancer-derived xenografts. Cell reports. 2013;4(6):1116-30.

22. Jeselsohn R, Buchwalter G, De Angelis C, Brown M, Schiff R. ESR1 mutations—a mechanism for acquired endocrine resistance in breast cancer. Nature reviews Clinical oncology. 2015;12(10):573.

23. Fanning SW, Mayne CG, Dharmarajan V, Carlson KE, Martin TA, Novick SJ, et al. Estrogen receptor alpha somatic mutations Y537S and D538G confer breast cancer endocrine resistance by stabilizing the activating function-2 binding conformation. Elife. 2016;5:e12792.

24. Martin L-A, Ribas R, Simigdala N, Schuster E, Pancholi S, Tenev T, et al. Discovery of naturally occurring ESR1 mutations in breast cancer cell lines modelling endocrine resistance. Nat Commun. 2017;8:1865.

25. Jeselsohn R, Bergholz JS, Pun M, Cornwell M, Liu W, Nardone A, et al. Allele-specific chromatin recruitment and therapeutic vulnerabilities of ESR1 activating mutations. Cancer Cell. 2018;33(2):173-86. e5.

26. Normanno N, De Luca A, Bianco C, Strizzi L, Mancino M, Maiello MR, et al. Epidermal growth factor receptor (EGFR) signaling in cancer. Gene. 2006;366(1):2-16.

27. Wieduwilt M, Moasser M. The epidermal growth factor receptor family: biology driving targeted therapeutics. Cell Mol Life Sci. 2008;65(10):1566-84.

28. Olayioye MA, Neve RM, Lane HA, Hynes NE. The ErbB signaling network: receptor heterodimerization in development and cancer. The EMBO journal. 2000;19(13):3159-67.

29. Scaltriti M, Baselga J. The epidermal growth factor receptor pathway: a model for targeted therapy. Clin Cancer Res. 2006;12(18):5268-72.

30. Normanno N, Bianco C, Strizzi L, Mancino M, Maiello M, Luca A, et al. The ErbB receptors and their ligands in cancer: an overview. Curr Drug Targets. 2005;6(3):243-57.

31. Herbst RS, Langer CJ, editors. Epidermal growth factor receptors as a target for cancer treatment: the emerging role of IMC-C225 in the treatment of lung and head and neck cancers. Semin Oncol; 2002: Elsevier.

32. Reis-Filho JS, Pinheiro C, Lambros M, Milanezi F, Carvalho S, Savage K, et al. EGFR amplification and lack of activating mutations in metaplastic breast carcinomas. J Pathol. 2006;209(4):445-53.

33. Dent R, Trudeau M, Pritchard KI, Hanna WM, Kahn HK, Sawka CA, et al. Triple-negative breast cancer: clinical features and patterns of recurrence. Clin Cancer Res. 2007;13(15):4429-34.

34. Zell JA, Tsang WY, Taylor TH, Mehta RS, Anton-Culver H. Prognostic impact of human epidermal growth factor-like receptor 2 and hormone receptor status in inflammatory breast cancer (IBC): analysis of 2,014 IBC patient cases from the California Cancer Registry. Breast Cancer Res. 2009;11(1):R9.

35. Masuda H, Zhang D, Bartholomeusz C, Doihara H, Hortobagyi GN, Ueno NT. Role of epidermal growth factor receptor in breast cancer. Breast cancer research and treatment. 2012;136(2):331-45.

36. Schiff R, Massarweh SA, Shou J, Bharwani L, Mohsin SK, Osborne CK. Cross-talk between estrogen receptor and growth factor pathways as a molecular target for overcoming endocrine resistance. Clin Cancer Res. 2004;10(1):331s-6s.

37. van Anken E, Romijn EP, Maggioni C, Mezghrani A, Sitia R, Braakman I, et al. Sequential waves of functionally related proteins are expressed when B cells prepare for antibody secretion. Immunity. 2003;18(2):243-53.

38. Castoria G, Giovannelli P, Lombardi M, De Rosa C, Giraldi T, De Falco A, et al. Tyrosine phosphorylation of estradiol receptor by Src regulates its hormone-dependent nuclear export and cell cycle progression in breast cancer cells. Oncogene. 2012;31(46):4868-77.

39. Migliaccio A, Castoria G, Di Domenico M, de Falco A, Bilancio A, Lombardi M, et al. Steroid-induced androgen receptor–oestradiol receptor β–Src complex triggers prostate cancer cell proliferation. The EMBO journal. 2000;19(20):5406-17.

40. Khare S, Bolt M, Wali R, Skarosi S, Roy H, Niedziela S, et al. 1, 25 dihydroxyvitamin D3 stimulates phospholipase C-gamma in rat colonocytes: role of c-Src in PLC-gamma activation. J Clin Invest. 1997;99(8):1831.

41. Dhar A, Shukla S. Electrotransjection of pp60v-src monoclonal antibody inhibits activation of phospholipase C in platelets. A new mechanism for platelet-activating factor responses. J Biol Chem. 1994;269(12):9123-7.

42. Summy JM, Gallick GE. Treatment for advanced tumors: SRC reclaims center stage. Clin Cancer Res. 2006;12(5):1398-401.

43. Irby RB, Yeatman TJ. Role of Src expression and activation in human cancer. Oncogene. 2000;19(49):5636.

44. Zhang S, Yu D. Targeting Src family kinases in anti-cancer therapies: turning promise into triumph. Trends Pharmacol Sci. 2012;33(3):122-8.

45. Giaccone G, Zucali P. Src as a potential therapeutic target in non-small-cell lung cancer. Ann Oncol. 2008;19(7):1219-23.

46. Zhang XH-F, Wang Q, Gerald W, Hudis CA, Norton L, Smid M, et al. Latent bone metastasis in breast cancer tied to Src-dependent survival signals. Cancer Cell. 2009;16(1):67-78.

47. Sun J, Zhou W, Kaliappan K, Nawaz Z, Slingerland JM. ERα phosphorylation at Y537 by Src triggers E6-AP-ERα binding, ERα ubiquitylation, promoter occupancy, and target gene expression. Mol Endocrinol. 2012;26(9):1567-77.

48. Boonyaratanakornkit V, Scott MP, Ribon V, Sherman L, Anderson SM, Maller JL, et al. Progesterone receptor contains a proline-rich motif that directly interacts with SH3 domains and activates c-Src family tyrosine kinases. Mol Cell. 2001;8(2):269-80.

49. Song RX, Zhang Z, Santen RJ. Estrogen rapid action via protein complex formation involving ERα and Src. Trends in Endocrinology & Metabolism. 2005;16(8):347-53.

50. Riggins RB, Schrecengost RS, Guerrero MS, Bouton AH. Pathways to tamoxifen resistance. Cancer Lett. 2007;256(1):1-24.

51. Xiao T, Li W, Wang X, Xu H, Yang J, Wu Q, et al. Estrogen-regulated feedback loop limits the efficacy of estrogen receptor–targeted breast cancer therapy. Proc Natl Acad Sci. 2018;115(31):7869-78.

52. Mayer EL, Krop IE. Advances in targeting SRC in the treatment of breast cancer and other solid malignancies. Clin Cancer Res. 2010;16(14):3526-32.

53. Harris KF, Shoji I, Cooper EM, Kumar S, Oda H, Howley PM. Ubiquitin-mediated degradation of active Src tyrosine kinase. Proc Natl Acad Sci. 1999;96(24):13738-43.

54. Roskoski Jr R. Src kinase regulation by phosphorylation and dephosphorylation. Biochem Biophys Res Commun. 2005;331(1):1-14.

55. Frame MC. Src in cancer: deregulation and consequences for cell behaviour. Biochimica et Biophysica Acta (BBA)-Reviews on Cancer. 2002;1602(2):114-30.

56. Aleksic T, Bechtel M, Krndija D, von Wichert G, Knobel B, Giehl K, et al. CUTL1 promotes tumor cell migration by decreasing proteasome-mediated Src degradation. Oncogene. 2007;26(40):5939.

57. Tan M, Li P, Klos KS, Lu J, Lan K-H, Nagata Y, et al. ErbB2 promotes Src synthesis and stability: novel mechanisms of Src activation that confer breast cancer metastasis. Cancer Res. 2005;65(5):1858-67.

58. Taipale M, Krykbaeva I, Koeva M, Kayatekin C, Westover KD, Karras GI, et al. Quantitative analysis of HSP90-client interactions reveals principles of substrate recognition. Cell. 2012;150(5):987-1001.

59. An WG, Schulte TW, Neckers LM. The heat shock protein 90 antagonist geldanamycin alters chaperone association with p210bcr-abl and v-src proteins before their degradation by the proteasome. Cell Growth and Differentiation-Publication American Association for Cancer Research. 2000;11(7):355-60.

60. Walter P, Ron D. The unfolded protein response: from stress pathway to homeostatic regulation. Science. 2011;334(6059):1081-6.

61. Ron D, Walter P. Signal integration in the endoplasmic reticulum unfolded protein response. Nature reviews Molecular cell biology. 2007;8(7):519-29.

62. Tsai YC, Weissman AM. The unfolded protein response, degradation from the endoplasmic reticulum, and cancer. Genes & cancer. 2010;1(7):764-78.

63. Andruska N, Zheng X, Yang X, Helferich WG, Shapiro DJ. Anticipatory estrogen activation of the unfolded protein response is linked to cell proliferation and poor survival in estrogen receptor alpha-positive breast cancer. Oncogene. 2015;34(29):3760-9.

64. Karali E, Bellou S, Stellas D, Klinakis A, Murphy C, Fotsis T. VEGF Signals through ATF6 and PERK to Promote Endothelial Cell Survival and Angiogenesis in the Absence of ER Stress. Mol Cell. 2014;54(4):559-72.

65. Malhotra JD, Kaufman RJ. Endoplasmic reticulum stress and oxidative stress: a vicious cycle or a double-edged sword? Antioxidants & redox signaling. 2007;9(12):2277-94.

66. Verfaillie T, Garg AD, Agostinis P. Targeting ER stress induced apoptosis and inflammation in cancer. Cancer Lett. 2013;332(2):249-64.

67. Breckenridge DG, Stojanovic M, Marcellus RC, Shore GC. Caspase cleavage product of BAP31 induces mitochondrial fission through endoplasmic reticulum calcium signals,

enhancing cytochrome c release to the cytosol. The Journal of cell biology. 2003;160(7):1115-27.

68. Andruska ND, Zheng X, Yang X, Mao C, Cherian MM, Mahapatra L, et al. Estrogen receptor α inhibitor activates the unfolded protein response, blocks protein synthesis, and induces tumor regression. Proc Natl Acad Sci. 2015;112(15):4737-42.

69. Livezey M, Huang R, Hergenrother PJ, Shapiro DJ. Strong and sustained activation of the anticipatory unfolded protein response induces necrotic cell death. Cell Death & Differentiation. 2018;25(10):1796.

70. Mao C, Livezey M, Kim JE, Shapiro DJ. Antiestrogen Resistant Cell Lines Expressing Estrogen Receptor alpha Mutations Upregulate the Unfolded Protein Response and are Killed by BHPI. Sci Rep. 2016;6:34753.

CHAPTER 2

ESTROGEN-INDEPENDENT MYC OVEREXPRESSION CONFERS ENDOCRINE THERAPY RESISTANCE ON BREAST CANCER CELLS EXPRESSING ERαY537S AND ERαD538G MUTATIONS [1]

ABSTRACT

Approximately 30% of metastatic breast cancers harbor estrogen receptor α (ERα) mutations associated with resistance to endocrine therapy and reduced survival. Consistent with their constitutive proliferation, T47D and MCF7 cells in which wild-type ERα is replaced by the most common mutations, ERαY537S and ERαD538G, exhibit partially estrogen-independent gene expression. A novel invasion/dissociation/rebinding assay demonstrated that the mutant cells have a higher tendency to dissociate from invasion sites and rebind to a second site. Compared to ERαD538G breast tumors, ERαY537S tumors exhibited a dramatic increase in lung metastasis. Transcriptome analysis showed that the ERαY537S and ERαD538G mutations each elicit a unique gene expression profile. Gene set enrichment analysis showed Myc target pathways are highly induced in mutant cells. Moreover, chromatin immunoprecipitation showed constitutive, fulvestrant-resistant, recruitment of ERα mutants to the Myc enhancer region, resulting in estrogen-independent Myc overexpression in mutant cells and tumors. Knockdown and virus transduction showed Myc is necessary and sufficient for ligand-independent proliferation of the mutant cells but had no effect on metastasis-related phenotypes. Thus,

[1] This chapter appeared in its entirety in *Cancer Letters*. Yu, L. *et al.* (2019) Estrogen-independent Myc overexpression confers endocrine therapy resistance on breast cancer cells expressing ERαY537S and ERαD538G mutations. *Cancer letters*, *442*, 373-382. Data in Figures 2.5 (F) and 2.6 (D, E) was obtained by Mr. Lawrence Wang and Mr. Darjan Duraki. Data in Figure 2.6 (B, C) was obtained by Dr. Chengjian Mao and data in Figure 2.11 (B) was obtained by Mr. Lawrence Wang.

Myc plays a key role in aggressive proliferation-related phenotypes exhibited by breast cancer cells expressing ERα mutations.

INTRODUCTION

At diagnosis, approximately 75% of breast cancers are estrogen receptor alpha (ERα) positive (1). Endocrine therapies for ERα positive tumors include aromatase inhibitors, tamoxifen, fulvestrant (ICI-182,780/Faslodex) and other selective estrogen receptor modulators, and degraders (2-4). Although endocrine therapies are effective initially, resistance often develops (5). While resistance mechanisms are diverse, approximately 30% of metastatic tumors harbor ERα ligand binding domain (LBD) mutations, most commonly ERαD538G and ERαY537S (6-8). These mutations are rare in primary tumors and increase after endocrine therapy (9, 10).

To characterize these aggressive tumors, we, and others used CRISPR/Cas9, long-term-estrogen-deprived selection and other methods to generate cell lines bearing ERα mutations (11-16). Consistent with their estrogen-independent proliferation and tamoxifen resistance (11), structural and modeling studies suggest ERαY537S and ERαD538G mutants are locked in active conformations and exhibit reduced affinity for 4-hydroxytamoxifen (OHT) (17). Moreover, ESR1 mutations increase breast cancer stem cell activity (16). Since invasiveness of these cell lines, was largely unstudied, we used a novel, invasion-dissociation-rebinding (IDR) assay to analyze metastasis-related properties. Compared to parental cells, T47D-ERαY537S (TYS) and T47D-ERαD538G (TDG) cells (11) exhibit increased invasiveness and TYS and TDG cells and MCF7-derived MCF7-Y537S and MCF7-D538G cells all exhibit increased dissociation and

rebinding at a second site. Patients whose breast cancers express the ERαY537S and ERαD538G mutations have 1-year and 6-month shorter lifespans, respectively, than patients whose tumors express wild type ERα (18). Notably, compared to the ERαD538G (TDG) tumors, the more lethal ERαY537S (TYS) tumors exhibited greatly increased lung metastases; wild type ERα (T47D) tumors did not metastasize. Thus, the aggressive phenotypes of cells expressing ERαY537S and ERαD538G include resistance to drugs targeting estrogen production and binding to ERα, estrogen-independent proliferation and an increase in stemness and metastasis-related properties.

How these aggressive phenotypes link to the mutant cells transcriptome was largely unknown. A few studies began transcriptome characterization (12, 14, 19), and recent studies identified specific coactivators and unique binding sites of mutant ERα (15, 20). Remaining to be done were detailed transcriptome comparisons of ERαD538G and ERαY537S mutant cells, analysis of invasiveness, and identification and analysis of specific genes contributing to the aggressive phenotypes of mutation-bearing tumors.

To identify pathways that might play a role in these aggressive phenotypes, we performed unbiased RNAseq analysis of global gene expression profiles. Compared to parental T47D cells, TYS and TDG cells exhibit distinct patterns of gene expression. Gene set enrichment analysis (GSEA) of T47D and MCF7 RNAseq data showed Myc targets are highly induced in mutant cells. Myc is important in diverse cellular processes including proliferation, biosynthesis and global metabolism(21, 22). Dysregulated Myc expression contributes to malignant transformation, tumor progression and reduced responsiveness to anticancer drugs(23-28). In breast cancer, Myc overexpression is associated with tamoxifen resistance *in vitro* and in patients(5).

Chromatin immunoprecipitation (ChIP) demonstrated estrogen-independent, fulvestrant-resistant, recruitment of ERαY537S and ERαD538G to the *Myc* enhancer. Moreover, cell and tumor studies demonstrated estrogen-independent Myc expression in the mutants is higher than in estrogen-treated controls. Myc knockdown blocked estrogen-independent growth of TYS and TDG cells. Notably, expression of Myc in estrogen-deprived T47D cells partially reproduces the estrogen-independent proliferation and antiestrogen resistance, but not the increased invasiveness, dissociation and rebinding, displayed by mutant cells. Our identification of a role for Myc in a sub-set of the aggressive phenotypes displayed by ERα mutant cells illustrates the utility of these cell models and transcriptome data as tools for identifying pathways that contribute to the aggressiveness of *ESR1* mutant cells.

MATERIALS AND METHODS

Cell culture and proliferation assays

Media and conditions were previously described (29). T47D, MCF7 and the mutant clones were generated and cultured as described(11, 14). Cells were authenticated at University of Arizona Genetics Core. E_2, fulvestrant and z-OHT were from Sigma. JQ1 was from Selleck. Cells proliferation assays were as described (29).

Generation of luciferase-expressing cell lines

The pcDNA3-Luc vector was transfected into T47D, TYS clone 4 and TDG clone 1 cells, respectively. Colonies were selected for 2 weeks in G418.

qRT-PCR and RNAseq data analysis

Cells were cultured and plated as described (29). For RNAseq, T47D, TYS and TDG cells were treated with vehicle (EtOH) or 10 nM E_2. Total RNA of three biological

replicates was collected and cDNA library were prepared using TruSeq Stranded mRNAseq Sample Prep kit (Illumina). Single-end RNA sequencing was performed by the University of Illinois High-Throughput Sequencing Unit (HiSeq 4000 (Illumina)). Software used for data analysis is in Table 1. Raw and processed data of RNAseq were deposited in NCBI GEO [GSE108304].

Western blot

Whole cell extracts were prepared and western blots were performed as described (29). Antibodies are in Table 2.

siRNA knockdowns

siRNA knockdowns were performed using DharmaFECT1 and 100 nM ON-TARGET plus non-targeting pool or SMARTpools for ERα and c-Myc (Dharmacon). Transfection conditions were as described (29).

2.6 Chromatin immunoprecipitation (ChIP)

Chromatin was prepared from three biological replicates incubated 30 min in 10 nM E_2 or pretreated with 500 nM fulvestrant for 10 min before E_2 addition. Samples were sheared using an M220 Focused-ultra sonicator (Covaris). ChIP assays were as described (30).

Lentivirus infection

Lentivirus was produced by cotransfecting pCDH-puro-cMyc (Addgene #46970) or pHIV-Luciferase vector (Addgene #21375) with packaging vectors pCI-VSVG (Addgene #1733) and psPAX2 (Addgene #12260) into HEK293 cells using Lipofectamine 3000 (Thermo Fisher).

Cell invasion assay

Millipore polycarbonate cell culture inserts (12 μm) were coated with 25 μg/ml collagen or Matrigel (Corning). 100,000 luciferase-expressing cells in 0.5 ml medium containing 0.1% BSA were placed in the upper chamber and 0.55 ml medium containing 20% CD-FBS were in bottom chamber (31, 32). After 24h, upper chamber cells were removed. 150 μl Bright-Glo™ (Promega) was added into the wells and luciferase activity was measured using a PHERAStar plate-reader (BMG Labtech).

Mouse xenograft

All animal studies were approved by the University of Illinois Institutional Animal Care (IACUC) committee. Five female mice were used for each cell line. Estrogen pellets (90 day; Innovative Research of America) were implanted subcutaneously 30 days prior to T47D-Luc cell injection; a second estrogen-release pellet was implanted 3 months after the first pellet. No estrogen supplementation was used in the TYS-Luc and TDG-Luc mice. 5×10^6 T47D, TYS and TDG cells in Matrigel stably expressing the luciferase gene (T47D-Luc, TYS-Luc and TDG-Luc) were grafted orthotopically into ovariectomized NSG mice. Mice were anesthetized, injected with luciferin substrate and tumor bioluminescence was monitored using an IVIS Spectrum CT live-animal imaging system (PerkinElmer). Based on the growth of the primary breast tumors, mice were sacrificed about 2 months (TYS-Luc), about 3 months (T47D-Luc) and about 4 months (TDG-Luc), after initiating tumor growth. Consistent with *in vitro* results for the cell lines, the TDG-Luc tumors have about 12-fold higher luciferase emission per mg excised breast tumor weight than the TYS-Luc tumors. Therefore, the TYS-Luc and TDG-Luc lung metastases data in Fig. 2E was normalized for the difference in luciferase

emission. Since no lung metastases were observed for T47D-Luc, normalization was not relevant.

Statistics

Each *in vitro* experiment was performed at least three times. Statistical significance was determined by an unpaired two-tailed Student's t-test or ANOVA using SPSS statistics (IBM). Data were presented as mean ± s.e.m and a p value of <0.05 was defined as statistically significant.

RESULTS

T47D-ERαY537S (TYS) and T47D-ERαD538G (TDG) cells display a constitutive gene expression pattern

To evaluate the effect of ERα mutations on gene expression, we performed RNAseq in T47D, TYS and TDG breast cancer cells. Without estrogen, T47D, TYS and TDG cells exhibit very different gene expression patterns. Expression of 3669 and 2592 genes were altered in TYS and TDG cells, respectively (Table 3); 2020 of these genes were shared by TYS and TDG cells (Fig. 1A). To evaluate expression of direct and indirect ERα target genes, we chose 4- and 24-hour E_2 treatment. After 4h E_2 treatment, 317 genes were differentially regulated in T47D cells; 272 of these genes are shared by one or both mutant cells (Fig. 2A). A heatmap of over 13,000 genes and a multi-dimensional scaling (MDS) plot show a modest effect of 4h E_2 treatment on the T47D transcriptome, with minimal effects on the mutants (Fig. 1B, Fig. 2D).

24h E_2 incubation dramatically increased differentially expressed T47D cell genes; most of these genes (1509/1748) were differentially expressed in one or both mutant cells (Fig. 2B). Compared to vehicle, the heatmap and MDS plot display a large shift of the E_2-

treated T47D transcriptome toward the TDG cells (Fig. 2C, E). To further compare T47D, TYS and TDG cells, we used qPCR to analyze expression of well-characterized ERα target genes. For all genes tested, estrogen responses were robust in T47D, reduced in TDG and minimal in TYS cells (Fig. 2F).

To test for off-target effects of CRISPR/Cas9, we evaluated expression of these genes both in additional clones of T47D-ERαY537S (clone 39) and T47D-ERαD538G (clone 28) and in MCF7 cell lines containing ERαY537S and ERαD538G mutations generated through virus infection, not CRISPR. Consistently, ERαY537S cells responded less to estrogen than ERαD538G and parental cells (Fig. 3, 4A). Overall, the data demonstrate estrogen-independent gene expression in the mutant cells.

ERαY537S and ERαD538G cells have distinct gene expression profiles and exhibit aggressive phenotypes

Although TYS and TDG cells both display ligand-independent gene expression, their gene expression profiles differ. MDS shows that after 24h E_2 treatment T47D cells shifted towards TDG cells, indicating that E_2-stimulated T47D and TDG cells have more closely related gene expression patterns. Notably, E_2 treatment had almost no effect on TYS gene expression (Fig. 2E). To further address potential off-target effects of CRISPR/Cas9 (33), we generated an MDS plot from raw RNAseq datasets of MCF7, and virus-generated MCF7-Y537S and MCF7-D538G [SRA: SRP093386] (14) (Fig. 4C). Consistent with the T47D data, the estrogen-treated MCF7 gene expression profile is closer to the MCF7-D538G cell profile and MCF7-Y537S cells respond least to estrogen.

To begin to explore the interplay between gene expression patterns and the aggressive phenotypes induced by ERα mutations, we examined proliferation and resistance to endocrine therapies. Parental T47D cells did not grow in estrogen-depleted medium, while TYS and TDG cells (Fig. 5A), other mutant T47D clones and MCF7-Y537S and MCF7-D538G cells all exhibited robust estrogen-independent proliferation (Fig. 5B, C). We used dose-response studies to evaluate resistance to endocrine therapies. In T47D cells, proliferation was nearly abolished by a 25- to 100-fold molar excess over estrogen of z-4-hydroxytamoxifen (OHT), or fulvestrant/ICI. In contrast, TYS and TDG cells exhibited partial resistance to OHT and fulvestrant (Fig. 5A). Notably, in MCF7 cells, a 50-fold molar excess of OHT or fulvestrant abolished estrogen induced cell proliferation, but had no effect on proliferation of MCF7-Y537S and MCF7-D538G cells (Fig. 5C). Thus, both T47D- and MCF7-derived cell lines containing ERαY537S and ERαD538G exhibit estrogen-independent proliferation and resistance to OHT and fulvestrant.

Although *ESR1* mutations are observed in metastatic breast cancers, metastasis is difficult to model in cell culture. To probe steps in metastasis beyond invasion, we developed a quantitative invasion-dissociation-rebinding (IDR) assay (Fig. 6A). Using T47D, TYS and TDG cell lines stably expressing luciferase, we quantified both total cells that invaded through collagen- or Matrigel-coated membranes (Fig. 6B; Invaded Cells) and cells that invaded and then dissociated from their membrane invasion site and rebound to a second site (Fig. 6B; IDR cells). ERα mutations significantly increased invasiveness. Even though more TDG cells invaded through membranes, more TYS cells dissociated and rebound (Fig. 5D, Fig. 6B, C). Using lentiviral transduction of luciferase, we performed IDR assays on MCF7, MCF7-Y537S and MCF7-D538G cells. Compared

to MCF7 cells, ERα mutations did not increase invasion, but strongly elevated dissociation and rebinding (Fig. 5E). Increased ability to dissociate and rebind at a second site is a previously unexplored metastasis-related property of ERα mutant cells.

We evaluated the ability of orthotopic breast tumors derived from TYS-Luc (ERαY537S) and TDG-Luc (ERαD538G) cells to metastasize to lung and investigated whether invasion or dissociation-rebinding correlated with *in vivo* metastatic potential. As a control, we used estrogen-supplemented T47D-Luc, which expresses wild type ERα. All the mice grew primary tumors (Fig. 5F). Because the light output from the large primary breast tumors masks signals from lung metastases, we evaluated the extent of lung metastasis using *ex vivo* bioluminescent imaging (BLI) of lungs excised from tumor bearing mice. Consistent with earlier reports (34, 35), lung metastases were not detected in mice harboring T47D-Luc xenografts (Fig. 6D). All mice harboring primary breast tumors expressing ERαY537S and ERαD538G developed lung metastases (Fig. 6D). Since light emission per mg of TDG-Luc breast tumor is 12-fold higher than from TYS-Luc breast tumors, the moderately lower visualized level of metastasis seen in the lungs of TDG-Luc tumors compared to TYS-Luc tumors (Fig. 6D) reflects a dramatically lower level of lung metastasis. Normalized for this difference in light emission, lung metastases from mice with primary TYS-Luc breast tumors averaged 32 times higher signals than lung metastases from mice harboring primary TDG breast tumors (Fig. 6E). A >20-fold increase in metastases in mice harboring TYS-Luc breast tumors compared to TDG-Luc tumors is also observed if the metastases data is calculated as the ratio of light emission by each lung metastases relative to light emission from the primary breast tumor in that mouse.

ERαY537S and ERαD538G mutations elicit constitutive hormone-independent pathway alterations

To probe pathways related to therapy resistance and metastatic potential in ERαY537S and ERαD538G cells, we used the RNAseq datasets to perform GSEA. Highly upregulated pathways were largely consistent across T47D and MCF7 mutant cells, with little estrogen dependence (Fig. 7, 8). Consistent with estrogen-independence, without estrogen, estrogen response pathways were upregulated in mutant cells (Fig. 7A). Cell cycle related pathways were constitutively elevated in mutant cells. Confirming our earlier observation (11), the tumor protective unfolded protein response (UPR) was upregulated in T47D and MCF7 mutant cells.

Consistent with direct regulation by ERα, in T47D cells after 4h estrogen treatment, “Estrogen_Response” pathways were the top upregulated pathways, (Fig. 7B). After 24h estrogen treatment, most pathways highly upregulated in mutant cells were also upregulated in parental T47D cells.

The Myc pathway exhibits constitutive and elevated activation in mutant cells

At 24 hours, Myc targets were the top upregulated pathway in mutant cells (Fig. 7, 8). There is a strong correlation between Myc targets and cancer stemness, which can lead to therapy resistance and metastasis(36). Compared to T47D cells, Myc target genes important in DNA replication, protein synthesis and cell cycle progression are constitutively overexpressed in TYS and TDG cells (Fig. 9A, B).

As expected, ERα knockdown blocked estrogen-stimulated proliferation of T47D cells and proliferation of TYS and TDG cells with and without E_2 (Fig. 10A). Consistent with a role for Myc, ERα knockdown also blocked estrogen stimulated Myc expression in T47D cells and reduced Myc expression in mutant cells (Fig. 10B).

We next assessed whether *Myc* expression in the TYS and TDG cells was constitutive and resistant to antagonists. Chromatin immunoprecipitation (ChIP) in T47D cells showed that E_2 stimulates, and a 50X excess of ICI/fulvestrant blocks, recruitment of ERα to the *Myc* enhancer region. Recruitment of ERαY537S was constitutive with little effect of E_2; binding of ERαD538G was partially constitutive and was further increased by E_2. ICI reduced, but did not eliminate binding of ERα mutants to *Myc* enhancer (Fig. 9C).

Moreover, compared to T47D cells, *Myc* mRNA expression in TYS and TDG cells was constitutive and elevated (Fig. 9D). Notably, compared to estrogen-treated T47D tumors, vehicle-treated TYS and TDG tumors exhibited higher *Myc* mRNA expression (Fig. 9E). Consistent with the ChIP, OHT or ICI abolished E_2-induction of *Myc* mRNA in T47D cells, but reduced *Myc* levels less than 50% in TYS and TDG cells (Fig. 9D). Western blot analysis confirmed that, in T47D cells, Myc protein exhibits fulvestrant-sensitive is E_2-induction. In contrast, in TYS and TDG cells, Myc levels are high in vehicle-treated cells, show little increase in response to E_2 and are only modestly sensitive to OHT and fulvestrant (Fig. 9F, G). Constitutive Myc expression and antiestrogen resistance were also observed in other T47D mutant clones and in MCF7 mutant cells (Fig. 10C, D)

In T47D cells, but not in the mutant cells, antiestrogens downregulated induction of mRNA and protein encoding Myc cell cycle effector targets, Cyclin E and E2F-2 (Fig. 9F, G, Fig. 10E, F). Although OHT and fulvestrant blocked E_2 induction of *E2F-2* mRNA in

mutant cells, it was still expressed at levels >5 fold higher than in T47D cells (Fig. 10E). These data help explain why TYS and TDG cells continue to proliferate during endocrine therapy.

Myc expression is required for estrogen-independent proliferation of TYS and TDG cells and is sufficient to confer partial resistance to endocrine therapy

To further evaluate Myc's role, we altered its level. After RNAi knockdown, levels of Myc protein in mutant cells and vehicle treated T47D cells were similar (Fig. 11A). Myc knockdown greatly reduced E_2 stimulated proliferation of T47D cells and abolished estrogen-independent proliferation of mutant cells (Fig. 11B). Targeting Myc expression through the bromodomain inhibitor JQ1 is an emerging therapeutic strategy(37, 38). JQ1 reduced Myc expression by ~50% (Fig. 11C) and abolished proliferation of T47D, TYS and TDG cells (Fig. 11D). As a bromodomain inhibitor, JQ1 acts on diverse targets. These data suggest other pathways promote proliferation in TYS and TDG cells by working synergistically with Myc.

Since reducing constitutive Myc expression abolished estrogen-independent proliferation of TYS and TDG cells, we explored whether constitutive Myc expression in estrogen-deprived T47D cells could recapitulate their aggressive phenotypes. T47D cells were infected with lentivirus expressing Myc, or a luciferase control. After infection, Myc protein levels in T47D cells were increased to levels similar to those in TYS and TDG cells (Fig. 11C, E). Myc overexpression in OHT- and fulvestrant-treated T47D cells did not alter ERα levels, but increased levels of the downstream effector, Cyclin E (Fig. 11E). Constitutive Myc expression facilitated both E_2-independent and E_2-dependent

proliferation of T47D cells (Fig. 11F). Notably, compared to control cells, Myc overexpression increased resistance to OHT and fulvestrant (Fig. 11F). However, Myc overexpression had no effect on the number of invaded cells, or on the number of dissociated and rebound cells (Fig. 11G, H). Thus, while estrogen-independent expression of Myc in T47D cells does not reproduce the metastasis-related phenotypes exhibited by ERα mutant cells, Myc expression partially recapitulates their proliferation-related phenotypes of increased growth, estrogen-independent proliferation and resistance to OHT and fulvestrant.

DISCUSSION

Clustered mutations in the ERα LBD occur in 20-40% of ERα positive metastatic breast cancers (7, 10, 39). While all metastatic ERα positive breast cancers display resistance to endocrine therapy and ultimately to standard chemotherapy, patients with tumors harboring the common ERαY537S and ERαD538G mutations exhibit 1-year and 6-month shorter median survival than patients whose metastatic tumors contain wild type ERα (18). To identify roles of these mutations, transient transfection, CRISPR/Cas9 and other techniques were used to express ERα LBD mutations in breast cancer cells (7, 9, 13-15).

Transcriptome level studies of cells bearing *ESR1* mutations are limited and were either restricted to a single mutation (13), or lack extensive functional analysis (14). We compared T47D cells harboring ERαY537S and ERαD538G mutations and parental cells at two time points and confirmed several key observations with the MCF7 dataset. Surprisingly, the MDS results show that the mutations are not simply constitutively active ERα, and instead exhibit unique gene expression patterns.

These ERα LBD mutations occur primarily after patients have received endocrine therapy (7, 9, 10, 40). Very recently, naturally occurring *ESR1* Y537C and Y537S mutations were identified by selection in long-term-estrogen-deprived MCF7 cells (12). Taken together, these studies, and the data we present, show that the changes in the Y537 and D538 *ESR1* mutations are sufficient to confer on breast cancer cells partial resistance to antiestrogens and estrogen-independent gene expression and cell proliferation. Across different clones, different parental cell lines and zygosity status, expression of most mRNAs tested exhibited a higher basal level and lower estrogen response in ERαY537S cells than in ERαD538G cells. Compared to cells expressing ERαD538G, we (Fig. 5A) and others, observe increased antiestrogen resistance in cell lines expressing ERαY537S (11, 14). These data suggest enhanced estrogen-independent gene expression in breast cancer cells expressing ERαY537S may confer unique properties that influence tumor behavior and response to therapy.

Previous studies focused almost entirely on proliferation-related properties of *ESR1* mutations. However, *ESR1* mutations were detected at higher allele frequency in metastases than in the primary breast cancers (41, 42). To probe the role of *ESR1* mutations in metastasis-related properties we improved conventional transwell assays (32) which fail to detect invaded cells that partially recapitulate the metastasis-related property of cell dissociation from the membrane and reattachment at a second site. Using T47D, TYS and TDG cells that stably express luciferase and luciferase-expressing lentivirus in MCF7 cell lines, we used our invasion-dissociation-rebinding assay to quantitate both the number of invaded cells and the number of invaded cells that then dissociate from the membrane and rebind on the bottom of the well. In the *in vitro*

invasion-dissociation-rebinding assay, ERα mutations significantly increase both T47D cell invasion and dissociation-rebinding. Consistent with the cell-based data, our *in vivo* data shows that the ERα mutations drive metastasis in otherwise non-metastatic T47D tumors. These data illustrate the value of the IDR assay (Fig. 6A). The dramatic increase in lung metastasis of TYS tumors compared to TDG tumors (Fig. 6E) was not predicted by the widely used Matrigel and collagen invasion assays, which show increased invasion by TDG cells (Fig. 6C). In contrast, the dissociation rebinding assay, which shows strongly increased dissociation and rebinding by the TYS cells compared to the TDG cells (Fig. 6C), is much more consistent with the *in vivo* lung metastasis data (Fig. 6E). While metastasis is an exceptionally complex multi-step process that cannot be fully modeled with cell-based assays, our data shows that, compared to the traditional Matrigel invasion assay, our simple *in vitro* IDR assay explores cell properties that correlate with *in vivo* metastatic frequency. Thus, the IDR assay provides a useful *in vitro* model for investigation of metastasis-related properties.

To identify pathways driving these aggressive phenotypes of ERα mutant cells, we performed GSEA using T47D and MCF7 RNAseq datasets. Compared to parental cells, Myc target genes were highly enriched in T47D and MCF7 mutant cells; other upregulated pathways like “E2F targets” and “G2M checkpoint” are tightly correlated with Myc expression. Myc directly induces expression of cell cycle regulators, including Cyclin D, Cyclin E and E2Fs (43, 44). Myc also promotes cell cycle progression by regulating CDK phosphorylation and antagonizing cell cycle inhibitor expression (45, 46). In estrogen-deprived ERαY537S and ERαD538G cells, Myc was highly induced, suggesting Myc might play an important role in their E_2-independent proliferation. Myc knockdown

demonstrated that Myc is necessary for E_2-independent proliferation of the TYS and TDG cells. Constitutive Myc expression in E_2-deprived T47D cells was sufficient to induce moderate E_2-independent proliferation. Moreover, TYS and TDG cells developed estrogen-independent tumors in ovariectomized mice; Myc expression was highly elevated in these tumors. Myc overexpression in tumors has been correlated with cancer stemness, which leads to reduced responsiveness to anticancer drugs and increased metastatic potential (24, 25, 36). In breast cancer cells, overexpression of Myc and its downstream targets Cyclin E1 and Cyclin D1 results in decreased sensitivity to antiestrogens (47, 48). An analysis of Myc in 399 patients with ERα positive breast cancer showed that higher levels of Myc expression were associated with shorter relapse free survival (48). Notably, while these studies and our data demonstrate an important role for Myc in proliferation-related phenotypes and therapy resistance, Myc expression in T47D cells had no effect on metastasis-related invasion, dissociation and rebinding.

In addition to Myc upregulation, these cell lines exhibit alterations in protective pathways associated with resistance to cell death. The UPR was upregulated in E_2-treated T47D and MCF7 cells and in ERαY537S and ERαD538G mutants. UPR upregulation is consistent with our recent work demonstrating E_2-activation of the anticipatory UPR in ERα containing T47D and MCF7 breast cancer cells (49), in PEO4 ovarian cancer cells (50), and estrogen-independent UPR activation in TYS and TDG cells (11). Since increased expression of a UPR gene index was tightly correlated with reduced time to tumor recurrence, tamoxifen resistance and reduced survival (49), these pro-survival changes may contribute to the pathology of tumors expressing ERα mutations.

FIGURES AND TABLES

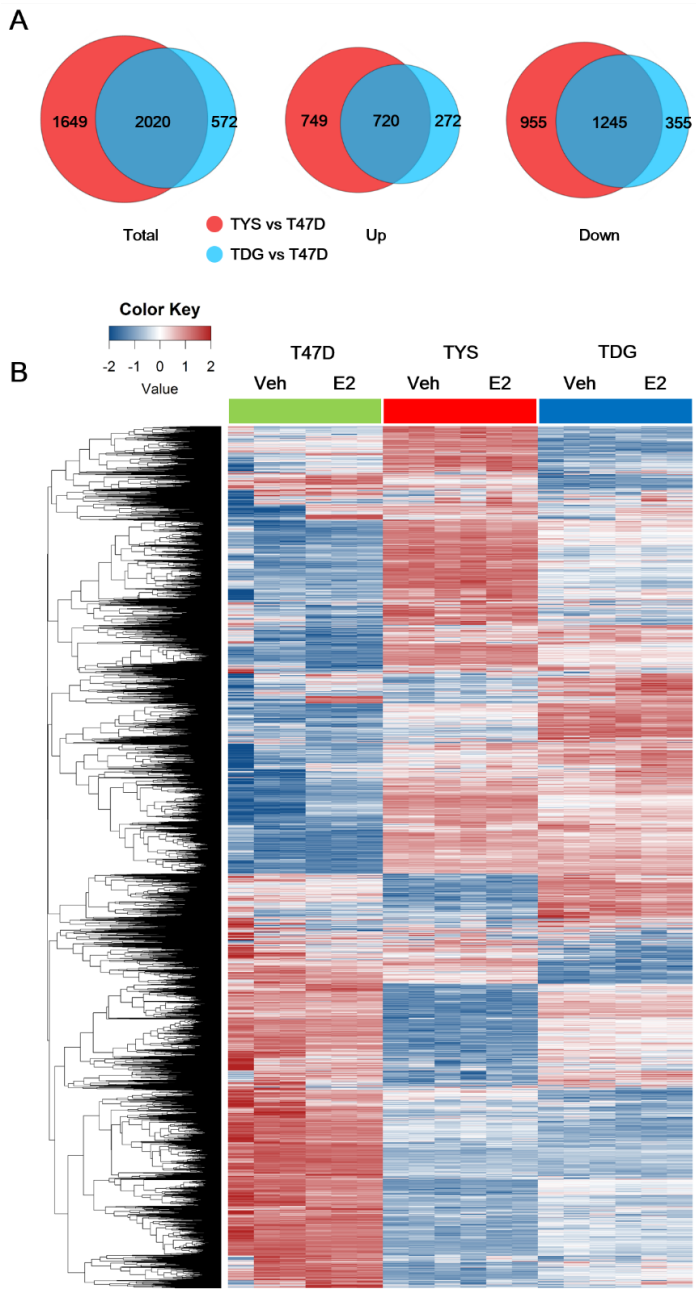

Figure 2.1 Gene expression patterns in TYS and TDG cells. A Venn diagrams comparing genes with absolute fold change >2 and false discovery rate <0.05 in vehicle-treated TYS and TDG cells. Up- and down-regulated genes were analyzed in two Venn diagrams. **B** Heatmap showing log counts per million (CPM) of genes that have CPM >1 in at least 3 samples after 4h E_2 treatment.

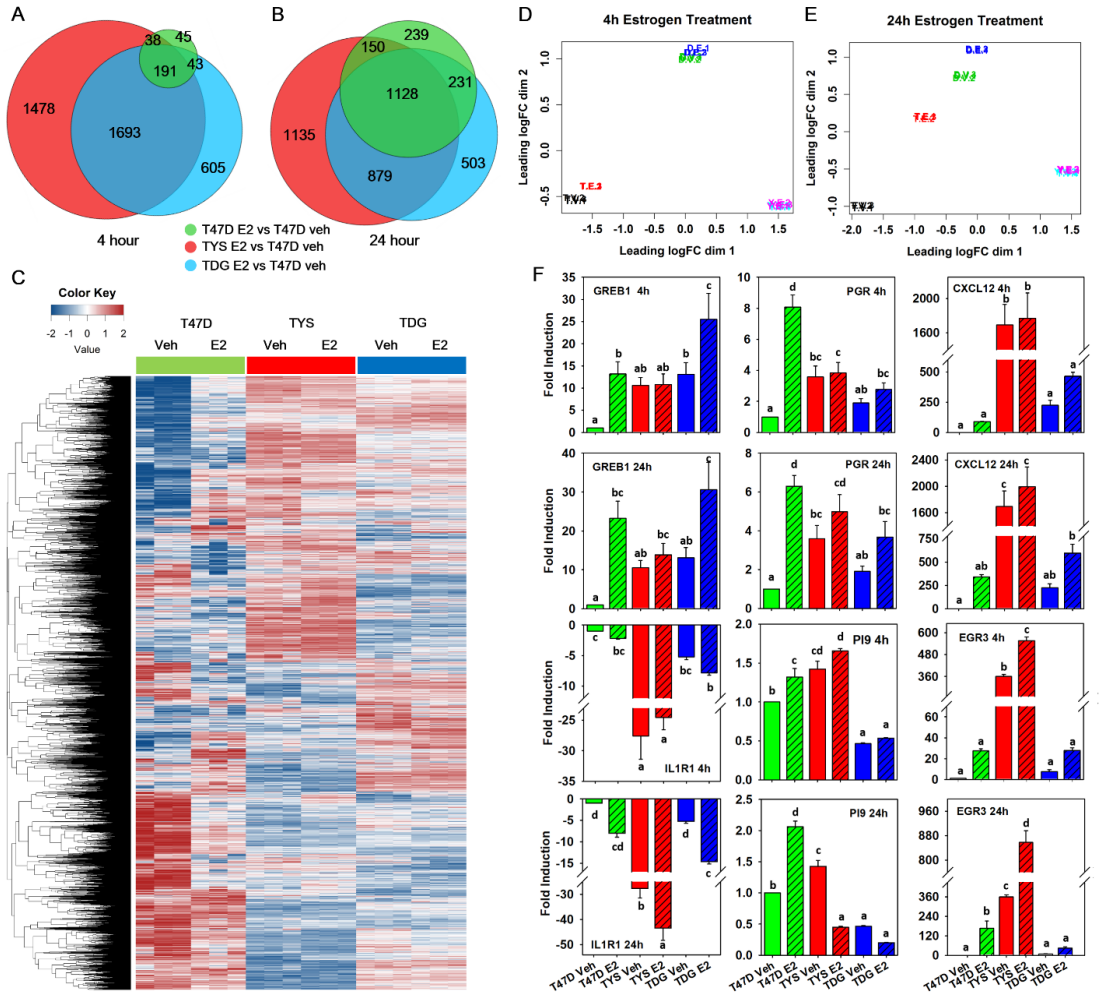

Figure 2.2 TYS and TDG cells exhibit unique gene expression patterns. A,B Venn diagrams comparing genes with absolute fold change >2 and false discovery rate (FDR) q-value <0.05 in T47D, TYS and TDG cells after 4h **A** and 24h **B** E_2 treatment. **C** Heatmap showing log counts per million (CPM) of genes that have CPM >1 in at least 3 samples after 24h E_2 treatment. **D,E** Multi-dimensional scaling (MDS) plot of RNAseq samples 4h **D** and 24h **E** after E_2 addition. Similarities of gene expression patterns were calculated and mapped for T47D (T), TYS (Y) and TDG (D) cells treated with vehicle (V) or estrogen (E). Data from each of the three biological replicates is shown. **F** Real-time PCR analysis of GREB1, PGR, CXCL12, IL1R1, PI9 and EGR3 in T47D, TYS and TDG cells after addition of vehicle or E_2 for 4h or 24h. (mean ± s.e.m., n=3). Different letters indicate a significant difference among groups ($P<0.05$) using one-way ANOVA followed by Duncan's *post hoc* test.

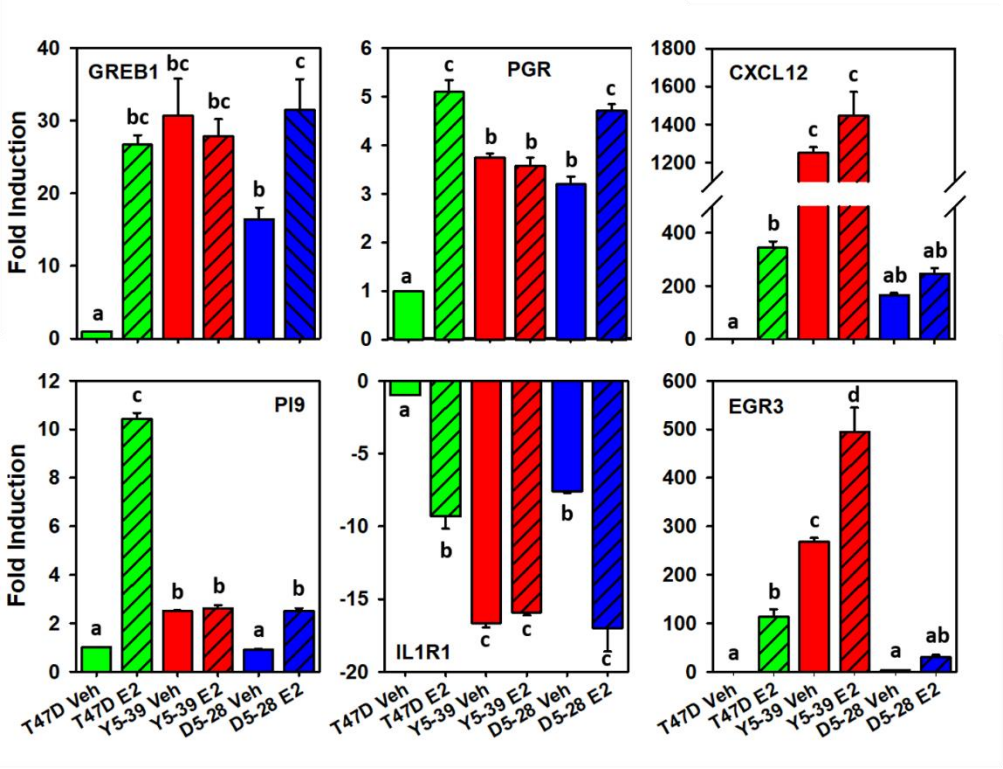

Figure 2.3 ERαY537S and ERαD538G mutations promote constitutive expression of ERα target genes. Real-time PCR analysis of GREB1, PGR, CXCL12, PI9, IL1R1 and EGR3 in T47D, and a second set of clonal cell lines, T47D-ERαY537S (clone 39) and T47D-ERαD538G (clone 28) that are distinct from TYS and and TDG cells, after addition of vehicle or E_2 for 24 h (mean ± s.e.m., n=3). Different letters indicate a significant difference among groups ($P<0.05$) using one-way ANOVA followed by Tukey's *post hoc* test.

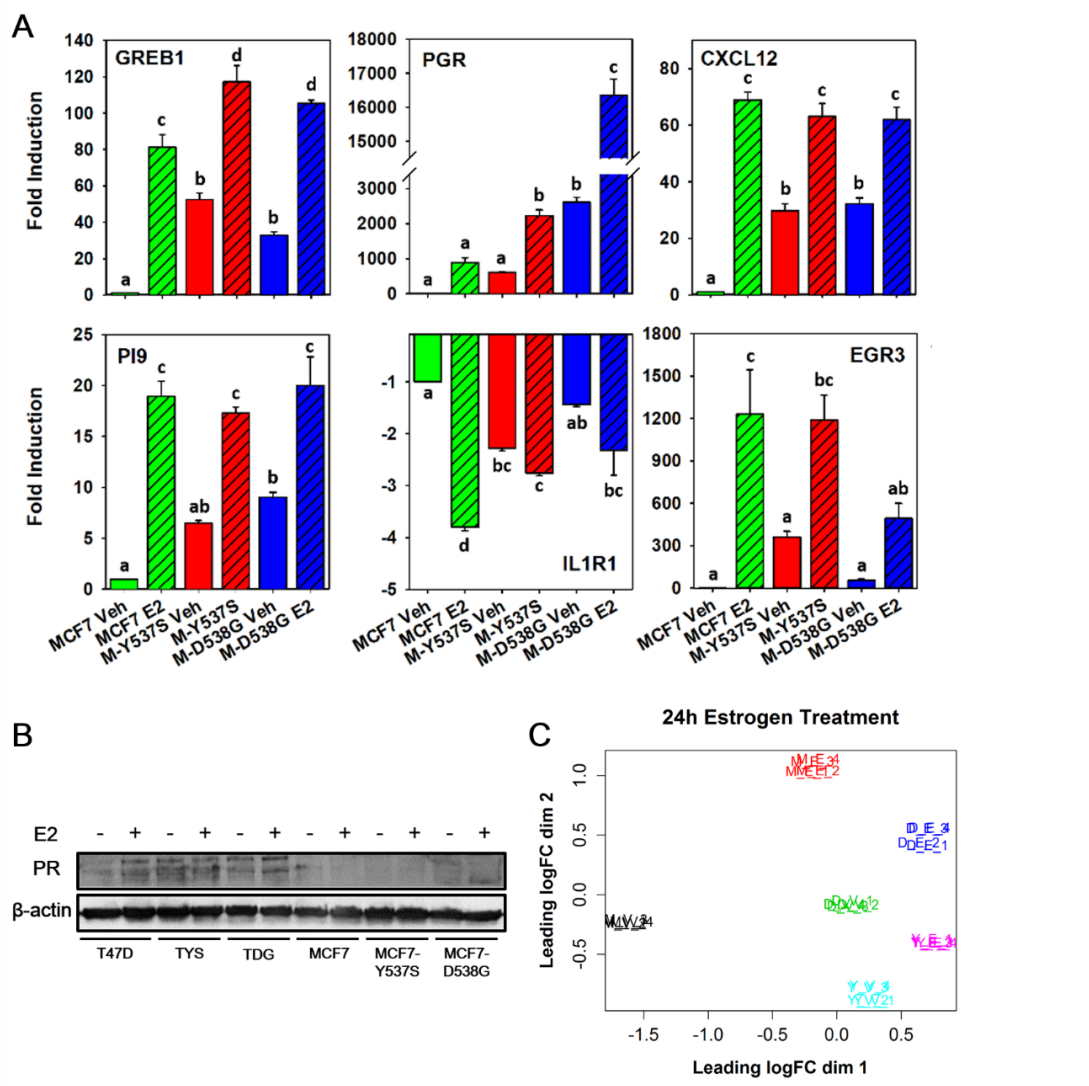

Figure 2.4 Gene expression patterns in MCF7, MCF7-Y537S and MCF7-D538G cells. **A** Real-time PCR analysis of GREB1, PGR, CXCL12, PI9, IL1R1 and EGR3 in MCF7, MCF7-Y537S and MCF7-D538G cells after addition of vehicle or E_2 for 24 h. n=3 ± s.e.m.. The dramatic Fold Induction of PR mRNA is due to extremely low basal levels of PR mRNA in our estrogen starved MCF7 cells. Different letters indicate a significant difference among groups (P<0.05) using one-way ANOVA followed by Tukey's *post hoc* test. **B** Western blot showing progesterone receptor (PR) levels following treatment of cells with vehicle or 1 nM E_2 for 24h. **C** Multi-dimensional scaling (MDS) plot of RNAseq samples 24h after E_2 addition. Similarities of gene expression patterns were calculated and mapped for MCF7 (M), MCF7-Y537S (Y) and MCF7-D538G (D) cells treated with vehicle (V) or estrogen (E).

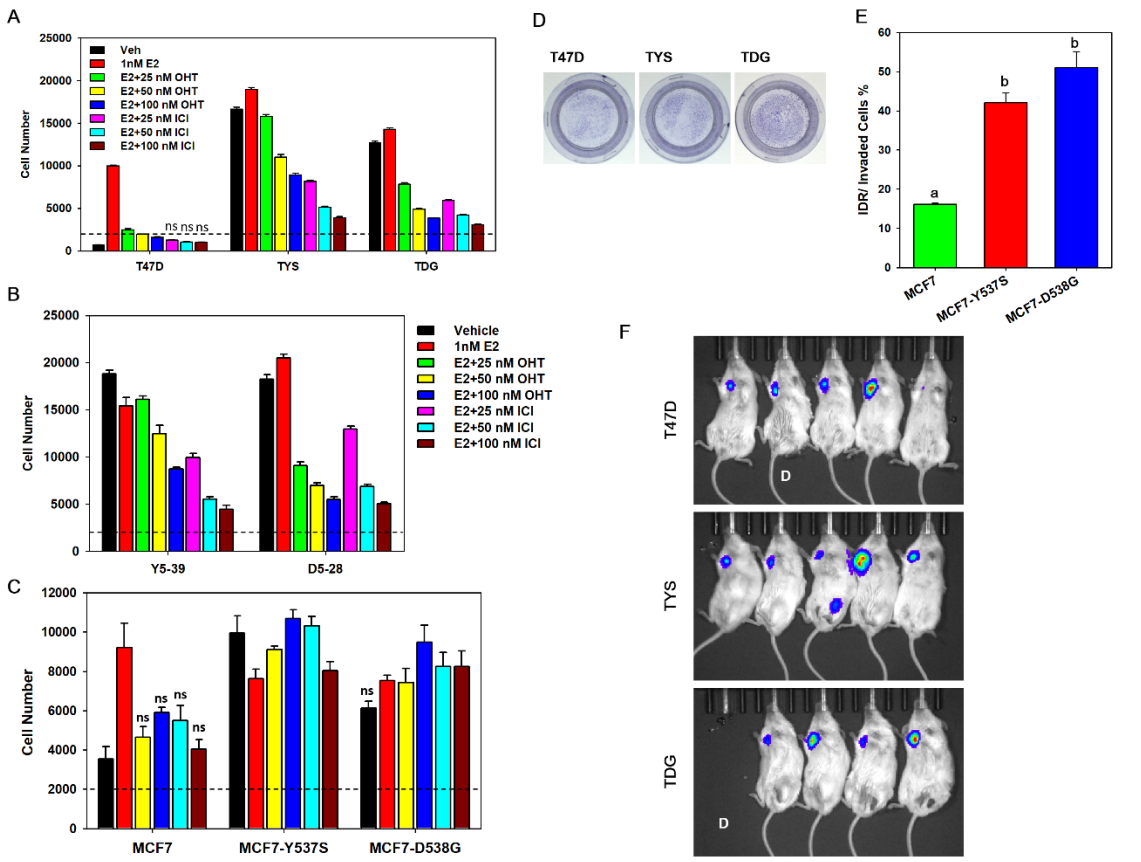

Figure 2.5 ERαY537S and ERαD538G mutant cells exhibit estrogen-independent cell proliferation and partial resistance to antiestrogens. A MTS assay of T47D, TYS and TDG cells, grown 4 days in 10% CD-FBS, treated with the indicated concentrations of E_2, OHT and fulvestrant/ICI. For each treatment condition, the data from TYS and TDG cells was significantly different from the corresponding T47D cell data (*** P<0.001). **B** MTS assay of T47D-ERαY537S (clone 39) and T47D-ERαD538G (clone 28) cells, grown in 10% CD-FBS, treated with the indicated concentrations of E_2, OHT and fulvestrant/ICI. **C** MTS assay of MCF7, MCF7-Y537S and MCF7-D538G cells, grown in 1% CD-calf serum, treated with the indicated concentrations of E_2, OHT and fulvestrant/ICI. **A, B, C** '---' denotes day 0 cell number, (2000 cells/well). The graph shows mean growth at day 4 ± s.e.m (n=6). One-way ANOVA was used to evaluate statistical significance. ns, not significant. **D** Representative crystal violet staining images showing more TYS and TDG cells invaded through the collagen-coated membrane. **E** IDR assay of MCF7, MCF7-Y537S and MCF7-D538G cells with matrigel-coated membranes and chambers. The data represents the percent of invaded cells that have dissociated from the membrane and

Figure 2.5 (cont.) rebound at the bottom of the well (IDR/Invaded Cells %) (mean ± s.e.m., n=5, letters denote significant differences between groups). **F** Representative BLI images of the mice with WT T47D cells + E2 pellets, TYS and TDG xenografts. One mouse from the T47D and one from TDG group died prior to *ex vivo* lung imaging. 'D' denotes the dead animals. These photographs were made using IVIS exposure times that allow visualization of differences between individual mice within each test group. For example, because of the higher light output of the TDG-Luc cells, a very short exposure was used for the TDG tumors.

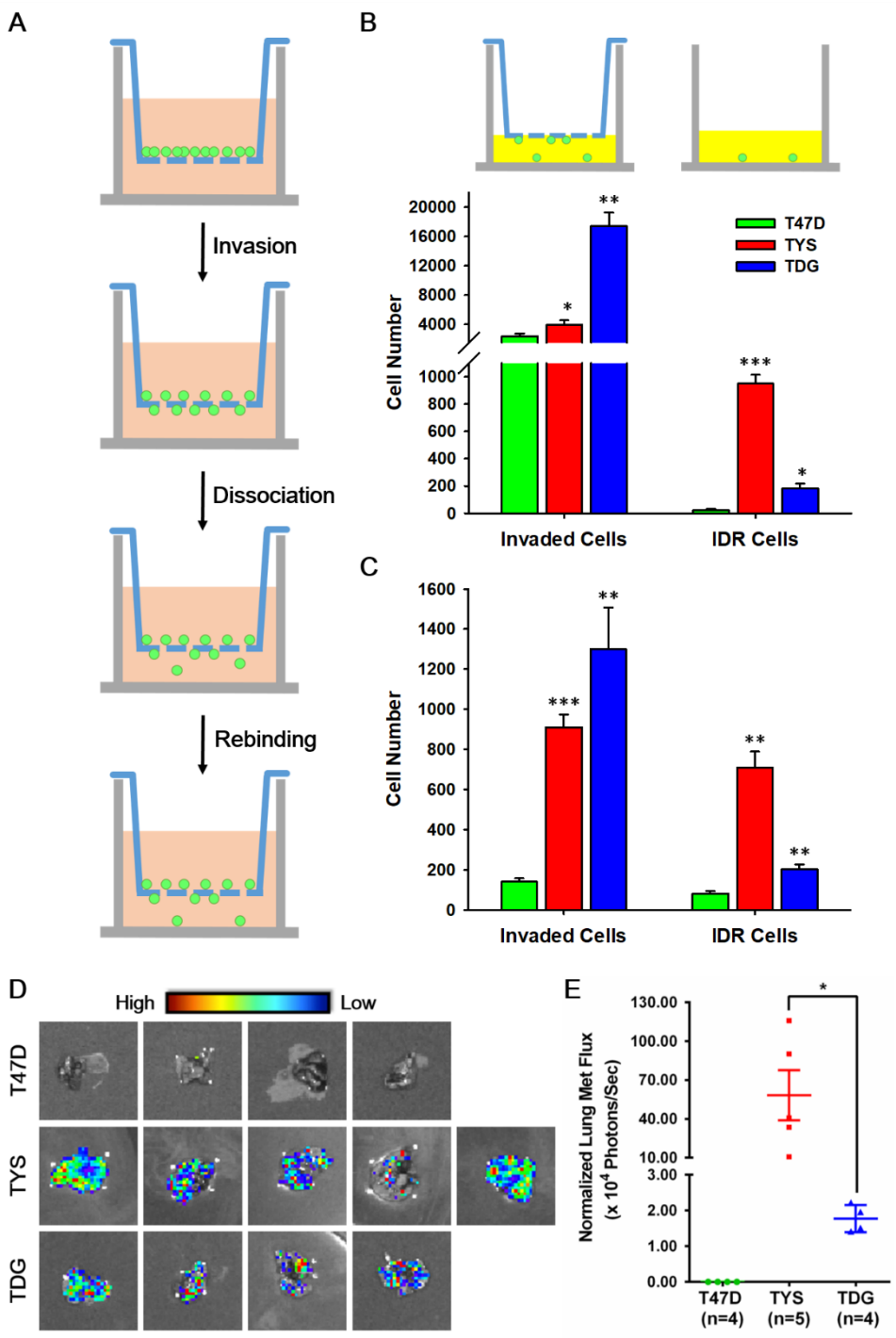

Figure 2.6 ERα Y537S and D538G mutations increase breast cell invasiveness and promote a metastatic phenotype. A Schematic of the invasion-dissociation-rebinding (IDR) assay. **B** The upper panel illustrates measurement of total invaded cells and IDR (invaded then dissociated and rebound) cells. IDR assay of T47D, TYS and TDG cells with collagen- **B** or matrigel-coated **C** membranes and chambers (n=5). Cell number

Figure 2.6 (cont.) calculated from a standard curve of light units (luciferase activity) versus cell number for each cell line. **D** *Ex vivo* imaging of excised lungs from xenograft bearing mice. As shown in the High to Low spectrum band, white dots are not bioluminescent signals. E Quantification of the bioluminescent signal in the lung areas shown in Fig. 2D. Shown as mean flux ± s.e.m.. The fluxes of lung metastases were normalized for the emission efficiency determined by tumor flux/ tumor weight. Similar results were obtained when the data was calculated as lung flux/ primary breast tumor flux. * Indicates a significant difference among groups using student t test. *P<0.05, **P<0.005, ***P<0.001. ns, not significant.

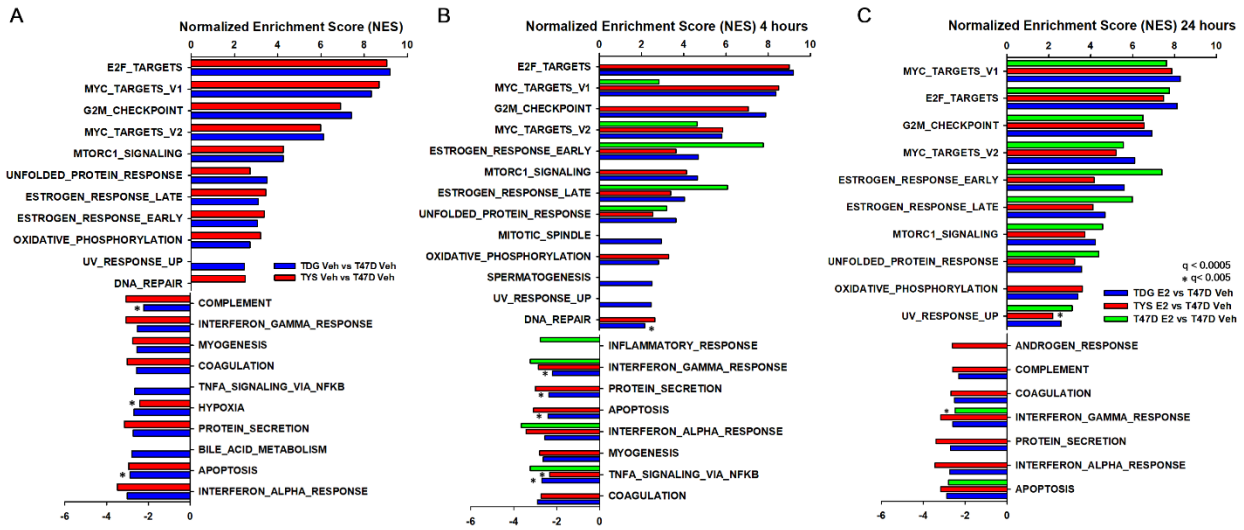

Figure 2.7 Estrogen upregulated pathways are constitutively activated in TYS and TDG cells. Gene set enrichment analysis (GSEA) using the 'hallmark gene set' as the reference dataset. The bar chart shows the normalized enrichment scores (NES) of pathways that are significantly up- or down-regulated in pair-wise comparisons between vehicle **A** 4h E_2 **B** and 24h E_2 **C** treated T47D, TYS and TDG cells and vehicle-treated T47D cells. All pathways had a false discovery rate q<0.0005 except those marked *, which were q<0.005.

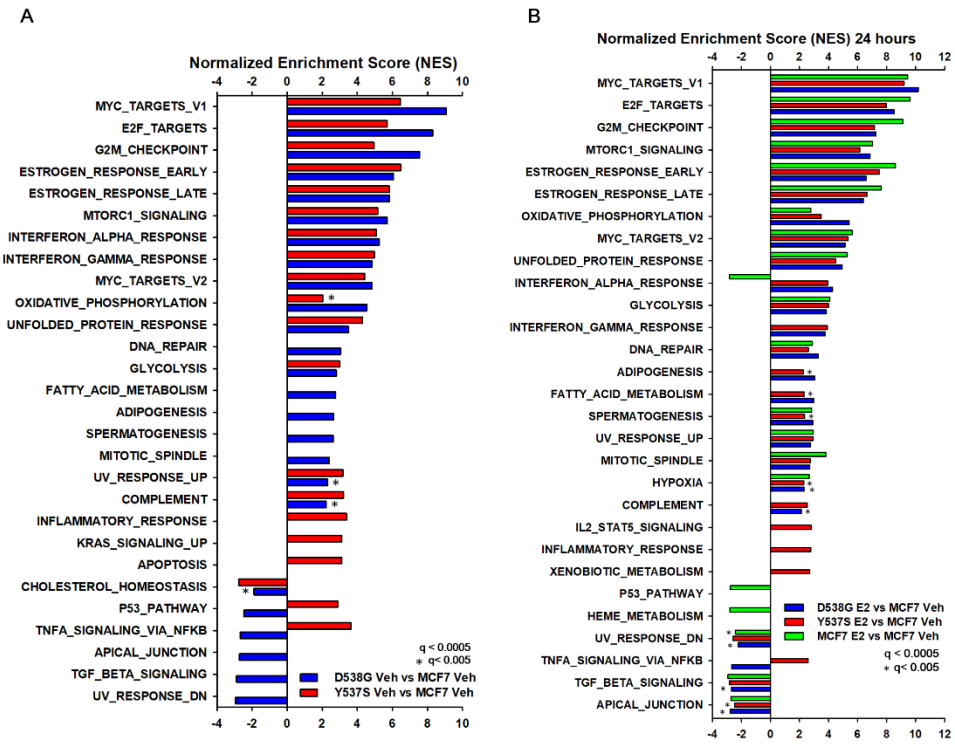

Figure 2.8 Estrogen upregulated pathways are constitutively activated in the MCF7-Y537S and MCF7-D538G cells. Gene set enrichment analysis (GSEA) using the 'hallmark gene set' as the reference dataset. The bar chart shows the normalized enrichment scores (NES) of pathways that are significantly up- or down-regulated in pair-wise comparisons between vehicle **A** and 24h E_2 **B** treated MCF7, MCF7-Y537S and MCF7-D538G cells and vehicle-treated MCF7 cells. All pathways had a false discovery rate q<0.0005 except those marked *, which were q<0.005.

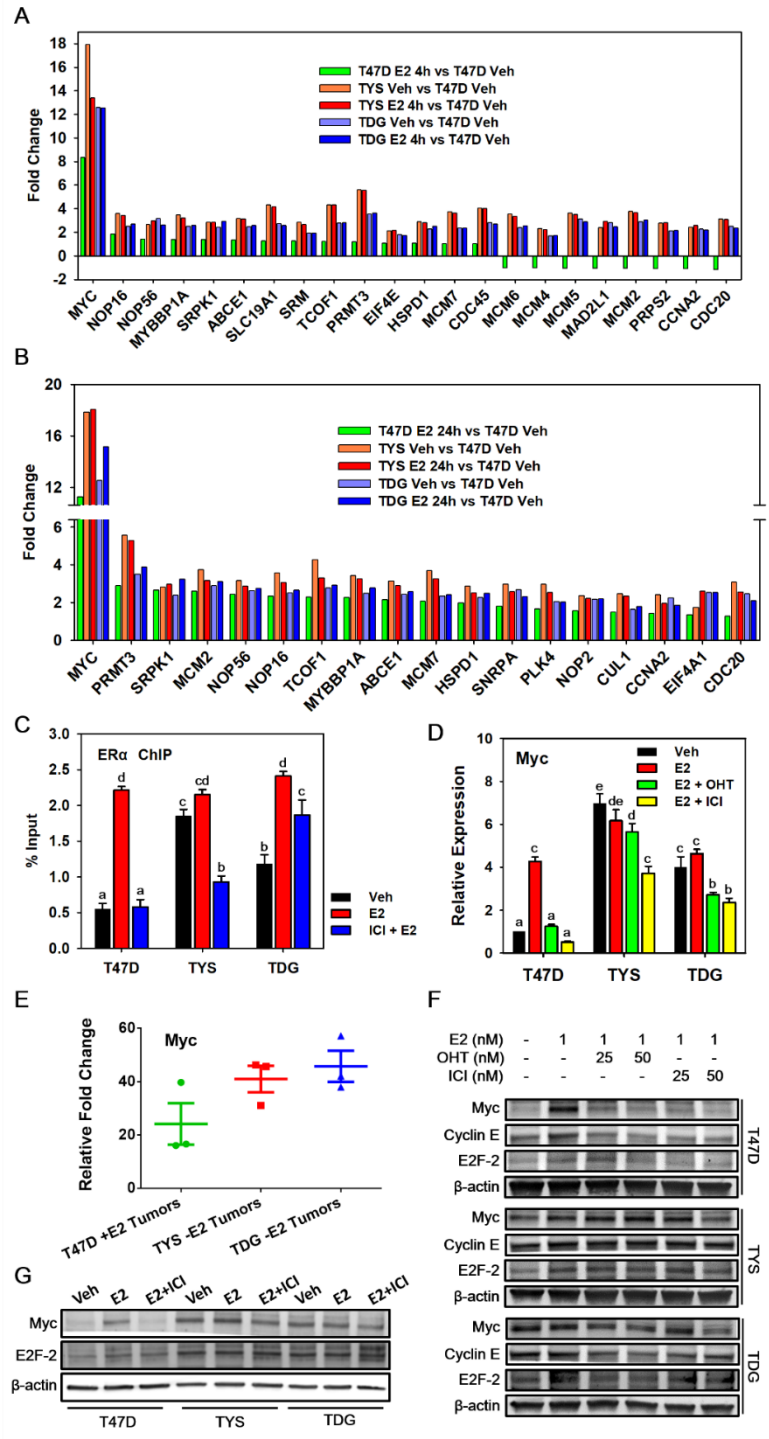

Figure 2.9 Myc is overexpressed and contributes to antiestrogen resistance in TYS and TDG cells. A,B Bar charts showing the RNAseq mean fold change of Myc target genes in T47D, TYS and TDG cells after addition of E_2 for 4h **A** or 24h **B**. **C** ChIP was performed in T47D, TYS and TDG cells treated with or without 500 nM fulvestrant/ICI for

Figure 2.9 (cont.) 10 min before adding 10 nM E_2 for 30 min. Real-time PCR was used to analyze the enrichment of ERα binding sites at the Myc enhancer region.(51) **D** qRT-PCR analysis of *Myc* mRNA levels in T47D and mutant cells after treatment for 24h with 1 nM E_2, 1 nM E_2 + 25 nM OHT, or 1 nM E_2 + 25 nM fulvestrant/ICI. **E** qRT- PCR analysis of *Myc* mRNA levels in tumors induced with estrogen (T47D) or without added estrogen (TYS and TDG). **C,D,E** Mean ± s.e.m., n=3. Different letters indicate a significant difference among groups ($p < 0.05$) using one-way ANOVA followed by Tukey's *post hoc* test. **F** Western blot analysis of Myc, Cyclin E and E2F-2 levels in T47D, TYS and TDG cells after 24h in the indicated concentrations of vehicle, E_2, OHT and fulvestrant. **G** Western blot analysis of Myc and E2F-2 protein levels following 24h treatment with vehicle, or 1 nM E_2, with or without 50 nM fulvestrant.

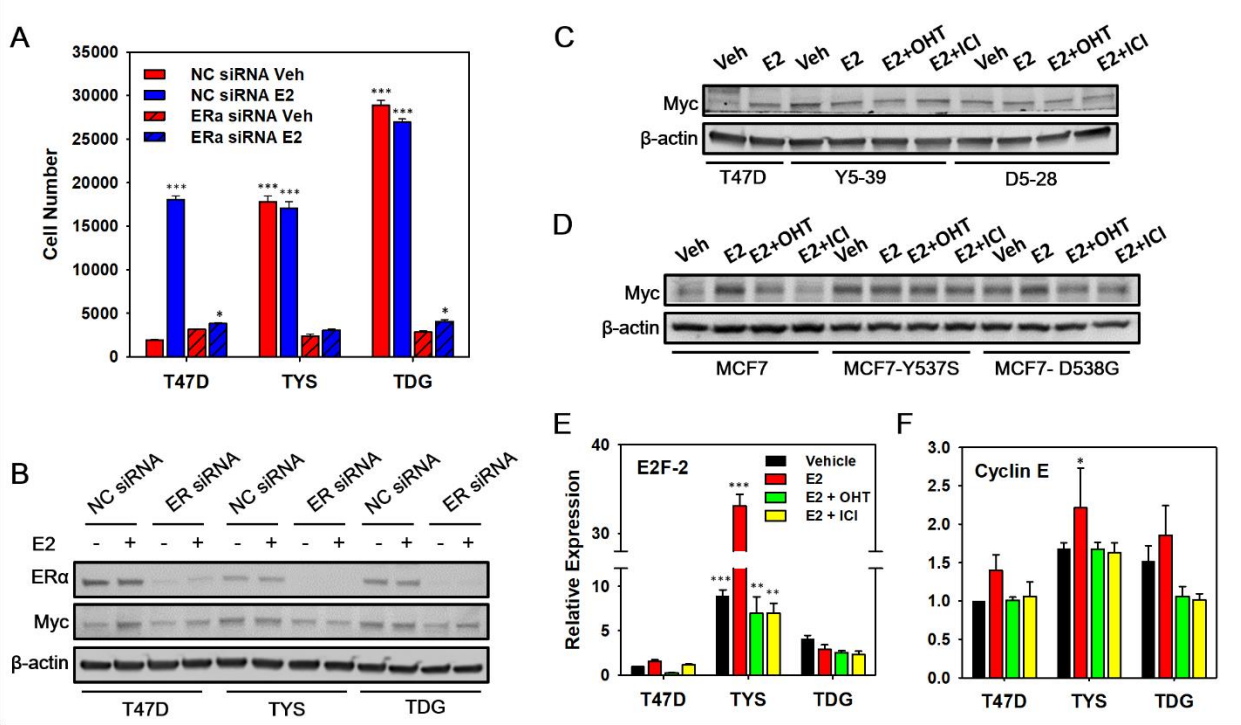

Figure 2.10 Myc expression is directly regulated by ERα and is partially antiestrogen-resistant in TYS and TDG cells. A Proliferation of T47D, TYS and TDG cells treated with 100 nM non-coding (NC) or ERα SMARTpool siRNA for 24h followed by treatment with vehicle or 1 nM E_2 for 96h (mean ± s.e.m., n=6). **B** Western blot analysis of ERα and Myc protein levels after treatment of T47D, TYS and TDG cells with 100 nM non-coding (NC) or ERα SMARTpool siRNA followed by treatment with vehicle or 1 nM E_2 for 24h. **C,D** Western blot analysis of Myc levels in T47D, T47D-ERαY537S (clone 39) and T47D-ERαD538G (clone 28) cells **C** and in MCF7, MCF7-Y537S and MCF7-D538G cells **D** after 24h treatment with vehicle, 1 nM E_2, 50 nM OHT and 50 nM fulvestrant. **E** qRT-PCR analysis of E2F-2 and **F** Cyclin E mRNA levels in T47D and mutant cells after treatment with 1 nM E_2, 1 nM E_2 + 25 nM OHT, or 1 nM E_2 + 25 nM ICI for 24h. * indicates a significant difference among groups using one-way ANOVA followed by Tukey's *post hoc* test. *P<0.05, **P<0.005, ***P<0.001.

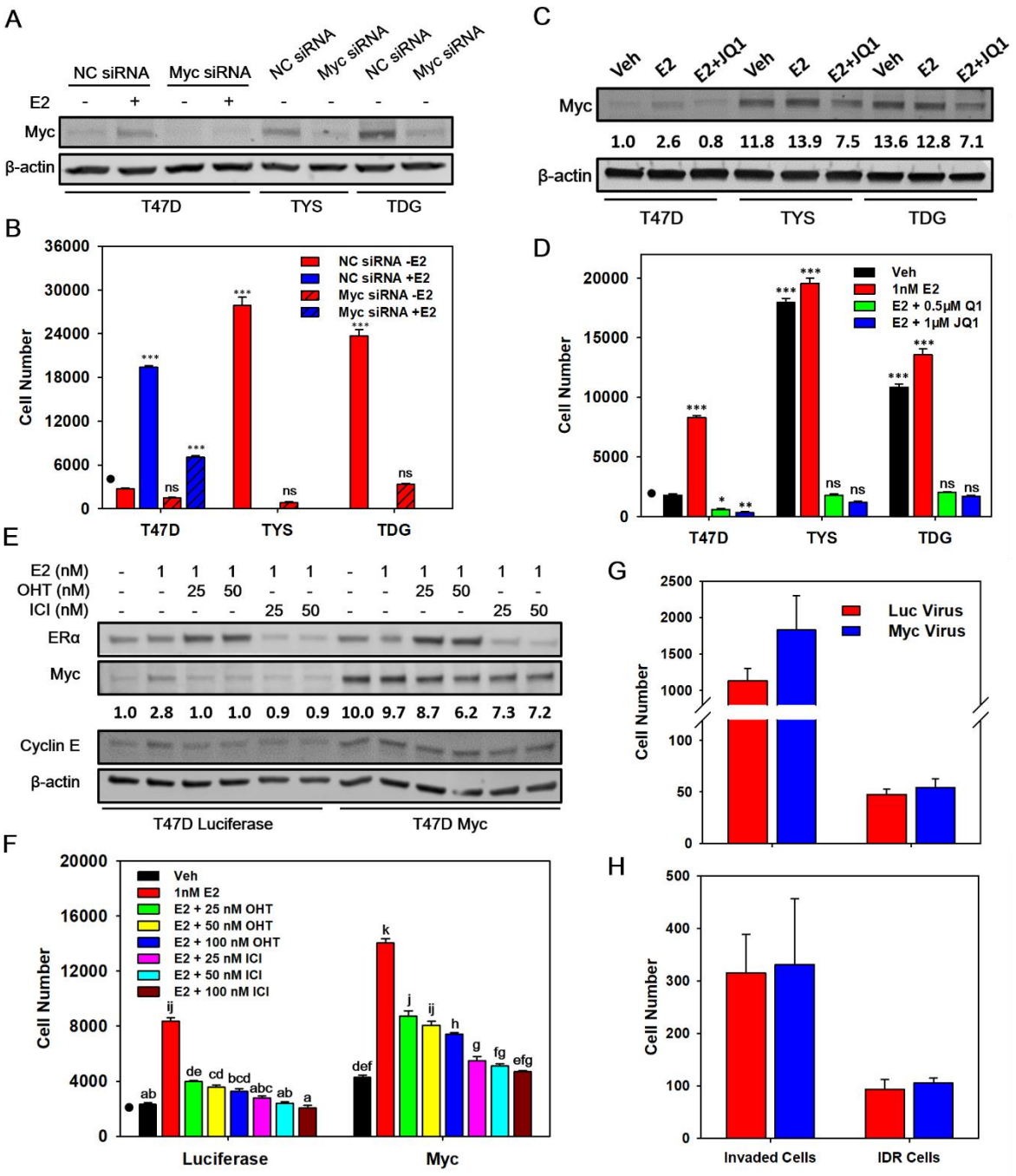

Figure 2.11 Myc is necessary and sufficient for estrogen-independent cell proliferation and antiestrogen resistance, but does not affect invasiveness. A Western blot showing Myc protein levels after treatment of T47D, TYS and TDG cells with 100 nM non-coding (NC) or Myc SMARTpool siRNA for 24h, followed by treatment with vehicle or 1 nM E_2 for 24h. **B** Proliferation of T47D, TYS and TDG cells treated with 100 nM NC or Myc SMARTpool siRNA, followed by treatment with vehicle or 1 nM E_2 for 96

Figure 2.11 (cont.) h (mean ± s.e.m., n=6). **C** Western blot showing Myc levels following treatment of cells with vehicle or 1 nM E_2 with, or without, 1 μM JQ1 for 8h. **D** Proliferation of T47D, TYS and TDG cells treated with vehicle, E_2, or E_2 plus 0.5 or 1 μM JQ1 for 96 h (mean ± s.e.m., n=6). **E** Western blot showing ERα, Myc and Cyclin E levels in T47D, TYS and TDG cells treated with Myc-lentivirus or control luciferase-lentivirus, followed by the indicated concentrations of E_2, OHT and ICI for 24h. **F** Proliferation of T47D, TYS and TDG cells, after transduction with Myc or control lentivirus containing medium for 24h, followed by treatment with the indicated concentrations of E_2, OHT and ICI for 4 days. (mean ± s.e.m., n=6). **B,D,F** '•' denotes cell number at day 0. **C,E** Myc protein levels were quantitated using a PhosphorImager and ImageQuant. **B,D** * indicates a significant difference among groups using one-way ANOVA followed by Tukey's *post hoc* test. *P<0.05, **P<0.005, ***P<0.001. ns, not significant. **F** Different letters indicate a significant difference among groups (P<0.05) using one-way ANOVA followed by Tukey's *post hoc* test. **G,H** IDR assay of T47D cells transduced with Myc-lentivirus or luciferase-lentivirus with collagen- **G** or matrigel-coated **H** membrane and chamber (mean ± s.e.m., n=5). Cells were transduced with virus and after 1 day total invaded cells and cells that invaded, then dissociated and rebound (IDR) were measured using their luciferase activity and a standard curve for each cell line of luciferase activity versus cell number.

Table 2.1

Software and reference genome used for RNAseq analysis.

Software and Reference	Version
STAR aligner	2.5.1b
Ensembl genome annotation	GRch38.88
Subread (featureCounts)	1.5.0
edgeR	3.16.5
GSEA	2.2.4

Table 2.2

Antibodies used in the immunoblot analysis.

Target protein	Catalog number	Manufacturer
c-Myc	sc-40	Santa Cruz
ERα	sc-8002	Santa Cruz
E2F-2	sc-9967	Santa Cruz
Cyclin E	sc-247	Santa Cruz
β-actin	A1978	Sigma-Aldrich

Table 2.3

Differentially regulated genes in T47D, TYS and TDG cells after estrogen treatment. Genes with fold change > 2 and false discovery rate < 0.05 were analyzed and numbers of genes in each category are shown.

Cell/ Treatment	Gene numbers		
	Up	Down	Total
T47D E_2 4h	245	72	317
T47D E_2 24h	809	939	1748
TYS	1469	2200	3669
TYS E_2 4h	1479	2191	3670
TYS E_2 24h	1373	1919	3292
TDG	992	1600	2592
TDG E_2 4h	1070	1732	2802
TDG E_2 24h	1093	1648	2741

REFERENCES

1. Clark GM, Osborne CK, McGuire WL. Correlations between estrogen receptor, progesterone receptor, and patient characteristics in human breast cancer. J Clin Oncol. 1984;2(10):1102-9.

2. Fisher B, Costantino JP, Wickerham DL, Redmond CK, Kavanah M, Cronin WM, et al. Tamoxifen for prevention of breast cancer: report of the National Surgical Adjuvant Breast and Bowel Project P-1 Study. J Natl Cancer Inst. 1998;90(18):1371-88.

3. Howell A, Robertson JF, Quaresma Albano J, Aschermannova A, Mauriac L, Kleeberg UR, et al. Fulvestrant, formerly ICI 182,780, is as effective as anastrozole in postmenopausal women with advanced breast cancer progressing after prior endocrine treatment. J Clin Oncol. 2002;20(16):3396-403.

4. Dowsett M, Cuzick J, Ingle J, Coates A, Forbes J, Bliss J, et al. Meta-analysis of breast cancer outcomes in adjuvant trials of aromatase inhibitors versus tamoxifen. J Clin Oncol. 2009;28(3):509-18.

5. Musgrove EA, Sutherland RL. Biological determinants of endocrine resistance in breast cancer. Nat Rev Cancer. 2009;9(9):631-43.

6. Alluri PG, Speers C, Chinnaiyan AM. Estrogen receptor mutations and their role in breast cancer progression. Breast Cancer Res. 2014 Dec 12;16(6):494.

7. Robinson DR, Wu Y-M, Vats P, Su F, Lonigro RJ, Cao X, et al. Activating ESR1 mutations in hormone-resistant metastatic breast cancer. Nat Genet. 2013;45(12):1446-51.

8. Gu G, Fuqua SA. ESR1 mutations in breast cancer: proof-of-concept challenges clinical action. Clin Cancer Res. 2016;22(5):1034-6.

9. Jeselsohn R, Yelensky R, Buchwalter G, Frampton G, Meric-Bernstam F, Gonzalez-Angulo AM, et al. Emergence of constitutively active estrogen receptor-α mutations in pretreated advanced estrogen receptor–positive breast cancer. Clin Cancer Res. 2014;20(7):1757-67.

10. Sefrioui D, Perdrix A, Sarafan-Vasseur N, Dolfus C, Dujon A, Picquenot JM, et al. monitoring ESR1 mutations by circulating tumor DNA in aromatase inhibitor resistant metastatic breast cancer. Int J Cancer. 2015;137(10):2513-9.

11. Mao C, Livezey M, Kim JE, Shapiro DJ. Antiestrogen Resistant Cell Lines Expressing Estrogen Receptor α Mutations Upregulate the Unfolded Protein Response and are Killed by BHPI. Scientific Reports. 2016 Oct 7
6:34753.

12. Martin L-A, Ribas R, Simigdala N, Schuster E, Pancholi S, Tenev T, et al. Discovery of naturally occurring ESR1 mutations in breast cancer cell lines modelling endocrine resistance. Nat Commun. 2017;8:1865.

13. Harrod A, Fulton J, Nguyen VT, Periyasamy M, Ramos-Garcia L, Lai C-F, et al. Genomic modelling of the ESR1 Y537S mutation for evaluating function and new therapeutic approaches for metastatic breast cancer. Oncogene. 2017 Apr 20;36(16):2286-96.

14. Bahreini A, Li Z, Wang P, Levine KM, Tasdemir N, Cao L, et al. Mutation site and context dependent effects of ESR1 mutation in genome-edited breast cancer cell models. Breast Cancer Res. 2017;19(1):60.

15. Jeselsohn R, Bergholz JS, Pun M, Cornwell M, Liu W, Nardone A, et al. Allele-specific chromatin recruitment and therapeutic vulnerabilities of ESR1 activating mutations. Cancer Cell. 2018;33(2):173-86. e5.

16. Gelsomino L, Panza S, Giordano C, Barone I, Gu G, Spina E, et al. Mutations in the estrogen receptor alpha hormone binding domain promote stem cell phenotype through notch activation in breast cancer cell lines. Cancer Lett. 2018;428:12-20.

17. Fanning SW, Mayne CG, Dharmarajan V, Carlson KE, Martin TA, Novick SJ, et al. Estrogen receptor alpha somatic mutations Y537S and D538G confer breast cancer endocrine resistance by stabilizing the activating function-2 binding conformation. Elife. 2016;5:e12792.

18. Chandarlapaty S, Chen D, He W, Sung P, Samoila A, You D, et al. Prevalence of ESR1 mutations in cell-free DNA and outcomes in metastatic breast cancer: a secondary analysis of the BOLERO-2 clinical trial. JAMA oncology. 2016;2(10):1310-5.

19. Harrod A, Fulton J, Nguyen VTM, Periyasamy M, Ramos-Garcia L, Lai CF, et al. Genomic modelling of the ESR1 Y537S mutation for evaluating function and new therapeutic approaches for metastatic breast cancer. Oncogene. 2017 Apr 20;36(16):2286-96. PubMed PMID: 27748765. Pubmed Central PMCID: PMC5245767. Epub 2016/10/18. eng.

20. Gates LA, Gu G, Chen Y, Rohira AD, Lei JT, Hamilton RA, et al. Proteomic proiling identiies key coactivators utilized by mutant ERα proteins as potential new therapeutic targets. 2018.

21. Gabay M, Li Y, Felsher DW. MYC activation is a hallmark of cancer initiation and maintenance. Cold Spring Harb Perspect Med. 2014;4(6):a014241.

22. Kress TR, Sabò A, Amati B. MYC: connecting selective transcriptional control to global RNA production. Nat Rev Cancer. 2015;15(10):593-607.

23. Li L, Osdal T, Ho Y, Chun S, McDonald T, Agarwal P, et al. SIRT1 activation by a c-MYC oncogenic network promotes the maintenance and drug resistance of human FLT3-ITD acute Myeloid Leukemia stem cells. Cell stem cell. 2014;15(4):431-46.

24. Yang X, Cai H, Liang Y, Chen L, Wang X, Si R, et al. Inhibition of c-Myc by let-7b mimic reverses mutidrug resistance in gastric cancer cells. Oncol Rep. 2015;33(4):1723-30.

25. Shajahan-Haq AN, Cook KL, Schwartz-Roberts JL, Eltayeb AE, Demas DM, Warri AM, et al. MYC regulates the unfolded protein response and glucose and glutamine uptake in endocrine resistant breast cancer. Mol Cancer. 2014;13(1):239.

26. Ladanyi M, Park CK, Lewis R, Jhanwar SC, Healey JH, Huvos AG. Sporadic amplification of the MYC gene in human osteosarcomas. Diagn Mol Pathol. 1993;2(3):163-7.

27. Schneider-Stock R, Boltze C, Jäger V, Epplen J, Landt O, Peters B, et al. Elevated telomerase activity, c-MYC-, and hTERT mRNA expression: association with tumour progression in malignant lipomatous tumours. J Pathol. 2003;199(4):517-25.

28. Escot C, Theillet C, Lidereau R, Spyratos F, Champeme M-H, Gest J, et al. Genetic alteration of the c-myc protooncogene (MYC) in human primary breast carcinomas. Proc Natl Acad Sci. 1986;83(13):4834-8.

29. Yu L, Andruska N, Zheng X, Shapiro DJ. Anticipatory Activation of the Unfolded Protein Response by Epidermal Growth Factor is Required for Immediate Early Gene Expression and Cell Proliferation. Mol Cell Endocrinol. 2016;422:31-41.

30. Krieg AJ, Krieg SA, Ahn BS, Shapiro DJ. Interplay between estrogen response element sequence and ligands controls in vivo binding of estrogen receptor to regulated genes. J Biol Chem. 2004;279(6):5025-34.

31. Pedraz-Cuesta E, Fredsted J, Jensen HH, Bornebusch A, Nejsum LN, Kragelund BB, et al. Prolactin Signaling Stimulates Invasion via Na+/H+ Exchanger NHE1 in T47D Human Breast Cancer Cells. Mol Endocrinol. 2016;30(7):693-708.

32. Platet N, Garcia M. A new bioassay using transient transfection for invasion-related gene analysis. Invasion and Metastasis. 1998;18(4):198-208.

33. Kosicki M, Tomberg K, Bradley A. Repair of double-strand breaks induced by CRISPR–Cas9 leads to large deletions and complex rearrangements. Nat Biotechnol. 2018.

34. Murthy MS, Scanlon EF, Jelachich ML, Klipstein S, Goldschmidt RA. Growth and metastasis of human breast cancers in athymic nude mice. Clin Exp Metastasis. 1995;13(1):3-15.

35. Walsh MD, Luckie SM, Cummings MC, Antalis TM, McGuckin MA. Heterogeneity of MUC1 expression by human breast carcinoma cell lines in vivo and in vitro. Breast cancer research and treatment. 1999;58(3):253-64.

36. Malta TM, Sokolov A, Gentles AJ, Burzykowski T, Poisson L, Weinstein JN, et al. Machine learning identifies stemness features associated with oncogenic dedifferentiation. Cell. 2018;173(2):338-54. e15.

37. Delmore JE, Issa GC, Lemieux ME, Rahl PB, Shi J, Jacobs HM, et al. BET bromodomain inhibition as a therapeutic strategy to target c-Myc. Cell. 2011;146(6):904-17.

38. Mertz JA, Conery AR, Bryant BM, Sandy P, Balasubramanian S, Mele DA, et al. Targeting MYC dependence in cancer by inhibiting BET bromodomains. Proc Natl Acad Sci. 2011;108(40):16669-74.

39. Merenbakh-Lamin K, Ben-Baruch N, Yeheskel A, Dvir A, Soussan-Gutman L, Jeselsohn R, et al. D538G mutation in estrogen receptor-α: a novel mechanism for acquired endocrine resistance in breast cancer. Cancer Res. 2013;73(23):6856-64.

40. Toy W, Shen Y, Won H, Green B, Sakr RA, Will M, et al. ESR1 ligand-binding domain mutations in hormone-resistant breast cancer. Nat Genet. 2013;45(12):1439-45.

41. Takeshita T, Yamamoto Y, Yamamoto-Ibusuki M, Inao T, Sueta A, Fujiwara S, et al. Droplet digital polymerase chain reaction assay for screening of ESR1 mutations in 325 breast cancer specimens. Transl Res. 2015;166(6):540-53. e2.

42. Wang P, Bahreini A, Gyanchandani R, Lucas PC, Hartmaier RJ, Watters RJ, et al. Sensitive detection of mono-and polyclonal ESR1 mutations in primary tumors, metastatic lesions, and cell-free DNA of breast cancer patients. Clin Cancer Res. 2016;22(5):1130-7.

43. Sears R, Ohtani K, Nevins JR. Identification of positively and negatively acting elements regulating expression of the E2F2 gene in response to cell growth signals. Mol Cell Biol. 1997;17(9):5227-35.

44. Pérez-Roger I, Solomon DL, Sewing A, Land H. Myc activation of cyclin E/Cdk2 kinase involves induction of cyclin E gene transcription and inhibition of p27 Kip1 binding to newly formed complexes. Oncogene. 1997;14(20).

45. Gartel AL, Ye X, Goufman E, Shianov P, Hay N, Najmabadi F, et al. Myc represses the p21 (WAF1/CIP1) promoter and interacts with Sp1/Sp3. Proc Natl Acad Sci. 2001;98(8):4510-5.

46. Bretones G, Delgado MD, León J. Myc and cell cycle control. Biochim Biophys Acta. 2015;1849(5):506-16.

47. Venditti M, Iwasiow B, Orr FW, Shiu RP. C-myc gene expression alone is sufficient to confer resistance to antiestrogen in human breast cancer cells. Int J Cancer. 2002;99(1):35-42.

48. Miller TW, Balko JM, Ghazoui Z, Dunbier A, Anderson H, Dowsett M, et al. A gene expression signature from human breast cancer cells with acquired hormone independence identifies MYC as a mediator of antiestrogen resistance. Clin Cancer Res. 2011;17(7):2024-34.

49. Andruska N, Zheng X, Yang X, Helferich WG, Shapiro DJ. Anticipatory estrogen activation of the unfolded protein response is linked to cell proliferation and poor survival in estrogen receptor alpha-positive breast cancer. Oncogene. 2015 Jul;34(29):3760-9. PubMed PMID: 25263449. Pubmed Central PMCID: PMC4377305. Epub 2014/09/30. eng.

50. Zheng X, Andruska N, Lambrecht MJ, He S, Parissenti A, Hergenrother PJ, et al. Targeting multidrug-resistant ovarian cancer through estrogen receptor α dependent ATP depletion caused by hyperactivation of the unfolded protein response. Oncotarget. 2018;9(19):14741.

51. Roderick JE, Tesell J, Shultz LD, Brehm MA, Greiner DL, Harris MH, et al. c-Myc inhibition prevents leukemia initiation in mice and impairs the growth of relapsed and induction failure pediatric T-ALL cells. Blood. 2014;123(7):1040-50.

CHAPTER 3

ANTICIPATORY ACTIVATION OF THE UNFOLDED PROTEIN RESPONSE BY EPIDERMAL GROWTH FACTOR IS REQUIRED FOR IMMEDIATE EARLY GENE EXPRESSION AND CELL PROLIFERATION [2]

ABSTRACT

The onco-protein epidermal growth factor (EGF) initiates a cascade that includes activation of the ERK and AKT signaling pathways and alters gene expression. We describe a new action of EGF-EGF receptor (EGFR), rapid anticipatory activation of the endoplasmic reticulum stress sensor, the unfolded protein response (UPR). Within 2 min., EGF elicits EGFR dependent activation of phospholipase C γ (PLCγ), producing inositol triphosphate (IP3), which binds to IP3 receptor (IP3R), opening the endoplasmic reticulum IP3R Ca^{2+} channels, resulting in increased intracellular Ca^{2+}. This calcium release leads to transient and moderate activation of the IRE1α and ATF6α arms of the UPR, resulting in induction of BiP chaperone. Knockdown or inhibition of EGFR, PLCγ or IP3R blocks the increase in intracellular Ca^{2+}. While blocking the increase in intracellular Ca^{2+} by locking the IP3R calcium channel with 2-APB had no effect on EGF activation of the ERK or AKT signaling pathways, it abolished the rapid EGF-mediated induction and repression of gene expression. Knockdown of ATF6α or XBP1, which regulate UPR-induced chaperone production, inhibited EGF stimulated cell proliferation. Supporting biological

[2] This chapter appeared in its entirety in *Molecular and Cellular Endocrinology*. Yu, L. *et al.* (2016) Anticipatory activation of the unfolded protein response by epidermal growth factor is required for immediate early gene expression and cell proliferation. *Molecular and cellular endocrinology*, 422, 31-41. Data in Figures 3.3 (C), 3.5 (A,B), 3.8 (A,B,H), 3.11 and Table 3.1 was obtained by Dr. Neal Andruska. Data in Figure 3.8 (C,D,E) was obtained by Dr. Xiaobin Zheng.

relevance, increased levels of EGF receptor during tumor progression were correlated with increased expression of the UPR gene signature. Anticipatory activation of the UPR is a new role for EGF. Since UPR activation occurs in <2 minutes, it is an initial cell response when EGF binds EGFR.

INTRODUCTION

Epidermal growth factor (EGF) stimulates cell proliferation and tumor growth by binding to a family of epidermal growth-factor receptors (EGFRs). The EGFR family consists of four members: ErbB1 (EGFR), ErbB2 (HER2/neu), ErbB3, and ErbB4 (1). Binding of EGF to EGFR leads to formation of activated EGFR dimer, which exhibits increased autophosphorylation. Phosphorylated EGFR activates several cell signaling pathways, including the ERK and AKT pathways and rapidly alters gene expression. The activated signaling pathways and altered gene expression program promote cell proliferation and invasion, and are anti-apoptotic (2).

EGF receptor is overexpressed in many human cancers including lung, pancreatic, brain, bladder, and breast cancer (3-5). EGFR is expressed in most breast cancers and is overexpressed in ~50% of triple-negative ($ER\alpha^-$, PR^-, and $HER2/neu^-$) breast cancers and in highly-aggressive invasive breast cancer (IBC) (6-8). EGFR overexpression is associated with larger tumors, poor differentiation, and poor clinical outcome (2, 9, 10). Activated EGFR reduces sensitivity to anticancer drugs. Although, responses to EGFR inhibitors given alone were modest (11-13), sustained inhibition of EGFR with erlotinib led to increased doxorubicin response and death of triple-negative breast tumors (14).

This suggests that EGFR inhibitors may enhance chemosensitivity of breast tumors to cytotoxic agents.

The ability of EGF-EGFR to reduce sensitivity to anticancer drugs suggested activated EGFR might alter responses to chemotherapy-induced stress by influencing the activity of stress response pathways. The sensor system for endoplasmic reticulum stress is the unfolded protein response. In the well-studied “reactive” mode of UPR activation, UPR sensors react to an excess of unfolded or misfolded protein, metabolic stress or anticancer drugs by activating signaling pathways that increase protein-folding capacity and reduce protein production (15, 16). Moderate activation of the UPR is protective. Consistent with the protective role of the UPR, a correlation between UPR activation and resistance to therapy has been described for several cancers (17-21). It was widely accepted that UPR activation in tumors arose by clonal evolution and selection of cells that survived in part because they responded to therapy-induced stress by activating the UPR (22, 23). In contrast to this well-known “reactive” mode of UPR activation, a little studied alternative mode of UPR activation termed “anticipatory” UPR activation occurs in the absence of endoplasmic reticulum stress (16). Anticipatory UPR activation was initially described in B-cells. Differentiation factors interleukin 4 and lipopolysaccharide induce UPR activation in B lymphocytes prior to increased immunoglobulin synthesis. Very recent studies demonstrate that estrogen in humans (24), ecdysone in insects (25, 26) and human vascular endothelial growth factor (VEGF) (27) elicit biologically significant anticipatory activation of the UPR. Bioinformatic studies indicate that anticipatory estrogen activation of the UPR occurs early in breast cancer development, prior to detection and initiation of therapy (24).

Many, but not all, mitogenic hormones elicit anticipatory activation of the UPR as an early event in the proliferation program. We therefore tested whether EGF elicits anticipatory activation of the UPR and whether rapid activation of the anticipatory UPR pathway is important for subsequent actions of EGF-EGFR. We demonstrate EGF-EGFR-mediated rapid anticipatory activation of the UPR through activation of phospholipase C γ (PLCγ), resulting in increased production of inositol triphosphate (IP_3). The IP_3 binds to and opens endoplasmic reticulum IP_3 receptors (IP_3R) leading to rapid efflux of calcium stored in the lumen of the endoplasmic reticulum into the cytosol. This activates the UPR, resulting in induction of the anti-apoptoptic chaperone BiP/GRP78/HSPA5 (28). Although intracellular calcium was increased in ~1 min., blocking the increase in intracellular calcium did not inhibit subsequent EGF-EGFR activation of the ERK and AKT signaling pathways. However, blocking the increase in intracellular calcium completely inhibited EGF-EGFR induction of pro-proliferation immediate early gene expression and reversed EGF-EGFR mediated down-regulation of pro-apoptotic genes. Moreover, knockdown of the chaperone-inducing arms of the UPR strongly inhibited EGF stimulated cell proliferation. Anticipatory activation of the UPR is a newly revealed early action of EGF-EGFR with very different effects on plasma membrane and nuclear EGF-EGFR-regulated pathways.

MATERIALS AND METHODS

Cell Culture

MDA MB-468 cells were maintained in phenol-red free DMEM/F12, supplemented with 10% fetal bovine serum ([FBS], Atlanta Biological, Atlanta, GA). MCF10A cells were

maintained in DMEM/F12, supplemented with 2% charcoal-dextran (cd)-stripped FBS. MCF10A cells were supplemented with 0.5 μg/ml hydrocortisone, 10 μg/ml insulin, 20 ng/ml epidermal growth factor (EGF), and 0.1 μg/ml cholera toxin. HCC1954 cells were maintained in RPMI1640, supplemented with 10% FBS. T47D cells were maintained in MEM, supplemented with 10% FBS. Estrogens were removed from the medium by maintaining T47D cells for at least three days in 10% charcoal dextran treated FBS (cd-FBS), and cells were plated in MEM containing 10% cd-calf serum.

Cell Proliferation Assays

Cell proliferation assays were carried out as described (24, 29). Briefly, cells were plated in 96-well plates at the following densities: MDA MB-468 (2,000 cells/well), T47D (2,000 cells/well), MCF10A (1,000 cells/well), and HCC-1954 (2,000 cells/well). Cell viability was determined using CellTiter 96® Aqueous One Solution Cell Proliferation Assay (MTS, Promega, WI). Cell number was determined from a standard curve of absorbance versus cell number for each cell line.

Luciferase Assay

Luciferase assay were as previously described (30). Hela cells were plated (300,000 cells/well in 1 ml) in 6-well plates in 10% CD-CS 3 days before transfection. On the day of transfection, the medium was changed to 0.2 ml of Opti-MEM (Invitrogen). DNA and Lipofectamine 3000 (Invitrogen) were diluted in Opti-MEM. A total of 2500 ng of DNA (1260 ng of XBP1-Luc, 40 ng Renilla-Luc and 1200 ng IP3 phosphatase or PTZ carrier) was transfected into each well at a DNA:Lipofectamine 3000 ratio of 1:1. 24 h after

transfection, 20 ng/ml EGF was added and the cells were incubated for 24 h. Cells were then lysed in 100 µl of passive lysis buffer (Promega), and luciferase activity was determined using a Dual-Luciferase Reporter Assay (Promega #E1910). XBP1-Luc and Renilla-Luc plasmids were constructed and modified by our lab. The IP3 phosphatase plasmid was previously described (31), and was generously provided by Dr. Mark Shapiro (University of Texas Health Science Center).

Western Blots

Western blotting was carried out as previously described (2, 5). Briefly, whole cell extracts were prepared using RIPA lysis buffer (Millipore, CA) and mini protease inhibitor mixture (Roche Applied Science, Germany). Bound antibodies were detected using horseradish peroxidase-conjugated secondary antibodies and chemiluminescent immunodetection. The following antibodies from Cell Signaling Technology (MA) were used: Phospho-eIF2α (Ser51) (#3398), eIF2α (#5324), Phospho-AKT (Thr308) (#13038P), AKT (#9272S) Phospho-p44/42 MAPK (#4370), p44/42 MAPK (#4695), BiP (#3177). Other antibodies used: pan-IP_3R (sc-28613; Santa Cruz Biotechnology), ATF6α (Imgenex, CA), β-Actin (Sigma, Saint Louis, MO), and α-Tubulin (Sigma, Saint Louis MO).

qRT-PCR Analysis

Cells were seeded into 6-well plates and grown to ~70% confluence. For EGF regulated gene expression assays, cells were washed two times with HEPES buffer (140 mM NaCl, 4.7 mM KCl, 1.13 mM MgCl2, 10 mM HEPES, 10 mM Glucose, pH = 7.4) and then incubated in medium containing 100 nM 2-APB (Sigma, Saint Louis MO) or 10 µM UO126

for 5 minutes at 37 °C before EGF treatment. Cells were treated with a saturating concentration (20 ng/ml) or a sub-saturating concentration (2 ng/ml) of EGF or vehicle-control for the indicated times, and RNA was extracted and purified using the Qiagen RNeasy kit. cDNA was prepared from 1 μg of RNA with M-MuLV reverse transcriptase from New England Biolabs. Diluted cDNA was used to perform quantitative RT-PCR using power SYBR® Green (Life technologies, NY) with actin as the internal control.

siRNA Knockdowns

siRNA knockdowns were performed using DharmaFECT1 Transfection Reagent and 100 nM ON-TARGETplus non-targeting pool or SMARTpools for PLCγ (PLCG1) or pan-IP3R (GE Healthcare, UK). The pan-IP_3R SmartPool consisted of three individual SmartPools, each at 33 nM, directed against each isoform of the IP_3R (ITPR1, ITPR2, and ITPR3).

Calcium Imaging

A calcium-sensitive dye, Fluo-4 AM, was used to measure cytoplasmic Ca^{2+}. Cells were grown on 35 mm fluorodish plates (World Precision Instruments, FL) for two days prior to experiments. Cells were loaded with 5 μM Fluo-4 AM (Life Technologies, NY) in calcium free HEPES buffer for 30 minutes at 37ºC. Cells were washed three times with the buffer and incubated for 10 minutes with either 2 mM $CaCl_2$ or without $CaCl_2$. Fluoresence was monitored for one minute to determine basal fluorescence intensity, and then the appropriate treatment was added. Measurements were taken using a Zeiss LSM 700 confocal microscope with a Plan-Four 20X objective (N.A. = 0.8) and 488-nM laser excitation (7% power). Images were obtained by monitoring fluorescence emission at 525

nM, and data analysis was performed using AxioVision and Zen software (Zeiss, Germany).

IP_3 Quantitation

MDA MB-468 cells were incubated for 10 minutes in 20 ng/ml EGF or vehicle. Intracellular IP_3 levels were determined by extracting cell lysate, and determining IP_3 levels in an assay based on competitive binding to a recombinant IP_3R fragment (Perkin Elmer, MA) that was saturated with ^3H-IP_3. Unlabeled IP_3 was used as a standard for the assays. $1.5x10^6$ MDA MB-468 cells were used in this assay and the protocol has been described recently (29).

Statistical Analysis

All data is reported as mean ± S.E.M. A two-tailed student's t-test is used for comparisons between groups. One-way ANOVA followed by LSD or Tukey's *post hoc* test is used for multiple comparisons with SPSS 13.0 for Windows (SPSS, Chicago, IL, USA). Significance was established when $p < 0.05$.

RESULTS

EGF Activates the UPR in Breast Cancer Cells

To assess whether EGF rapidly activates the UPR, we selected a diverse set of breast cancer cell lines with different expression levels of EGFR protein and different effects of EGF on cell proliferation. (*i*) ERα^+ T47D breast cancer cells express low levels of EGFR, and are EGF-dependent for cell proliferation (Fig. 1A) (29, 32); (*ii*) MCF10A

pre-tumorigenic breast cells grossly overexpress EGFR, express minimal levels of HER2/neu and are fully dependent on EGF for proliferation (Fig 1B); (*iii*) triple-negative MDA MB-468 breast cancer cells, grossly overexpress EGFR through gene amplification, and EGF does not stimulate their proliferation (Fig. 1C); and (*iv*) ERα^- HCC-1954 breast cancer cells, which overexpress equal amounts of EGFR and HER2/neu, and do not depend on EGF for cell proliferation (Fig. 1D) (33, 34).

To assess whether EGF activates the UPR, we focused on markers indicative of activation of each arm of the UPR (Fig. 2). The UPR regulates protein production by autophosphorylation of the transmembrane kinase, PERK (16, 35). p-PERK phosphorylates eukaryotic initiation factor 2α (eIF2α), resulting in transient inhibition of protein synthesis. The other UPR arms initiate with activation of the transcription factor ATF6α, leading to increased chaperone production and activation of the ER splicing factor IRE1α, which splices the transcription factor XBP1, leading to production of active spliced-XBP1, increased protein folding capacity and altered mRNA decay and translation (16, 35). We first assessed whether EGF could activate the IRE1α arm of the UPR. In response to UPR activation, active spliced-XBP1 (sp-XBP1) enters the nucleus and regulates expression of UPR targets (Fig. 2A). EGF rapidly activated the IRE1α arm of the UPR, as shown by increased splicing of XBP1 mRNA in T47D, MDA MB-468, HCC-1954 and MCF10A breast cancer cells (Fig. 3A). Pre-treating cells with the EGFR inhibitor, erlotinib, blocked EGF-induction of sp-XBP1 mRNA (Fig. 3B), demonstrating that activation of the IRE1α arm of the UPR is dependent on activation of EGFR. Although our primary focus was on EGF in breast cancer cells, EGF also activated the UPR in

HeLa cervical cancer cells as shown by activation of a transfected luciferase reporter activated by sp-XBP1 (Fig. 4).

We next evaluated whether EGF activates the ATF6α arm of the UPR. ATF6α activation involves release from the ER and transport to the Golgi apparatus where ATF6α undergoes proteolytic cleavage to form active p50-ATF6α (Fig. 2B) (16, 35, 36). Supporting rapid EGF activation the ATF6α arm of the UPR, EGF modestly increased proteolysis of ATF6α (Fig. 3C, Fig. 5B), which was blocked by pre-treatment with erolitinib (Fig. 5A).

p50-ATF6α regulates induction of BiP and other UPR-regulated chaperones (36, 37). Inducing BiP increases ER protein folding capacity, contributing to resolution of the stress, and helps reverse UPR activation (38). Overexpression of BiP is linked to a poor prognosis in breast and other cancers (39). EGF rapidly induced BiP mRNA in T47D, MDA MB-468, HCC-1954 and MCF10A breast cancer cells (Fig. 3D), leading to increases in BiP protein levels (Fig. 3F). Consistent with BiP induction being dependent on activation of EGFR, pre-treating MDA MB-468 cells with erlotinib blocked EGF-induction of BiP mRNA (Fig. 3E). While induction of BiP mRNA led to increases in BiP protein in T47D and MDA MB-468 cells (Fig. 3F), EGF did not increase BiP protein levels in pre-tumorigenic MCF10A cells (Fig. 5C). XBP1 can directly interact with and activate estrogen receptor α (40). Although the mechanism by which XBP1-ERα interaction might impact translation is unclear, this may provide an explanation for the different levels of BiP expression in estrogen receptor positive T47D cells and estrogen receptor negative MCF 10A cells. Alternatively, since BiP expression is elevated in breast cancer cells relative to surrounding normal tissue (41), the different stages of tumor development in non-

tumorigenic MCF10A cells compared to tumorigenic T47D and MDA-MB-468 cells may play a role.

Inducing BiP helps protect cancer cells against protein-misfolding and other forms of UPR stress (24). Extensive and sustained activation of the UPR is toxic. This enabled us to test whether prior exposure of MDA MB-468 cells to EGF or to a low concentration of the UPR activator tunicamycin (TUN) could alter the concentration of TUN required to subsequently induce cell death. Pretreating cells with EGF or with TUN increased the concentration of TUN required to induce cell death by ~2 fold (Fig. 6).

We next assessed whether EGF activates the PERK arm of the UPR. Activated PERK induces increased eIF2α phosphorylation (Fig. 2C). EGF induced a rapid increase in phosphorylation of eIF2α (Fig. 7A, B). Phosphorylation of eIF2α leads to preferential translation of ATF4 mRNA, and we observed a moderate and transient increase in ATF4 protein expression. In contrast, the toxic UPR activator, tunicamycin (TUN) robustly induced ATF4 (Fig. 7C, D). Because mild and transient activation of the PERK arm of the UPR does not induce the proapoptotic protein CHOP (24), CHOP was not induced by the EGF stimulated ATF4 (Fig. 7E, F). This data demonstrates that EGF elicits moderate and transient activation of all three arms of the UPR.

EGF Activates the UPR through a PLCγ-dependent Mechanism

Because the pathway is activated in less than 2 min., it was unlikely that accumulation of misfolded protein or other forms of EGF-induced stress triggered UPR activation. We recently identified a different anticipatory pathway of UPR activation in which the estrogen, 17β-estradiol, bound to estrogen receptor α rapidly activates

phospholipase C γ (PLCγ). Active phosphorylated plasma membrane PLCγ, hydrolyzes PIP_2 to diacylglycerol (DAG) and inositol 1, 4, 5-triphosphate (IP_3). The IP_3 binds to endoplasmic reticulum IP_3 receptors opening the IP_3R Ca^{2+} channels and allowing efflux of Ca^{2+} stored in the lumen of the endoplasmic reticulum into the cytosol. This activates the UPR. Consistent with a role for Ca^{2+} efflux in UPR activation, the well-studied UPR activator thapsigargin rapidly activates the UPR by depleting Ca^{2+} stores in the lumen of the ER and increasing cytosol Ca^{2+} (24). Although EGF has been reported to activate PLCγ, the consequences of PLCγ activation were unknown (42). We therefore evaluated the role of Ca^{2+} release in EGF activation of the UPR.

EGF induced rapid phosphorylation and activation of PLCγ in T47D and MDA MB-468 breast cancer cells (Fig. 8A, B). EGF-mediated phosphorylation of PLCγ was blocked by pre-treatment with the EGFR inhibitor, erlotinib (Fig. 8A, B). PLCγ activation rapidly induced IP_3 (Fig. 8C).

To assess changes in the level of intracellular Ca^{2+}, we used the calcium sensitive dye Fluo-4 AM. In the absence of extracellular Ca^{2+}, EGF elicited a transient increase in fluorescence in MDA MB-468 cells (Fig. 8D). Since the increase in cytosol Ca^{2+} occurs in the absence of extracellular Ca^{2+}, this suggested that the source of intracellular Ca^{2+} was the Ca^{2+} stored in the lumen of the endoplasmic reticulum. To identify the Ca^{2+} channels responsible for promoting the release of Ca^{2+} from the ER, we assessed whether the EGFR inhibitor erlotinib or 2-APB, which locks the IP_3R Ca^{2+} channel, blocks the EGF-mediated increase in cytosol Ca^{2+}. Pre-treatment of MDA MB-468 cells with erlotinib, or with 2-APB, followed by EGF, blocked the increase in intracellular Ca^{2+} (Fig. 8D, E). To further confirm that PLCγ activation is required for EGF to activate the UPR, we performed

siRNA knockdown of PLCγ, and assessed whether EGF was still capable of activating the UPR and inducing the widely used surrogate marker for UPR activation, the chaperone BiP. Knockdown of PLCγ blocked phosphorylation of eIF2α and induction of BiP (Fig. 8F, G). Similarly, knockdown of IP_3Rs blocked EGF-induction of BiP protein (Fig. 8H). These data demonstrate that PLCγ activation, resulting in opening of the ER IP_3 receptor, mediates transient EGF activation of the UPR. (Pathway: EGF-EGFR-p (active) → p-PLCγ (active) → IP_3↑→ IP_3:IP_3R (open)→ Ca^{2+}↑→ UPR (activated)→ BiP↑).

Activation of the Anticipatory UPR Pathway is Required for EGF-EGFR-mediated Gene Expression and is Important for Cell Proliferation

The EGF-EGFR mediated anticipatory pathway of UPR activation can be divided into a rapid early segment that involves activation of PLCγ, increased IP_3, opening of the IP_3R calcium channel and increased intracellular calcium and a late segment that involves activation of the 3 arms of the UPR and induction of BiP chaperone. Since the EGF induced increase in intracellular Ca^{2+} occurs in ~1 min. (Fig. 8D, E), it may precede other actions of EGF. We therefore tested whether the increase in intracellular calcium is important in subsequent rapid effects of EGF. These rapid pathways include rapid activation of the ERK and AKT signaling pathways and induction of pro-proliferation immediate early genes and rapid repression of pro-apoptotic genes. EGF-EGFR induction of immediate early genes, EGR1 and Fos is thought to play a role in EGF-mediated cell proliferation (38, 43). To test whether the extremely rapid increase in intracellular Ca^{2+} is important for subsequent EGF induction of EGR1 and Fos, we used sub-saturating biologically relevant concentrations of EGF. Fos and EGR1 mRNAs were robustly (>10

fold) induced after only 20 min. of EGF treatment. Blocking the EGF mediated increase in intracellular calcium with 2-APB completely blocked EGF induction of EGR1 and Fos mRNAs (Fig. 9A). Since 2-APB also prevents EGF-mediated down-regulation of the pro-apoptotic BIK and BIM mRNAs (Fig. 9B), 2-APB is acting as a selective modulator of EGF-mediated gene expression and not as a general inhibitor of transcription. As expected, inhibition of ERK signaling with the ERK inhibitor UO1026 also blocked EGF-induction of Fos and EGR1 mRNAs (Fig. 9A). To test whether elevated intracellular calcium was stimulating ERK activation (44), and activated ERK then induced immediate early gene expression, we examined the effect of 2-APB on rapid EGF activation of the ERK and AKT signaling pathways. Under the same conditions used in the gene expression experiment, 2-APB did not inhibit rapid and robust EGF activation of the ERK and AKT (protein kinase B) signaling pathways (Fig. 9C). Since 2-APB did not block EGF activation of the ERK pathway, the elevated level of intracellular calcium is a previously undescribed independent regulator of EGF-induced gene expression that works together with ERK activation to regulate immediate early gene expression.

UPR-induced-chaperones, like BiP/GRP78, are thought to be important for cell proliferation (45, 46). We therefore evaluated the effect of UPR activation in EGF stimulated proliferation of T47D cells. Activation of the ATF6α and IRE1α arms of the UPR induces chaperone production. However, the IRE1α arm of the UPR also play a role in mRNA decay and JNK mediated apoptosis (47). To dissect out the role of chaperone induction, instead of carrying out an IRE1α knockdown, we knocked down XBP1 which encodes the spliced XBP1 transcription factor when cleaved by the activated IRE1α. Compared to the control siRNA, knockdown of the XBP1 arm of the UPR produced a

highly significant 28% decline in EGF stimulated cell proliferation, while ATF6 knockdown produced a 35% decline (Fig. 9D). These data indicate that EGF induced UPR activation and the subsequent chaperone production plays an important role in EGF stimulated cell proliferation.

Overexpression of EGFR and HER2/neu is Correlated with Increased UPR Activation

The UPR plays an important role in cancer cell migration, metastasis and resistance to therapy-induced apoptosis. Consistent with a role for the anticipatory UPR pathway in the oncogenic actions of EGF, a recent report found that PLCγ signaling was important for EGF to induce an aggressive pro-metastastic phenotype (48). We therefore evaluated whether overexpression of HER2/neu or EGFR was correlated with increased activation of the UPR in tumors by evaluating a UPR gene signature (24) in several publically available patient tumor cohorts.

To assess UPR activity early in EGFR$^+$ breast cancer development, we compared EGF receptor family member expression level and UPR pathway activity in samples of histologically normal breast epithelium, ductal carcinoma in situ (DCIS) and invasive ductal carcinoma (IDC). Compared with normal epithelium, DCIS and IDC samples displayed elevated levels of EGF receptor family members mRNA (Fig. 11A). Additionally, DCIS and IDC samples displayed elevated markers of UPR activation. Besides the classic UPR maker genes, additional UPR related genes were correlated with increased expression of EGFR. Specifically, SERP1 mRNA, a marker for IRE1α activation (49), TRIB3, which is a marker of PERK activation (50), and BiP chaperone, which is a marker

of ATF6α activation (Fig. 11B). These data suggest that UPR activation is correlated with EGF receptor family member expression.

Using data from an independent cohort of 114 ERα^- breast cancers, we explored whether the expression of HER2 mRNA correlates with the expression of UPR genes. The expression of several UPR genes displayed highly significant correlation with the expression of HER2 genes (Table 1).

DISCUSSION

Cancer progression is often correlated with increased protein synthesis and poor glucose and oxygen supply in the microenvironment (51, 52). In response to these different intrinsic and extrinsic stresses, cancer cells activate the UPR pathway. UPR activation has been described in several human tumors including myeloma (53), lymphoma (54) and carcinoma of the breast (55). The role of UPR activation in resistance of breast cancer and other tumors to tamoxifen and other therapeutics has been extensively studied (23). XBP1 is upregulated in antiestrogen resistant breast cancer cells (56). It interacts with and regulates the activity of estrogen receptor (40, 57), NFκB (58) and apoptosis related proteins (59); this may contribute to drug resistance in these cells. Induction of BiP and other chaperones may also play a role in this protective UPR activation (49).

These studies have focused on the reactive mode of UPR activation in which cells respond to stress by activating the UPR and, if moderate and transient, the UPR is protective (24, 60). In this reactive form of UPR activation, diverse stressors increase the level of unfolded or misfolded proteins in the lumen of the endoplasmic reticulum. This

activates sensors in the endoplasmic reticulum membrane that both sense the stress and activate the 3 major arms of the UPR (Fig. 2) (15, 16, 61, 62).

Here we describe a fundamentally different type of very rapid UPR activation that anticipates future needs and occurs in the absence of cell stress or accumulation of unfolded proteins. In less than 2 minutes EGF triggers PLCγ-mediated opening of endoplasmic reticulum IP_3R calcium channels and release of Ca^{2+} into the cytosol. This increase in cytosol Ca^{2+} stimulates activation of all three arms of the UPR. Anticipatory activation of the UPR is a newly identified common pathway shared by several mitogenic hormones. We suggest this newly unveiled pathway is used by many, but not all, mitogenic hormones to prepare cells for the increased protein folding load that will occur during subsequent hormone-stimulated cell proliferation. Although this pathway is conserved from peptide hormones to steroid hormones, there are important differences in the activation mechanisms. VEGF induced UPR activation is not inhibited by blocking the ER calcium signal (27). However, EGF mediated activation of the UPR is totally dependent on IP_3 mediated calcium release from the ER.

Supporting biological relevance of the UPR pathway, EGFR levels and expression levels of UPR related genes were strongly correlated in samples from 114 ERα negative breast cancers. Moreover, there was a parallel increase in EGFR content and UPR gene index components as cells progress from normal mammary epithelial cells to DCIS and then to IDC. Thus the EGF induced anticipatory UPR pathway not only facilitates tumor cell proliferation but likely also helps protect cancer cells against subsequent apoptosis induced by hypoxia, nutrient deprivation and therapy. Since hypoxia, nutrient deprivation and therapy can all stimulate reactive UPR activation, the anticipatory and reactive modes

of UPR activation lead to UPR engagement throughout the entire cycle of tumor development and therapy.

Since a key feature of rapid anticipatory activation of the UPR is an increase in cytosolic calcium, we explored the effect of blocking this increase on well-known actions of EGF-EGFR. The mitogenic action of EGF is mediated in part by regulation of immediate early gene expression. Two major EGF-induced immediate early genes, *c-fos* and *egr1* encode transcription factors important for cell cycle progression (63, 64). Rapid (5-30 min) EGF-EGFR activation of the ERK signaling pathway is essential for early gene expression (Fig. 9A and 10) (43). Cytosolic calcium levels play an important role in regulating ERK activation (65, 66). Moreover a massive increase in cytosol calcium due to strong and sustained cytotoxic UPR activation is sufficient to activate the ERK pathway (44). However, blocking the transient and moderate increase in cytosol Ca^{2+} induced by EGF-EGFR activation of the protective anticipatory UPR pathway did not inhibit EGF-EGFR activation of the ERK or AKT signaling pathways (Fig.9 and 10). Since blocking the EGF-induced increase in cytosol Ca^{2+} abolished induction and repression of gene expression by EGF, the anticipatory UPR pathway is not regulating immediate early gene expression by controlling ERK activation. ERK activation and the elevated calcium resulting from activation of the early stages of the anticipatory UPR pathway are independent EGF activated pathways that converge at the level of immediate early gene expression. Since 2-APB blocks EGF-induced immediate early gene expression without affecting EGF activation of the ERK and AKT signaling pathways, 2-APB represents a useful new probe for dissecting the roles of immediate early gene expression and ERK and AKT activation in downstream actions of EGF. In contrast to 2-APB, the equally useful simultaneous

RNAi knockdown of all 3 functionally overlapping, but non-homologous, endoplasmic reticulum IP_3R channels (Fig. 8H) is technically challenging and has rarely been reported.

Accumulating evidence suggests a role for UPR chaperones in regulation of cell proliferation. One of the most abundant and well characterized UPR-induced chaperones, GRP78/BiP, influences proliferation of embryonic cells (46). In a GRP78 heterozygous mice model where the level of BiP was reduced by about half, growth of breast tumors was significantly reduced (45). These results suggest UPR chaperones have functions other than facilitating protein folding within the ER. Using siRNA, we knocked down the major UPR chaperone producing pathways, the XBP1 and ATF6 arms (Fig. 2 and 12), and significantly inhibited EGF stimulated cancer cell proliferation (Fig. 9D).

These results indicate that the EGF induced anticipatory UPR pathway facilitates EGF stimulated cell proliferation in at least two ways. First, it releases calcium from endoplasmic reticulum stores and cooperates with the ERK signaling pathway to regulate immediate early gene expression. Second, it increases UPR chaperone production, which facilitates EGF stimulated cell proliferation.

Our studies add a new dimension to the cascade of events that occur when a cell is exposed to EGF.

FIGURES AND TABLE

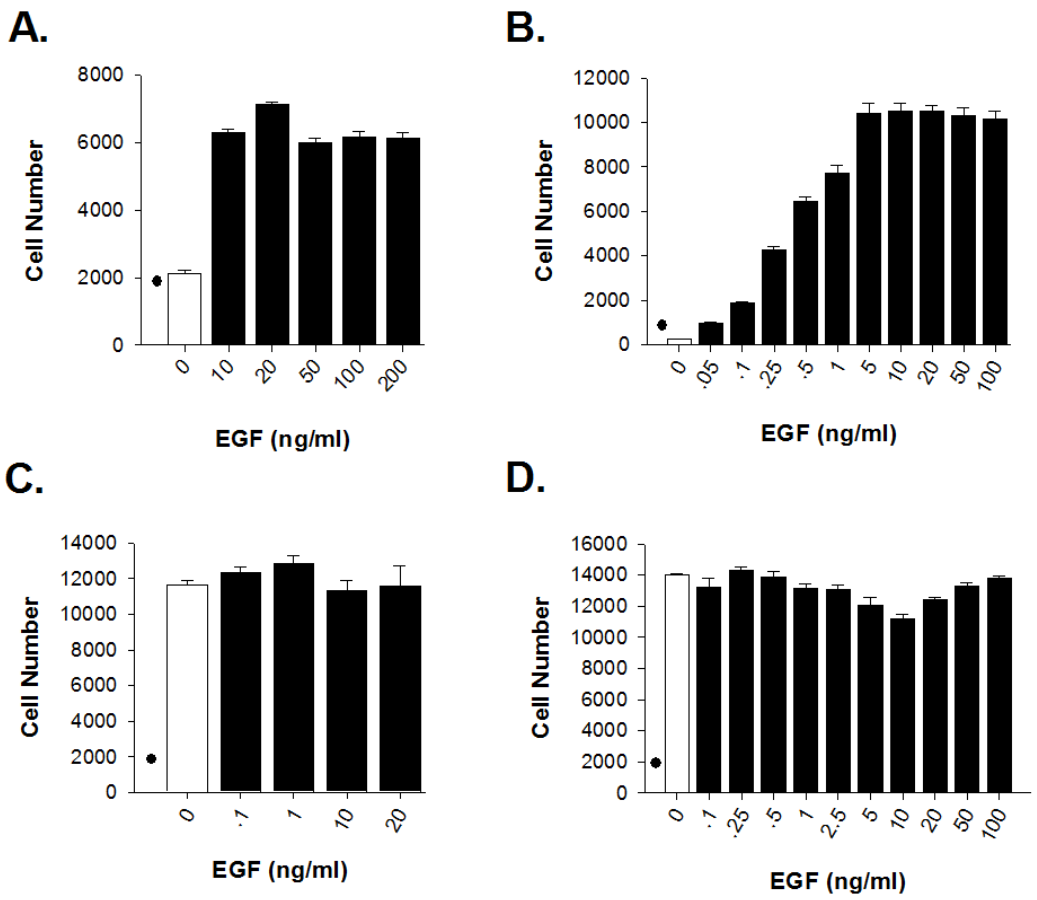

Figure 3.1 Effects of EGF on proliferation of breast cancer cell lines. Effects of EGF on proliferation of (**A**) T47D breast cancer cells, (**B**) pre-tumorigenic MCF10A cells, (**C**) MDA MB-468 breast cancer cells, and (**D**) HCC1954 breast cancer cells. "•" denotes cell number at day 0. Data is mean ± SEM (n = 6).

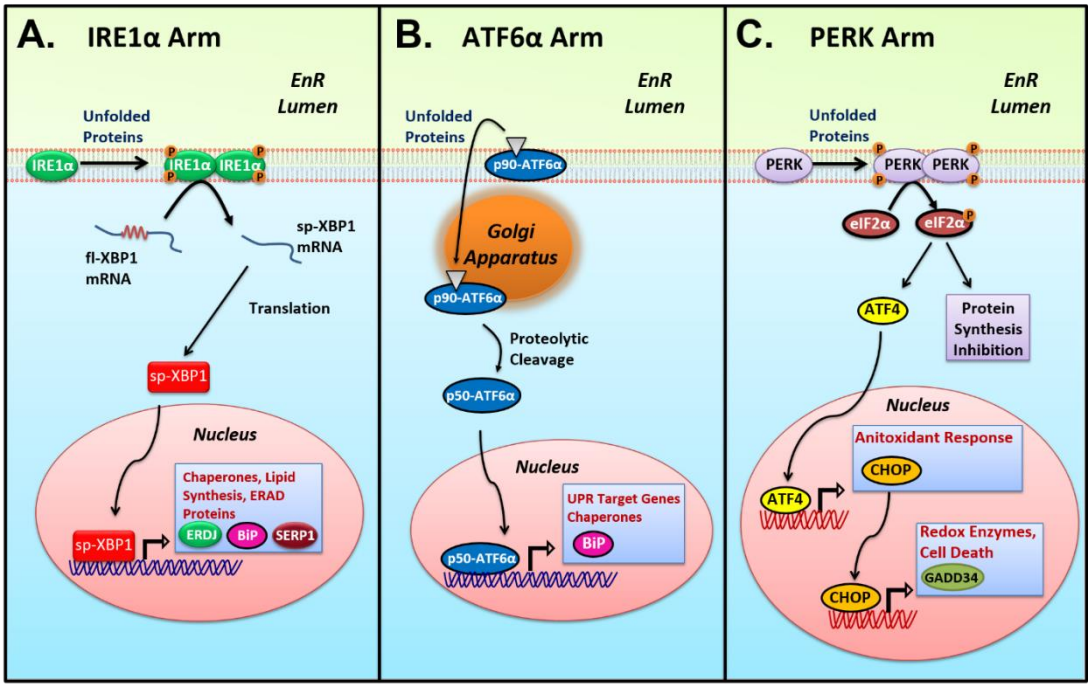

Figure 3.2 Endoplasmic reticulum (ER) stress activates the three arms of the UPR. (**A**) ER stress leads to the oligomerization, auto-phosphorylation, and activation of IRE1α. Activated IRE1α has endonuclease activity and removes an intron from full-length XBP1 (fl-XBP1) mRNA, producing spliced-XBP1 (sp-XBP1) mRNA. The translation product of sp-XBP1 increases lipid synthesis to expand ER capacity, induces ER-associated degradation (ERAD) genes to increase turnover of misfolded proteins. ERDJ, BiP and SERP1 are induced by sp-XBP1 expression. (**B**) ER stress promotes the translocation ATF6α, a transmembrane protein, from the ER to the Golgi apparatus. ATF6α is cleaved in the Golgi apparatus by two proteases and the cytosolic fragment (p50-ATF6α) is released after cleavage. p50-ATF6α increases protein-folding capacity of the ER by inducing BiP, GRP94, and other ER chaperones. (**C**) UPR activation leads to the oligomerization, auto-phosphorylation, and activation of the transmembrane kinase PERK. Phosphorylated PERK oligomer has kinase activity which phosphorylates eukaryotic initiation factor 2α (eIF2α), leading to general inhibition of protein synthesis. However, prolonged activation of eIF2α increases translation of certain mRNAs, including the transcription factor, ATF4 (67). ATF4, acting as a transcription factor, induces the expression of CHOP, which induces GADD34 and several pro-apoptotic genes which eventually leads to cell death.

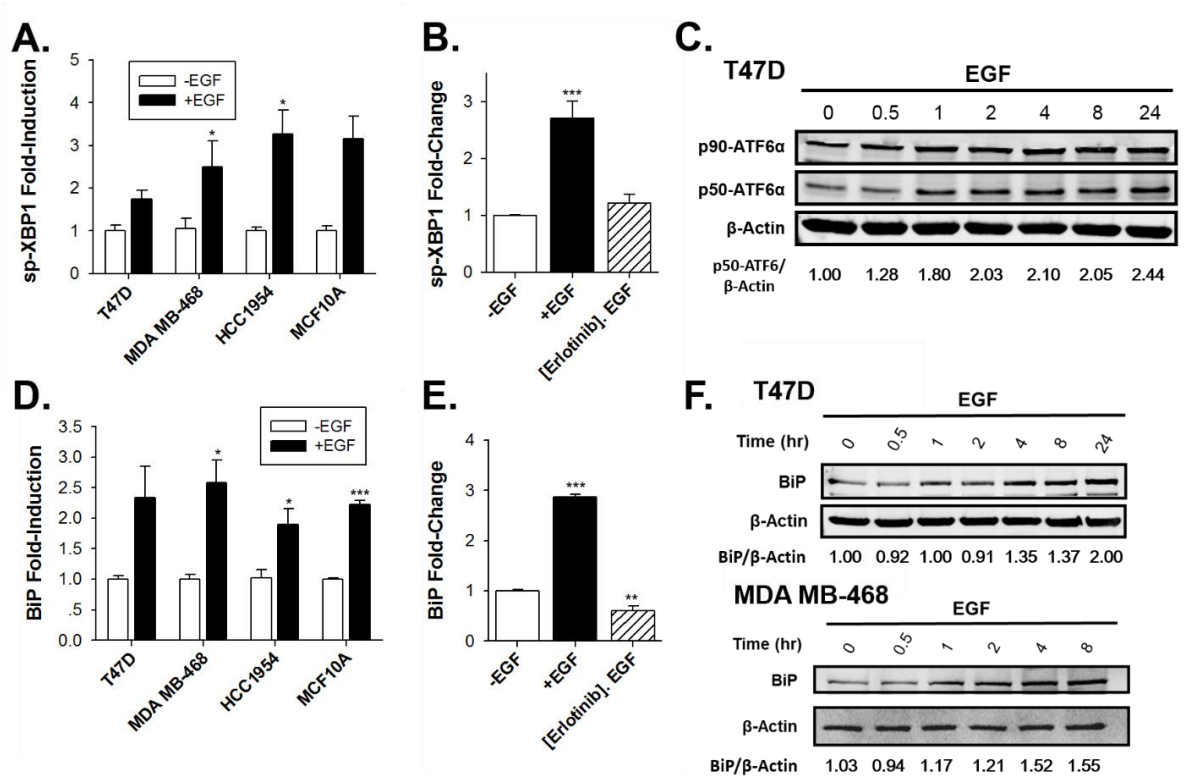

Figure 3.3 EGF activates the IRE1α and ATF6α arms of the UPR and induces production of the chaperone, BiP. (**A**) qRT-PCR comparing the effect of EGF on sp-XBP1 mRNA in T47D, MDA MB-468, HCC1954 and MCF10A cells after EGF treatment for 2 hours (n=3; -EGF set to 1). (**B**) qRT-PCR analysis of sp-XBP1 mRNA in MDA MB-468 breast cancer cells after pre-treating MDA MB-468 cells with erlotinib or with DMSO-vehicle for 30 minutes, following by treatment with EGF for 2 hours (n = 3; -EGF set to 1). (**C**) Western blot analysis showing full-length ATF6α (p90-ATF6α) and cleaved-ATF6α (p50-ATF6α) in EGF-treated T47D breast cancer cells. The numbers below the gel indicate the ratio of p50-ATF6α/β-actin. (D) qRT-PCR analysis of BiP mRNA in T47D, MDA MB-468, HCC1954 and MCF10A breast cell lines after treatment with EGF for 4 hours (n = 3; -EGF set to 1). (E) qRT-PCR analysis of BiP mRNA in MDA MB-468 breast cancer cells after pre-treating MDA MB-468 cells with erlotinib or DMSO vehicle for 30 minutes, following by treatment with EGF for 4 hours (n = 3; -EGF set to 1). (F) Western blot analysis of BiP protein levels in T47D, MDA MB-468 cells treated with EGF. The numbers below the gel are the ratio of BiP/β-actin. Data is the mean ± SEM (n = 3). *p<0.05; **p<0.01; ***p<0.001.

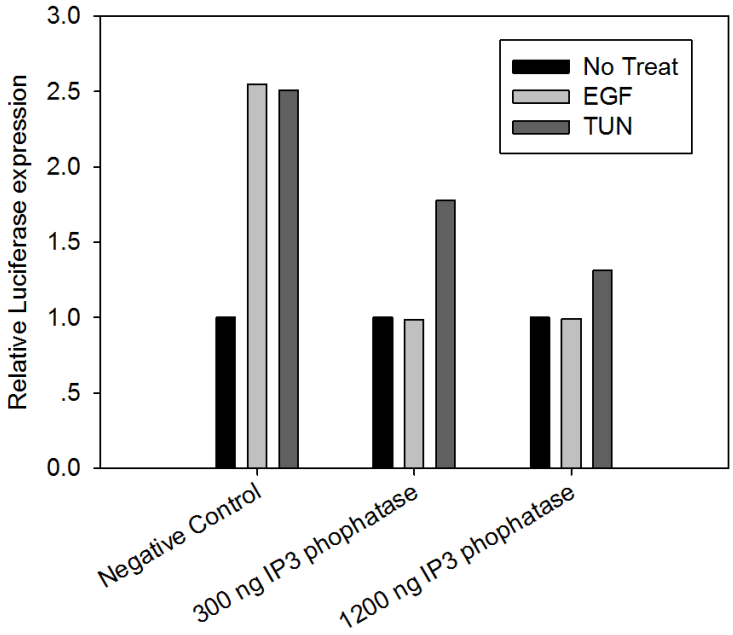

Figure 3.4 EGF activation of UPR is mediated through IP_3 induced calcium release. T47D cells were transfected with the indicated amounts of IP3 phosphatase, XBP1-luciferse reporter and renilla luciferase internal standard as described in Experimental Procedures. The transfected cells were treated with EGF (20 ng/ml) or TUN (10 µg/ml) and luciferase activity was determined. The data shows relative levels of XBP1-firefly luciferase expression normalized to renilla luciferase expression. The experiment shows that IP_3 phosphatase blocks EGF induced XBP1-Luciferase expression but has little effect on TUN stimulated luciferase expression (n=1).

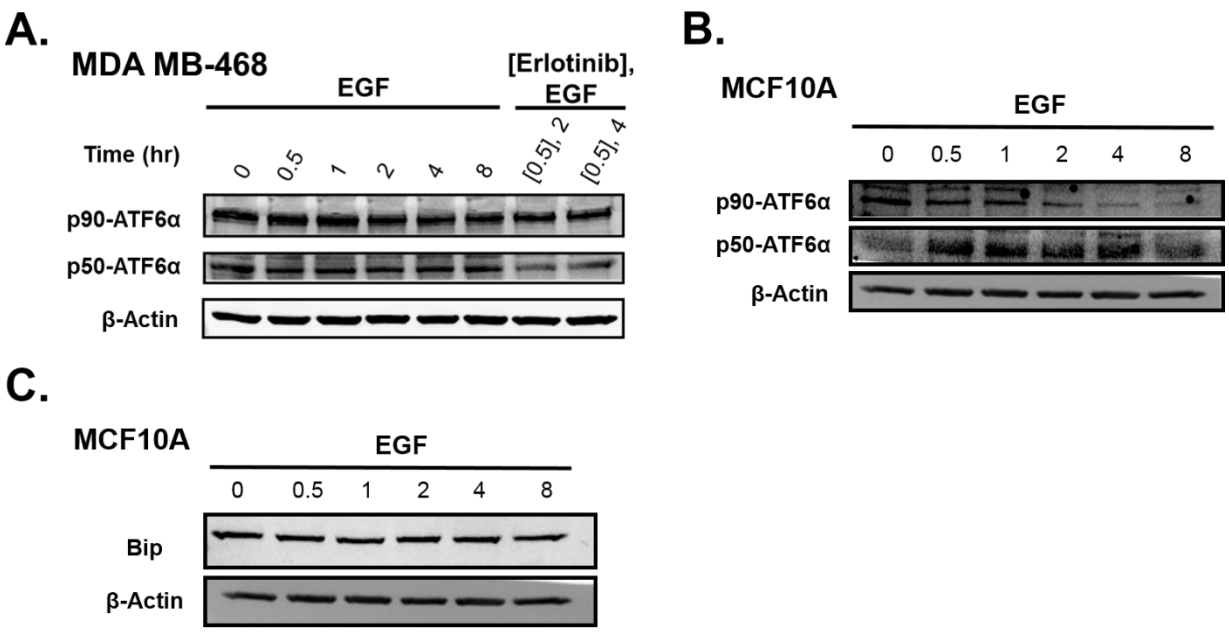

Figure 3.5 EGF activates the UPR. (**A**) EGF activates the ATF6α arm of the UPR in MDA MB-468 breast cancer cells. The increase in the level of cleaved, active ATF6α (p50-ATF6α) demonstrates activation of the ATF6α arm of the UPR. (**B**) Effects of EGF on cleaved-ATF6α (p50-ATF6α) and inactive, full-length ATF6α p90-ATF6α in non-tumorigenic MCF10A cells. (**C**) Effects of EGF on induction of BiP protein in non-tumorigenic MCF10A breast cells. In contrast to T47D and MDA MB-468 cells (see Figure 3.3F), EGF does not induce BiP protein in non-tumorigenic MCF10A cells.

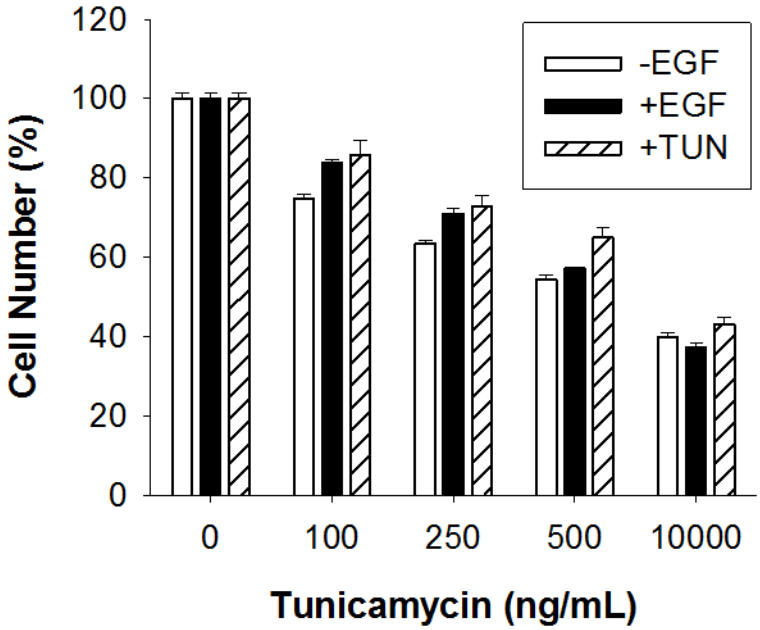

Figure 3.6 Prior EGF activation of the UPR protects MDA MB-468 from subsequent stress. MDA MB-468 cells were maintained in the presence of 20 ng/mL EGF, 250 ng/mL tunicamycin, or a vehicle control for 7 days prior to treating cells with the indicated concentrations of tunicamycin.

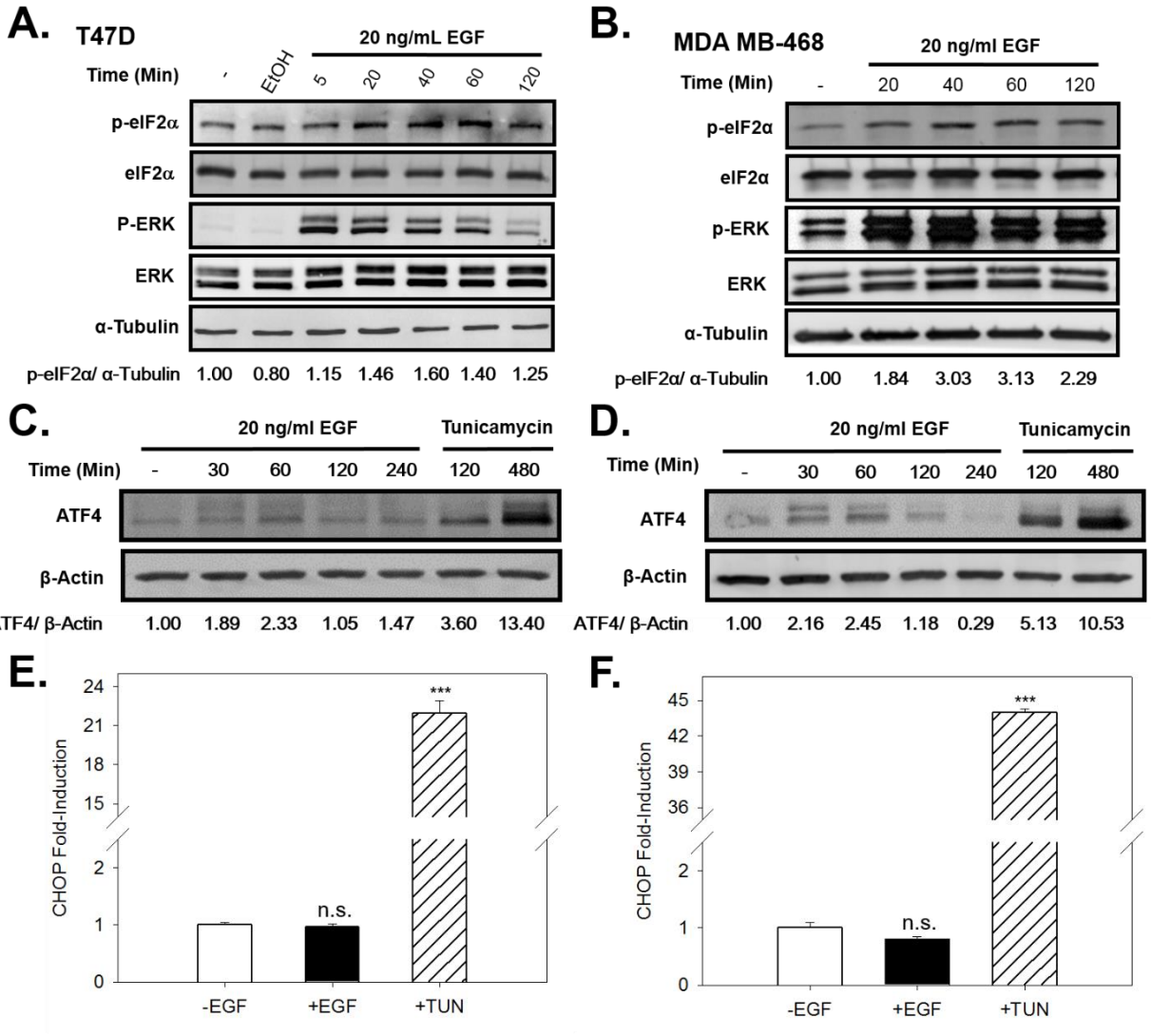

Figure 3.7 EGF activates the PERK arm of the UPR. Western blot analysis showing p-eIF2α levels and total eIF2α levels in ERα⁺ T47D cells (**A**) and in MDA MB-468 cells (**B**) treated with EGF for the indicated times. The numbers below the gel are the ratio of p-eIF2α/α-tubulin ratio. Western blot analysis of ATF4 levels following treatment of T47D cells (**C**) and MDA MB-468 cells (**D**) with EGF, or with the UPR activator tunicamycin. The numbers below the gel are the ratio of ATF4/β-actin. qRT-PCR analysis of CHOP mRNA following treatment of T47D cells (**E**) and MDA MB-468 cells (**F**) with EGF. Concentrations: EGF, 20 ng/ml, TUN, 10 µg/ml. Data is mean ± SEM (n=3). ***p<0.001. n.s., not significant.

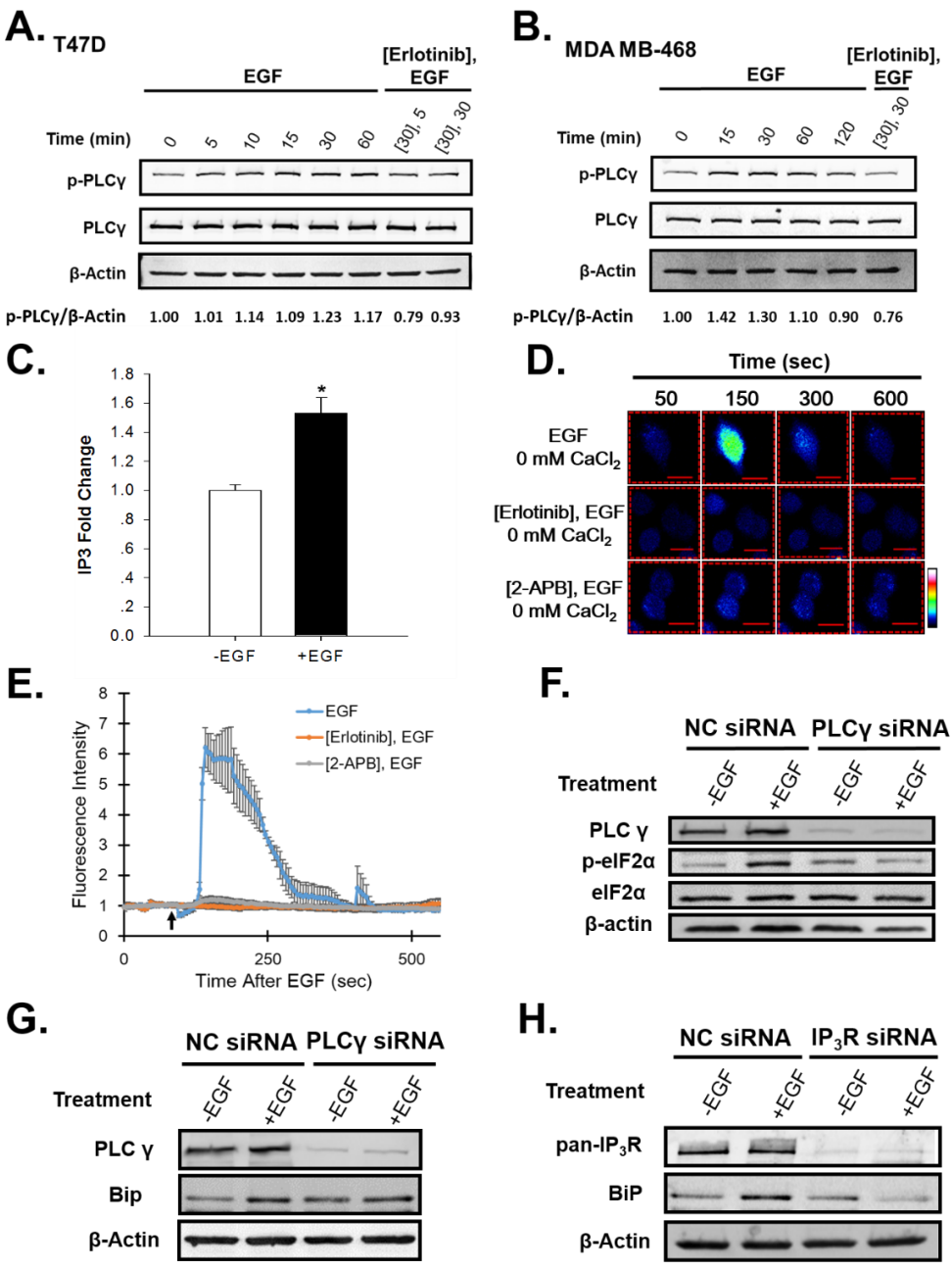

Figure 3.8 EGF activates the UPR through PLCγ-mediated opening of the IP_3R Ca^{2+} channels, leading to the release of Ca^{2+} from the ER into the cytosol, and UPR activation. Western blot analysis of p-PLCγ and total PLCγ protein levels after treatment of (**A**) T47D or (**B**) MDA MB-468 breast cancer cells with EGF or EGF + erlotinib. Cells were treated with either 10 μM erlotinib or vehicle-control, followed by 20 ng/ml EGF for the indicated times. The numbers below the gel are the ratio of p-PLCγ/β-actin. (**C**) Quantitation of intracellular IP_3 levels following treatment of MDA MB-468 cells for 10 min.

Figure 3.8 (cont.) with or without EGF (n=3). (**D**) EGF increases intracellular calcium levels in MDA MB-468 breast cancer cells in medium lacking calcium (0 mM $CaCl_2$). Visualization of intracellular Ca^{2+} using Fluo-4 AM. Color scale from basal Ca^{2+} to highest Ca^{2+}: blue, green, red, white. (**E**) Graph depicts quantitation of cytosolic calcium levels in MDA MB-468 breast cancer cells pre-treated with either vehicle-control, the EGFR inhibitor, erlotinib, or the IP_3R inhibitor, 2-amino propyl-benzoate (2-APB), followed by treatment with 20 ng/ml EGF in the absence of extracellular calcium (indicated by the black arrow, n = 10 cells). Calcium quantitation data is expressed as mean ± SE (n = 10). (**F**) Western blotting analysis of PLCγ, p-eIF2α and total eIF2α protein levels after treatment of T47D cells with 100 nM non-coding (NC) or PLCγ siRNA, followed by treatment with EGF (+EGF) or ethanol-vehicle (−EGF) for 30 minutes. (**G**) Western blotting analysis of PLCγ and BiP protein levels after treatment of T47D cells with 100 nM non-coding (NC) or PLCγ siRNA, followed by treatment with EGF (+EGF) or ethanol-vehicle (−EGF) for 4 h. (**H**) siRNA knockdown of the three isoforms of the IP_3R Ca^{2+} channel blocks EGF-induction of BiP protein in T47D breast cancer cells. Cells were treated with either 100 nM non-coding (NC) or IP_3R siRNA SmartPool, followed by treatment with 20 ng/mL EGF for 4 hours. IP_3R smartpool contained equal amounts of three individual SmartPools directed against each isoform of IP_3R. Data is mean ± SEM (n = 3); *$p<0.05$.

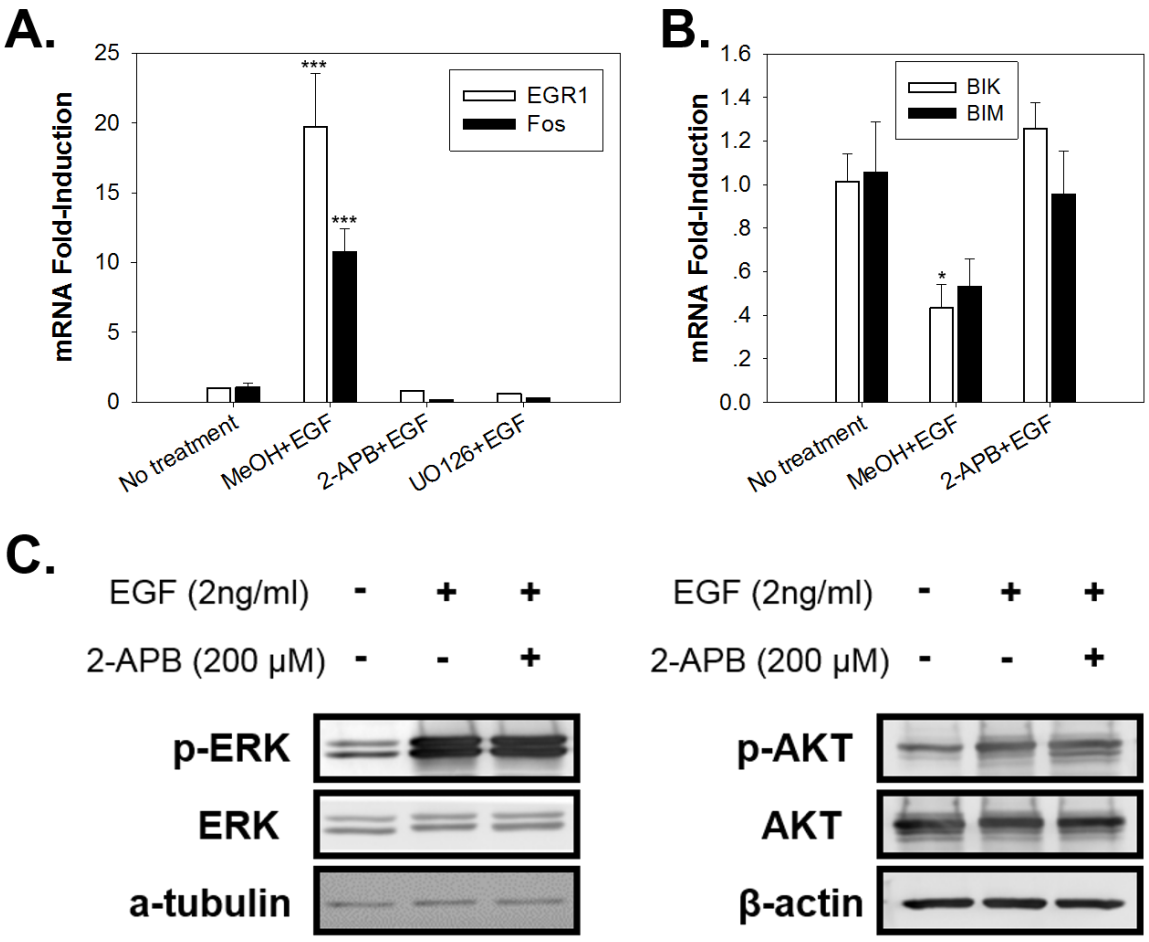

Figure 3.9 EGF induced UPR activation is required for EGF regulated gene expression and cell proliferation. (A and B) qRT-PCR of the oncogene mRNAs EGR1 and Fos and the pro-apoptotic mRNAs BIK and BIM in T47D cells pre-treated for 5 min. with ethanol, 2-APB or the ERK inhibitor UO126, then treated with 2 ng/ml EGF for 20 min. **(A)**, or 2 hours **(B)** (Ca^{2+}-free medium; n=3, mean ±SEM). **(C)** Western blot analysis showing p-ERK levels and total ERK and p-AKT and total AKT levels in T47D cells treated with 2 ng/mL EGF with or without 2-APB pretreatment. (D) EGF stimulated proliferation of T47D breast cancer cells treated with 100 nM non-coding (NC), ATF6 or XBP1 siRNA SmartPool (n=6). Proliferation rates were normalized to cells treated with non-coding (NC) siRNA. *p<0.05; ***p<0.001.

The effects of EGF on the UPR and downstream pathways are depicted in Fig. 3.10.

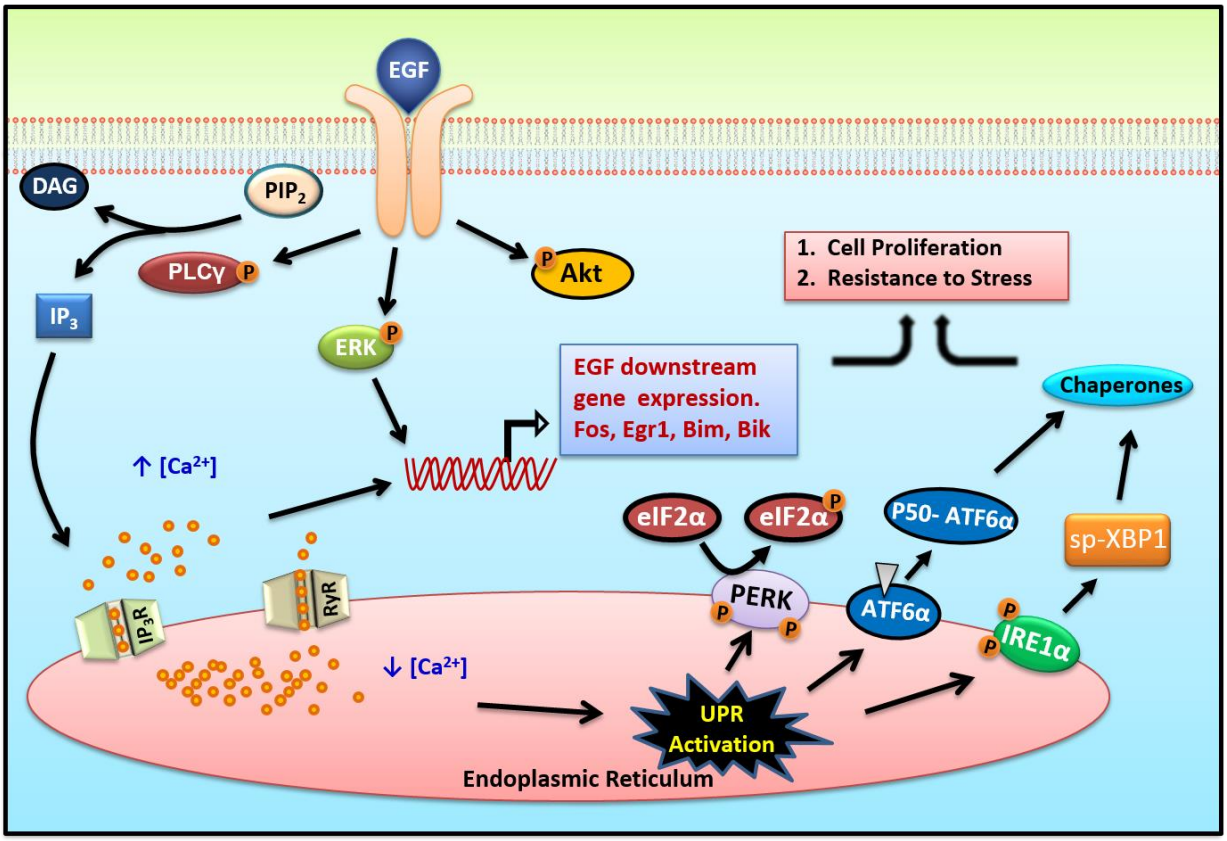

Figure 3.10 Schematic of the pathway of EGF induced anticipatory UPR activation.

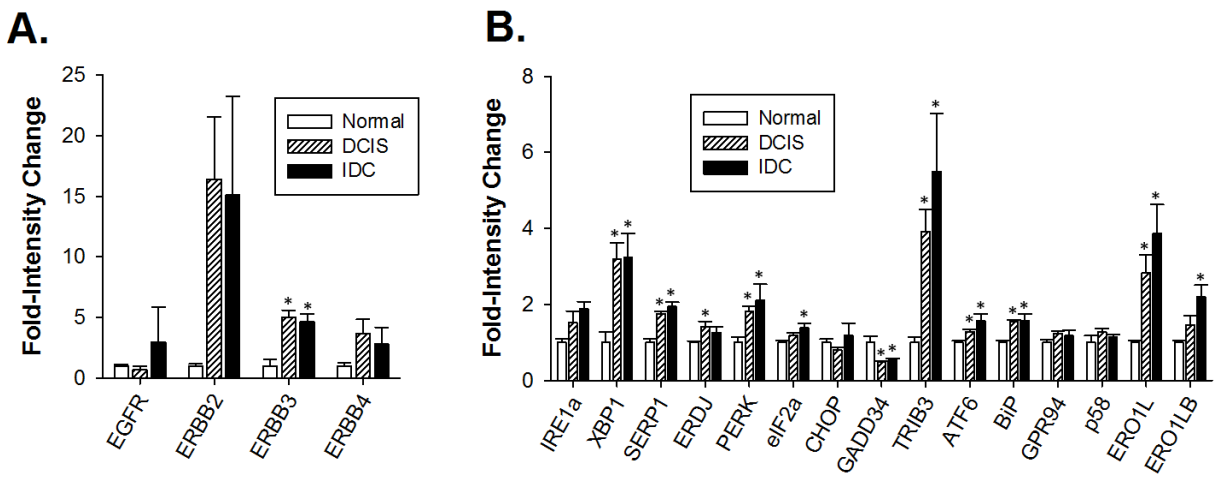

Figure 3.11 Increased expression of EGF receptors is correlated with increased expression of the UPR gene signature. Expression of (**A**) EGF receptors and (**B**) UPR sensors and UPR-regulated genes in samples from normal breast epithelial cells (n=5), ductal carcinoma in situ (n=9), and invasive ductal carcinoma (n=5). Normal epithelial samples were set to 1. Data is mean ± SEM, *p<0.05.

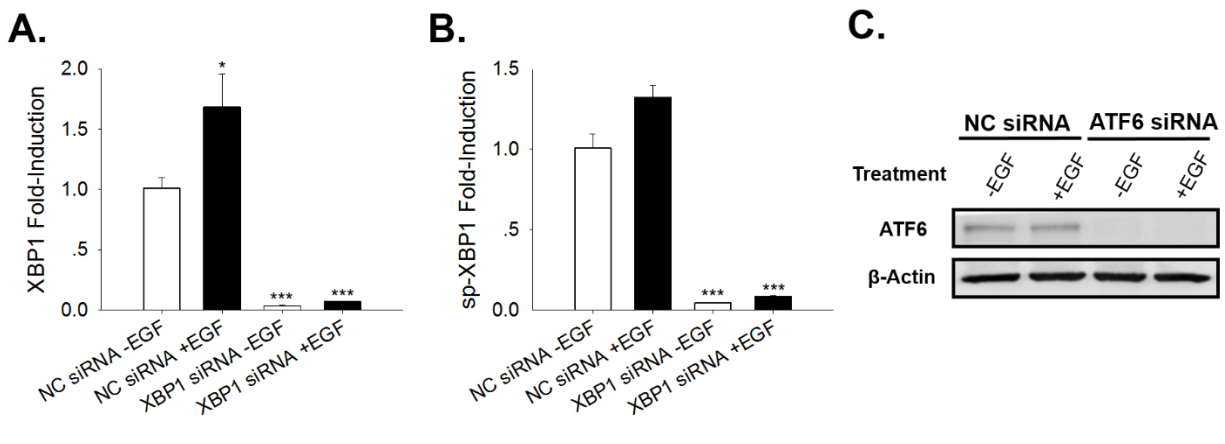

Figure 3.12 siRNA knockdown reduces levels of XBP1 and ATF6α. (A and B) qRT-PCR analysis of (A) XBP1 and (B) sp-XBP1 expression after treatment of T47D cells with 100 nM non-coding (NC) or XBP1 siRNA SmartPool, followed by treatment with EGF (+EGF) or PBS vehicle (− EGF) for 2 h. **(C)** Western blotting analysis of PLCγ, BiP and ATF6α protein levels after treatment of T47D cells with 100 nM non-coding (NC) or ATF6α siRNA SmartPool, followed by treatment with EGF (+EGF) or PBS vehicle (− EGF) for 2 h.

Table 3.1 Correlations between UPR-related mRNAs and ErbB2 mRNA levels in ERα- tumors

Pathway	Gene	HUGO Name	Her2/neu	p-value
PLCy	PLCy	PLCG1	0.339	8.2×10^{-4}
Calcium Channels	IP_3R2	ITPR2	-0.422	2.3×10^{-5}
	IP_3R3	ITPR3	0.500	$<10^{-7}$
XBP1 Arm of UPR	XBP1	XBP1	0.600	$<10^{-7}$
	SERP1	SERP1	0.235	0.012
PERK Arm of UPR	PERK	EIF2AK3	0.476	1×10^{-7}
	eIF2α	EIF2S1	0.352	1.3×10^{-4}
		TRIB3	0.468	2×10^{-7}
	ATF4	ATF4	0.300	1.2×10^{-3}
		HERPUD1	0.271	3.6×10^{-3}
	GADD34	PPP1R15A	0.257	5.9×10^{-3}
ATF6 Arm of UPR	ATF6α	ATF6	n.s.	-
	BiP	HSPA5	0.289	1.8×10^{-3}
	GRP94	HSP90B1	0.231	0.014
	$p58^{IPK}$	DNAJC3	0.205	0.03

Data from a cohort of 114 breast cancer patients (GSE20194). Spearman correlation coefficients and parametric p-values are shown in the table. “n.s.” indicates that no significant correlation was observed.

REFERENCES

1. Yarden Y, Pines G. The ERBB network: at last, cancer therapy meets systems biology. Nat Rev Cancer. 2012;12(8):553-63.

2. Masuda H, Zhang D, Bartholomeusz C, Doihara H, Hortobagyi GN, Ueno NT. Role of epidermal growth factor receptor in breast cancer. Breast Cancer Res Treat. 2012;136(2):331-45.

3. Herbst RS, Langer CJ, editors. Epidermal growth factor receptors as a target for cancer treatment: the emerging role of IMC-C225 in the treatment of lung and head and neck cancers. Semin Oncol; 2002: Elsevier.

4. Holbro T, Civenni G, Hynes NE. The ErbB receptors and their role in cancer progression. Exp Cell Res. 2003;284(1):99-110.

5. Saxena R, Dwivedi A. ErbB family receptor inhibitors as therapeutic agents in breast cancer: current status and future clinical perspective. Medicinal research reviews. 2012;32(1):166-215.

6. Dent R, Trudeau M, Pritchard KI, Hanna WM, Kahn HK, Sawka CA, et al. Triple-negative breast cancer: clinical features and patterns of recurrence. Clinical cancer research : an official journal of the American Association for Cancer Research. 2007;13(15 Pt 1):4429-34.

7. Zell JA, Tsang WY, Taylor TH, Mehta RS, Anton-Culver H. Prognostic impact of human epidermal growth factor-like receptor 2 and hormone receptor status in inflammatory breast cancer (IBC): analysis of 2,014 IBC patient cases from the California Cancer Registry. Breast cancer research : BCR. 2009;11(1):R9.

8. Reis-Filho JS, Pinheiro C, Lambros MB, Milanezi F, Carvalho S, Savage K, et al. EGFR amplification and lack of activating mutations in metaplastic breast carcinomas. The Journal of pathology. 2006;209(4):445-53.

9. Sainsbury JR, Farndon JR, Needham GK, Malcolm AJ, Harris AL. Epidermal-growth-factor receptor status as predictor of early recurrence of and death from breast cancer. Lancet. 1987;1(8547):1398-402.

10. Salomon DS, Brandt R, Ciardiello F, Normanno N. Epidermal growth factor-related peptides and their receptors in human malignancies. Critical reviews in oncology/hematology. 1995;19(3):183-232.

11. Baselga J, Albanell J, Ruiz A, Lluch A, Gascon P, Guillem V, et al. Phase II and tumor pharmacodynamic study of gefitinib in patients with advanced breast cancer. Journal of clinical oncology : official journal of the American Society of Clinical Oncology. 2005;23(23):5323-33.

12. Dickler MN, Cobleigh MA, Miller KD, Klein PM, Winer EP. Efficacy and safety of erlotinib in patients with locally advanced or metastatic breast cancer. Breast cancer research and treatment. 2009;115(1):115-21.

13. Baselga J, Arteaga CL. Critical update and emerging trends in epidermal growth factor receptor targeting in cancer. Journal of clinical oncology : official journal of the American Society of Clinical Oncology. 2005;23(11):2445-59.

14. Lee MJ, Ye AS, Gardino AK, Heijink AM, Sorger PK, MacBeath G, et al. Sequential application of anticancer drugs enhances cell death by rewiring apoptotic signaling networks. Cell. 2012;149(4):780-94.

15. Ron D, Walter P. Signal integration in the endoplasmic reticulum unfolded protein response. Nature reviews Molecular cell biology. 2007;8(7):519-29.

16. Walter P, Ron D. The unfolded protein response: from stress pathway to homeostatic regulation. Science. 2012;334(6059):1081-6.

17. Auf G, Jabouille A, Guérit S, Pineau R, Delugin M, Bouchecareilh M, et al. Inositol-requiring enzyme 1α is a key regulator of angiogenesis and invasion in malignant glioma. Proc Natl Acad Sci. 2010;107(35):15553-8.

18. Crozat A, Åman P, Mandahl N, Ron D. Fusion of CHOP to a novel RNA-binding protein in human myxoid liposarcoma. Nature. 1993;363(6430):640-4.

19. Nawrocki ST, Carew JS, Dunner K, Boise LH, Chiao PJ, Huang P, et al. Bortezomib inhibits PKR-like endoplasmic reticulum (ER) kinase and induces apoptosis via ER stress in human pancreatic cancer cells. Cancer Res. 2005;65(24):11510-9.

20. Shuda M, Kondoh N, Imazeki N, Tanaka K, Okada T, Mori K, et al. Activation of the ATF6, XBP1 and grp78 genes in human hepatocellular carcinoma: a possible involvement of the ER stress pathway in hepatocarcinogenesis. Journal of hepatology. 2003;38(5):605-14.

21. Prabhu A, Sarcar B, Kahali S, Shan Y, Chinnaiyan P. Targeting the unfolded protein response in glioblastoma cells with the fusion protein EGF-SubA. PloS one. 2012;7(12):e52265.

22. Clarke R, Tyson JJ, Dixon JM. Endocrine resistance in breast cancer–an overview and update. Mol Cell Endocrinol. 2015.

23. Clarke R, Cook KL. Unfolding the role of stress response signaling in endocrine resistant breast cancers. Frontiers in oncology. 2015;5.

24. Andruska N, Zheng X, Yang X, Helferich W, Shapiro D. Anticipatory estrogen activation of the unfolded protein response is linked to cell proliferation and poor survival in estrogen receptor α-positive breast cancer. Oncogene. 2014.

25. Liu W, Cai M-J, Zheng C-C, Wang J-X, Zhao X-F. Phospholipase Cγ1 Connects the Cell Membrane Pathway to the Nuclear Receptor Pathway in Insect Steroid Hormone Signaling. J Biol Chem. 2014;289(19):13026-41.

26. Dong D-J, Jing Y-P, Liu W, Wang J-X, Zhao X-F. The steroid hormone 20-hydroxyecdysone upregulates Ste-20 family serine/threonine kinase Hippo to induce programmed cell death. J Biol Chem. 2015:jbc. M115. 643783.

27. Karali E, Bellou S, Stellas D, Klinakis A, Murphy C, Fotsis T. VEGF Signals through ATF6 and PERK to Promote Endothelial Cell Survival and Angiogenesis in the Absence of ER Stress. Mol Cell. 2014;54(4):559-72.

28. Lee AS. Glucose-regulated proteins in cancer: molecular mechanisms and therapeutic potential. Nat Rev Cancer. 2014;14(4):263-76.

29. Andruska ND, Zheng X, Yang X, Mao C, Cherian MM, Mahapatra L, et al. Estrogen receptor α inhibitor activates the unfolded protein response, blocks protein synthesis, and induces tumor regression. Proc Natl Acad Sci. 2015;112(15):4737-42.

30. Cherian MT, Wilson EM, Shapiro DJ. A competitive inhibitor that reduces recruitment of androgen receptor to androgen-responsive genes. J Biol Chem. 2012;287(28):23368-80.

31. Hernandez CC, Zaika O, Tolstykh GP, Shapiro MS. Regulation of neural KCNQ channels: signalling pathways, structural motifs and functional implications. The Journal of physiology. 2008;586(7):1811-21.

32. Pattarozzi A, Gatti M, Barbieri F, Würth R, Porcile C, Lunardi G, et al. 17β-Estradiol promotes breast cancer cell proliferation-inducing stromal cell-derived factor-1-mediated epidermal growth factor receptor transactivation: reversal by gefitinib pretreatment. Mol Pharmacol. 2008;73(1):191-202.

33. Sahin Ö, Löbke C, Korf U, Appelhans H, Sültmann H, Poustka A, et al. Combinatorial RNAi for quantitative protein network analysis. Proc Natl Acad Sci. 2007;104(16):6579-84.

34. Lin H, Hsieh F, Song H, Lin J. Elevated phosphorylation and activation of PDK-1/AKT pathway in human breast cancer. Br J Cancer. 2005;93(12):1372-81.

35. Ron D, Walter P. Signal integration in the endoplasmic reticulum unfolded protein response. Nat Rev Mol Cell Biol. 2007;8(7):519-29.

36. Wu J, Rutkowski DT, Dubois M, Swathirajan J, Saunders T, Wang J, et al. ATF6alpha optimizes long-term endoplasmic reticulum function to protect cells from chronic stress. Dev Cell. 2007;13(3):351-64.

37. Okada T, Yoshida H, Akazawa R, Negishi M, Mori K. Distinct roles of activating transcription factor 6 (ATF6) and double-stranded RNA-activated protein kinase-like endoplasmic reticulum kinase (PERK) in transcription during the mammalian unfolded protein response. The Biochemical journal. 2002;366(Pt 2):585-94.

38. Lee AS. GRP78 induction in cancer: therapeutic and prognostic implications. Cancer Res. 2007;67(8):3496-9.

39. Luo B, Lee AS. The critical roles of endoplasmic reticulum chaperones and unfolded protein response in tumorigenesis and anticancer therapies. Oncogene. 2013;32(7):805-18.

40. Ding L, Yan J, Zhu J, Zhong H, Lu Q, Wang Z, et al. Ligand-independent activation of estrogen receptor α by XBP-1. Nucleic Acids Res. 2003;31(18):5266-74.

41. Cook KL, Shajahan AN, Wärri A, Jin L, Hilakivi-Clarke LA, Clarke R. Glucose-regulated protein 78 controls cross-talk between apoptosis and autophagy to determine antiestrogen responsiveness. Cancer Res. 2012;72(13):3337-49.

42. Margolis B, Bellot F, Honegger A, Ullrich A, Schlessinger J, Zilberstein A. Tyrosine kinase activity is essential for the association of phospholipase C-gamma with the epidermal growth factor receptor. Mol Cell Biol. 1990;10(2):435-41.

43. Murphy LO, Smith S, Chen R-H, Fingar DC, Blenis J. Molecular interpretation of ERK signal duration by immediate early gene products. Nat Cell Biol. 2002;4(8):556-64.

44. Chao T, Byron K, Lee K, Villereal M, Rosner MR. Activation of MAP kinases by calcium-dependent and calcium-independent pathways. Stimulation by thapsigargin and epidermal growth factor. J Biol Chem. 1992;267(28):19876-83.

45. Dong D, Ni M, Li J, Xiong S, Ye W, Virrey JJ, et al. Critical role of the stress chaperone GRP78/BiP in tumor proliferation, survival, and tumor angiogenesis in transgene-induced mammary tumor development. Cancer Res. 2008;68(2):498-505.

46. Luo S, Mao C, Lee B, Lee AS. GRP78/BiP is required for cell proliferation and protecting the inner cell mass from apoptosis during early mouse embryonic development. Mol Cell Biol. 2006;26(15):5688-97.

47. Chen Y, Brandizzi F. IRE1: ER stress sensor and cell fate executor. Trends Cell Biol. 2013;23(11):547-55.

48. Dittmar T, Husemann A, Schewe Y, Nofer JR, Niggemann B, Zanker KS, et al. Induction of cancer cell migration by epidermal growth factor is initiated by specific

phosphorylation of tyrosine 1248 of c-erbB-2 receptor via EGFR. FASEB journal : official publication of the Federation of American Societies for Experimental Biology. 2002;16(13):1823-5.

49. Lee A-H, Iwakoshi NN, Glimcher LH. XBP-1 regulates a subset of endoplasmic reticulum resident chaperone genes in the unfolded protein response. Mol Cell Biol. 2003;23(21):7448-59.

50. Bromati CR, Lellis-Santos C, Yamanaka TS, Nogueira TC, Leonelli M, Caperuto LC, et al. UPR induces transient burst of apoptosis in islets of early lactating rats through reduced AKT phosphorylation via ATF4/CHOP stimulation of TRB3 expression. American Journal of Physiology-Regulatory, Integrative and Comparative Physiology. 2011;300(1):R92-R100.

51. Ruggero D. Translational control in cancer etiology. Cold Spring Harbor perspectives in biology. 2013;5(2):a012336.

52. Brown JM, Wilson WR. Exploiting tumour hypoxia in cancer treatment. Nat Rev Cancer. 2004;4(6):437-47.

53. Lee A-H, Iwakoshi NN, Anderson KC, Glimcher LH. Proteasome inhibitors disrupt the unfolded protein response in myeloma cells. Proc Natl Acad Sci. 2003;100(17):9946-51.

54. Jenner RG, Maillard K, Cattini N, Weiss RA, Boshoff C, Wooster R, et al. Kaposi's sarcoma-associated herpesvirus-infected primary effusion lymphoma has a plasma cell gene expression profile. Proc Natl Acad Sci. 2003;100(18):10399-404.

55. Lee E, Nichols P, Spicer D, Groshen S, Mimi CY, Lee AS. GRP78 as a novel predictor of responsiveness to chemotherapy in breast cancer. Cancer Res. 2006;66(16):7849-53.

56. Gomez BP, Riggins RB, Shajahan AN, Klimach U, Wang A, Crawford AC, et al. Human X-box binding protein-1 confers both estrogen independence and antiestrogen resistance in breast cancer cell lines. The FASEB Journal. 2007;21(14):4013-27.

57. Fang Y, Yan J, Ding L, Liu Y, Zhu J, Huang C, et al. XBP-1 increases ERα transcriptional activity through regulation of large-scale chromatin unfolding. Biochem Biophys Res Commun. 2004;323(1):269-74.

58. Gu Z, Lee RY, Skaar TC, Bouker KB, Welch JN, Lu J, et al. Association of interferon regulatory factor-1, nucleophosmin, nuclear factor-κB, and cyclic AMP response element binding with acquired resistance to Faslodex (ICI 182,780). Cancer Res. 2002;62(12):3428-37.

59. Moretti L, Cha YI, Niermann KJ, Lu B. Switch between apoptosis and autophagy: radiation-induced endoplasmic reticulum stress? Cell cycle. 2007;6(7):793-8.

60. Ma Y, Hendershot LM. The role of the unfolded protein response in tumour development: friend or foe? Nat Rev Cancer. 2004;4(12):966-77.

61. Okada T, Yoshida H, Akazawa R, Negishi M, Mori K. Distinct roles of activating transcription factor 6 (ATF6) and double-stranded RNA-activated protein kinase-like endoplasmic reticulum kinase (PERK) in transcription during the mammalian unfolded protein response. Biochem J. 2002;366:585-94.

62. Novoa I, Zeng H, Harding HP, Ron D. Feedback inhibition of the unfolded protein response by GADD34-mediated dephosphorylation of eIF2α. The Journal of cell biology. 2001;153(5):1011-22.

63. Zwang Y, Oren M, Yarden Y. Consistency test of the cell cycle: roles for p53 and EGR1. Cancer Res. 2012;72(5):1051-4.

64. Brown JR, Nigh E, Lee RJ, Ye H, Thompson MA, Saudou F, et al. Fos family members induce cell cycle entry by activating cyclin D1. Mol Cell Biol. 1998;18(9):5609-19.

65. Schmitt JM, Wayman GA, Nozaki N, Soderling TR. Calcium activation of ERK mediated by calmodulin kinase I. J Biol Chem. 2004;279(23):24064-72.

66. Agell N, Bachs O, Rocamora N, Villalonga P. Modulation of the Ras/Raf/MEK/ERK pathway by Ca 2+, and calmodulin. Cell Signal. 2002;14(8):649-54.

67. Walter P, Ron D. The unfolded protein response: from stress pathway to homeostatic regulation. Science. 2011;334(6059):1081-6.

CHAPTER 4

SRC COUPLES ESTROGEN RECEPTOR TO THE ANTICIPATORY UNFOLDED PROTEIN RESPONSE AND REGULATES CELL FATE UNDER STRESS

ABSTRACT

Accumulation of unfolded protein, or other forms of stress, activates the classical reactive unfolded protein response (UPR). Estrogen and other mitogenic hormones act through their receptors to rapidly elicit phosphorylation of phospholipase C γ (PLCγ), activating the PLCγ-mediated, tumor-protective, anti-apoptotic, anticipatory UPR. We show that the oncogene c-Src is a rate-limiting regulator whose tyrosine kinase activity couples estrogen and progesterone activation of their receptors to activation of the anticipatory UPR. Src-dependent, hormone-mediated activation of the protective anticipatory UPR protected cancer cells against subsequent UPR-mediated cell death. To probe the role of Src, we used the preclinical anticancer drug, BHPI, an estrogen receptor α (ERα) biomodulator that induces lethal hyperactivation of the anticipatory UPR, resulting in necrotic cancer cell death. After unbiased long-term selection for BHPI-resistant human breast cancer cells, 4/11 BHPI-resistant T47D clones and nearly all the MCF-7 clones exhibited reduced levels of normally growth-stimulating Src. Rapid, proteasome-independent turnover and loss of Src contributes to resistance to otherwise lethal concentrations of BHPI. Supporting the conclusion that the BHPI-resistant Src-deficient cells are defective in an early step in the anticipatory UPR, while BHPI failed to induce the UPR marker spliced XBP-1 mRNA, induction of sp-XBP1 by the reactive UPR activators tunicamycin and thapsigargin was unaffected. Moreover, Src overexpression

by virus transduction restored sensitivity to BHPI. Furthermore, in wild type cells, several-fold knockdown of Src, but not of ERα, strongly blocked BHPI-mediated UPR activation and subsequent HMGB1 release and necrotic cell death. Supporting Src linking estrogen and progesterone to activation of the anticipatory UPR, we identified extranuclear complexes of ERα:Src:PLCγ and progesterone receptor:Src:PLCγ. Thus, Src plays a previously undescribed pivotal role in activation of the tumor protective anticipatory UPR, thereby increasing the resilience of breast cancer cells. This is a new role for Src and the UPR in breast cancer.

INTRODUCTION

The endoplasmic reticulum (EnR) stress sensor, the unfolded protein response (UPR), plays a central role in the maintenance of protein folding quality control and homeostasis. In the well-studied reactive UPR, cancer cells respond to unfolded or misfolded proteins, hypoxia, nutritional deprivation and therapy-induced stress by activating the three arms of the UPR, PERK, IRE1α and ATF6α, reducing protein production and increasing protein folding capacity (1). Building on initial work in B cells (2), we, and others, described a protective anticipatory UPR pathway in which the mitogenic hormones, estrogen (E_2), epidermal growth factor (EGF) and vascular endothelial growth factor (VEGF) act through their respective receptors to pre-activate the UPR and anticipate future needs for increased protein folding capacity required to support hormone-stimulated cell proliferation (3-7). Notably, mild and transient E_2 and EGF activation of the anticipatory UPR elicits an adaptive response that protects cancer cells against subsequent UPR-mediated apoptosis (3, 4). Moreover, analysis of data from ~1,000 breast cancer patients

showed that estrogen (17β-estradiol, E_2)-estrogen receptor (ERα)-related activation of a UPR gene index at diagnosis was tightly correlated with subsequent tamoxifen resistance, tumor recurrence and a poor prognosis. While a role for ERα in activation of the anticipatory UPR was clearly established, the key rate-limiting regulator that couples E_2-ERα to tyrosine phosphorylation and activation of phospholipase C γ (PLCγ), initiating the anticipatory UPR pathway (Figure 1) was unknown (3, 4, 6). We demonstrate that the well-studied oncogene cellular Src (c-Src) is the activated rate-limiting tyrosine kinase that couples estrogen:ERα and progesterone:PR to activation of the anticipatory UPR.

The proto-oncogene c-Src is a non-receptor tyrosine kinase with critical roles in signaling pathways involved in cancer cell proliferation, survival, angiogenesis and metastasis (8-10). Although Src has been known to interact with ERα and PR (11-14), a role for Src in coupling ERα and PR action to the UPR had not been reported.

While moderate and transient activation of the reactive and anticipatory UPR pathways serves an adaptive function that promotes cancer progression and therapy resistance; severe unresolvable EnR stress elicits strong and sustained activation of the reactive UPR, activating multiple pro-apoptotic pathways (15-17). In contrast, we recently showed that strong and sustained activation of the anticipatory UPR results in ATP depletion and necrotic cell death (Figure 1) (18). We targeted the anticipatory UPR pathway with the promising preclinical breast cancer drug, BHPI, which acts through ERα to induce lethal anticipatory UPR hyperactivation (18-21). We explored the role of Src in both protective and cytotoxic anticipatory UPR activation. Our studies describe a previously unexplored, often rate-limiting role for Src in coupling steroid receptor action to life-death decisions based on activation of the protective and cytotoxic anticipatory UPR.

MATERIALS AND METHODS

Cell Culture and Reagents

T47D and MCF-7 cells were from ATCC. MCF7-ERαHA cells were provided by E. Alarid. T47D-ERαY537S (TYS) cells were made as described(20). BHPI resistant clones were derived from T47D cells. Cells were grown in the following conditions: T47D (MEM, 10% FBS), MCF-7 (MEM, 5% FBS), MCF7-ERαHA (DMEM, 10% FBS), TYS (MEM, 10% CD-FBS), BHPI-resistant clones (MEM, 10% FBS + 1 μM BHPI for T47D clones; MEM, 5% FBS + 5 μM BHPI for MCF-7 clones). Reagents used were: Dasatinib, Saracatinib, MG132 (Selleck Chemicals, TX), Tunicamycin (Sigma-Aldrich, MO), ^{35}S-methionine (Perkin Elmer, MA).

Western Blotting

Western blotting was carried out as previously described(22). The following primary antibodies were used: p-PLCγ (Cell Signaling Technology (CST) #14008), PLCγ (CST #5690), p-Src (CST #6943), Src (CST #2110), PR (CST #3153), BiP (CST #3177), p-ERK (CST #4370), ERK (CST #4695), p-eIF2α (CST #3398), eIF2α (CST #5324), p-PERK (CST #3179), PERK (CST #5683),ERα (Santa Cruz, sc-8002), HMGB1 (Abnova, H00003146-M08), β-actin (Sigma, A1978). Antibodies were proved with HRP-conjugated secondary antibodies (ThermoFisher, MA) and imaged with the ECL2 detection kit (ThermoFisher) using a PhosphorImager (GE Healthcare, IL).

Co-immunoprecipitation

Cells were lysed with non-denaturing lysis buffer (20 mM Tris HCl, pH 8; 137 mM NaCl; 1% NP-40; 2 mM EDTA) with proteinase inhibitor cocktail. Whole cell lysates obtained by

centrifugation were incubated with 1 μg of ERα (Santa Cruz, sc-543) or PR (Santa Cruz, sc-7208) antibody crosslinked protein A Dynabeads (ThermoFisher) overnight at 4°C. The immunocomplexes were then washed with washing buffer (10mM Tris, pH 7.4; 1mM EDTA; 1mM EGTA, pH 8.0; 150mM NaCl; 1% Triton X-100; 0.2mM sodium orthovanadate; protease inhibitor cocktail) three times and separated for immunoblotting analysis.

siRNA Knockdown

siRNA knockdowns were performed using DharmaFECT1 and 100 nM ON-TARGET plus non-targeting pool or SMARTpools for ERα, PLCγ and Src (Dharmacon, CO). Transfection conditions were as described(22).

Real-time PCR

300 000 cells were plated and cultured as described(22). Total RNA of three biological replicates was collected using a Qiagen RNAeasy kit and cDNA libraries were prepared using a ProtoScript® First Strand cDNA Synthesis Kit (NEB, MA).

Cell Proliferation Assay

Indicated number of cells were plated into 96-well plates. The next day, medium was changed to indicated treatment. The treatment medium was changed after 48 hr and cell numbers were measured with MTS reagent (Promega, WI) after 96 hr (72 hr for siRNA KD experiments) with indicated treatments.

ATP Measurement

ATP depletion assay was performed as previously described(18) and ATP levels were measured using ATPlite Luminescence Assay System (Perkin Elmer, MA). Luminescence was measured using a PHERAStar plate reader (BMG Labtech, Germany).

Cell Viability Assay

300 000 Cells were cultured and plated as previously described(18). Cell viability and cell volume after indicated treatment were measured using a Countess II cell counter (ThermoFisher).

Protein Synthesis Assay

Protein synthesis was analyzed by measuring incorporation of ^{35}S-methionine into newly synthesized proteins. Cells were incubated with indicated treatments and 3 µCi ^{35}S-methionine (Perkin Elmer) was added for the last 30 min. of treatment. Cells were washed, lysed and clarified by centrifugation. Supernatants were spotted onto Whatman 540 filter paper discs (Fisher Scientific, PA) and subsequently washed by 10% trichloroacetic acid (TCA) and 5% TCA. Trapped protein was solubilized, and filters were measured in a scintillation counter.

Lentivirus Production

Src cDNA was amplified and inserted into a pCDH-CMV-MCS-EF1-PURO vector using an In-Fusion HD cloning kit (Clontech, CA). Lentivirus was produced by cotransfecting pCDH-Src or pHIV-Luciferase vector (Addgene #21375) with packaging vectors pCI-VSVG (Addgene #1733) and psPAX2 (Addgene #12260) into HEK293 cells using Lipofectamine 3000 (ThermoFisher).

Statistical Analysis

RNAseq data of normal tissues and primary tumors were obtained from the TCGA Research Network. Samples were grouped by hormone receptors status determined by IHC. Pearson correlation test was used to determine gene expression correlation

coefficients. Two-tailed Student's t-test was used for comparisons between groups. One-way ANOVA followed by Tukey's *post hoc* test was used for multiple comparisons.

RESULTS

Steroid hormones activate phospholipase C γ through Src

Src is a major tyrosine kinase in cancer cells(9). Consistent with our earlier finding that UPR markers are elevated in ERα$^+$ mammary carcinoma(3), compared to normal mammary gland tissue, *Src* expression is significantly elevated in ERα$^+$ and in PR$^+$ mammary carcinomas (Figure 2a). To explore whether Src mediates estrogen-ERα activation of PLCγ, we evaluated the effect of Src inhibition or knockdown on estrogen-ERα stimulation of PLCγ phosphorylation. In ERα$^+$ T47D and MCF-7 human breast cancer cells E_2 increased phosphorylation and activation of Src and PLCγ with a maximum at 20 min. The Src inhibitor, dasatinib (Das), abolished phosphorylation and activation of Src and PLCγ (Figure 2b and 3a). PR interacts with Src through its proline-rich domain (14), suggesting progesterone (P_4) might also activate PLCγ and the anticipatory UPR through Src. P_4 treatment stimulated Src and PLCγ phosphorylation in T47D cells and in TYS cells which express the ERαY537S mutation that is associated with reduced survival in metastatic breast cancer (20, 22). Dasatinib pretreatment blocked the P_4-mediated increase in Src and PLCγ phosphorylation (Figure 2c and 3b). Notably, Src knockdown blocked E_2- and P_4-stimulated PLCγ phosphorylation (Figure 2d). Since a second set of Src siRNAs also blocked PLCγ phosphorylation (Figure 3c), these effects are not due to off-target effects of the siRNA.

Identification of multiprotein complexes containing ERα, Src and PLCγ and PR, Src and PLCγ

Rapid PLCγ phosphorylation stimulated by E_2 and P_4 suggested direct interactions between ERα, Src and PLCγ and PR, Src and PLCγ. Using co-immunoprecipitation (co-IP), we tested for the existence of ERα:Src:PLCγ and PR:Src:PLCγ complexes. Since membrane ERα is only ~5% of the total cellular pool(23), MCF7-ERαHA cells were used to increase total ERα expression (19). Compared to control lysates immunoprecipitated using non-specific rabbit IgG, immunoprecipitation with ERα antibody resulted in an E_2-dependent increase in co-immunoprecipitated Src and PLCγ (Figure 2e). In TYS cells where PR expression is high(22), Src and PLCγ co-immunoprecipitated with anti-PR but not with control rabbit IgG (Figure 2f). Unlike the ERα-Src-PLCγ complex, association of PR, Src and PLCγ was not further enhanced by progesterone. These data indicate that acting by direct physical association in multiprotein complexes, E_2-ERα and P_4-PR activate Src kinase and Src phosphorylates and activates PLCγ, initiating the anticipatory UPR.

Elevated Src expression enhances E_2 and P_4 activation of the anticipatory UPR and adaptation to drug-induced stress

Since we showed that UPR activation at diagnosis is strongly correlated with a poor prognosis in breast cancer(3), and Src both couples ERα to anticipatory UPR activation and is overexpressed in mammary carcinomas, we explored whether Src overexpression correlated with overexpression of the oncogenic UPR-induced chaperone HSPA5/BiP/GRP78 (24). *In vivo* data from The Cancer Genome Atlas (TCGA) demonstrated that in $ERα^+$ and PR^+ mammary carcinomas in which *Src* was also

upregulated, there was up-regulation of UPR marker genes, especially the IRE1α pathway targets *XBP1* and *HSPA5* (Figure 4a). Thus, Src-mediated PLCγ activation may be responsible for anticipatory UPR activation in these ERα and PR positive breast cancers. To test our hypothesis, we monitored levels of the UPR activation marker, spliced XBP1 mRNA (*sp-XBP1*). Both E_2 and P_4 increased *sp-XBP1* in breast cancer cells. Inhibiting Src with dasatinib or saracatinib significantly reduced sp-XBP1 mRNA levels (Figure 4b,c and 5a,b). sp-XBP1 is a transcription factor and induces BiP and other EnR chaperones (25). Consistent with their induction of sp-XBP1 mRNA, E_2 and P_4 elevated BiP expression in T47D cells and Src knockdown blocked BiP induction (Figure 4d). Estrogen pretreatment elicits chaperone induction and renders cells resistant to exposure to lethal concentrations of tunicamycin (TUN) (3). In contrast to estrogen, which increases cell proliferation, complicating analysis, progesterone did not activate the pro-proliferation ERK pathway (Figure 4e), or increase cell number (Figure 5c,d). Notably, pretreating cells with P_4 elicited 4-fold and 2-fold increases in the concentration of TUN required to induce apoptosis in T47D and TYS cells, respectively; blocking UPR activation with dasatinib re-sensitized cells to TUN (Figure 4f,g). Thus, Src-mediated anticipatory activation of the UPR, resulting in increased chaperone production, and protects tumor cells against apoptotic cell death induced by prolonged EnR stresses.

Src is required for strong and sustained activation of the UPR

BHPI, acting through ERα, elicits strong and sustained activation of the anticipatory UPR (18, 19). Opening of IP_3R calcium channels induces sustained Ca^{2+} release from the EnR. To restore Ca^{2+} homeostasis, sarco/endoplasmic reticulum Ca^{2+}-ATPase (SERCA) pumps use ATP to pump Ca^{2+} back into the EnR lumen (19), creating a futile

cycle of pumping and release that depletes intracellular ATP. BHPI stimulated a ~40% decline in ATP levels, which was partially blocked by Src knockdown (Figure 6a). We next explored whether Src was critical for strong UPR activation. BHPI robustly induced sp-XBP1 mRNA and dasatinib largely blocked sp-XBP1 induction (Figure 6b). BHPI strongly stimulates the PERK arm of the UPR leading to protein synthesis inhibition(19). Pretreatment with dasatinib blocked BHPI-induced PERK activation reducing downstream phosphorylation of eIF2α (Figure 7a,b).

Sustained UPR activation induced by BHPI results in classical necrosis phenotypes, including plasma membrane disruption and leakage of intracellular contents(18). We assessed loss of membrane integrity by monitoring leakage into the medium of the widely used marker, high mobility group box 1 (HMGB1). 24h BHPI treatment increased HMGB1 release and Src knockdown reduced HMGB1 leakage (Figure 6c). To evaluate cell viability, we quantitated cell death using an automated trypan blue exclusion assay. In T47D, TYS and MCF-7 cells, ablating Src signaling by knockdown or with dasatinib, nearly abolished BHPI's ability to induce cell death. Moreover, a longer three-day MTS assay confirmed that Src knockdown reversed BHPI inhibition of cell proliferation (Figure 6d-f). Src knockdown only reduces Src protein ~3-fold (Figure 4c), suggesting Src, not ERα might be limiting for activation of the anticipatory UPR. To explore this, we evaluated the effect of ERα knockdown on BHPI inhibition of cell proliferation. Although the extent of ERα knockdown was at least as great as Src knockdown (Figures 4c and 7c), ERα knockdown did not block BHPI inhibition of cell proliferation (Figure 7d). These data suggest that Src, not ERα, is limiting in the complex that initiates activation of the anticipatory UPR.

In ER$^+$ breast cancer cells Src downregulation confers resistance to BHPI

To explore Src's roles in the anticipatory UPR and in development of resistance to BHPI in tumor cells, we performed long-term selections for breast cancer cells resistant to growth inhibition by BHPI. Initially, BHPI treatment led to rapid death of nearly all cells. Over many weeks BHPI-resistant colonies grew out. We isolated T47D and MCF-7 colonies that survived long-term selection in 1 μM (T47D) and 5 μM (MCF-7) BHPI. BHPI-resistance could arise due to changes that diminish lethal BHPI hyperactivation of the anticipatory UPR, or from changes in growth or death pathways that counter UPR hyperactivation. We therefore compared the effect of the apoptosis inducer staurosporine (STS) as well as BHPI in T47D and MCF-7 cells and in BHPI-resistant T47D clone 1 (TB1) and MCF-7 clone 5 (MB5) cells. Flow cytometry showed that while both BHPI and STS induced cell death in the wild-type T47D and MCF-7 cells, only STS induced death of the BHPI-resistant TB1 and MB5 cells (Figure 8).

Since the TB1 cells were not broadly resistant to cell death, we initially explored effects on proteins in the anticipatory UPR pathway and on UPR activation. Since long-term treatment with aromatase inhibitors selects for tumors that contain constitutively active ERα mutations and BHPI acts through ERα, it seemed possible we would identify mutations in ERα with diminished interaction with BHPI. Interestingly, sequencing of all 11 BHPI-resistant T47D clones showed there were no mutations in ERα. Since BHPI acts through the ERα-Src-PLCγ complex to hyperactivate the anticipatory UPR pathway, we explored the levels of these proteins in the BHPI-resistant clones. Consistent with a rate-limiting role for Src in the anticipatory UPR, 4 of 11 T47D clones (clone 1, 3, 4 and 11) and 7 of 8 MCF-7 clones showed reduced Src expression (Figure 9a and 10a). Several

BHPI-resistant clones displayed reduced levels of ERα. We further characterized T47D clones: TB1 (moderately reduced Src, ERα and PLCγ), TB3 (reduced Src) and TB11 (reduced ERα, PLCγ and slightly reduced Src) and MCF-7 clone MB5 (reduced Src and ERα) and MB7 (reduced Src and ERα). T47D clone TB8 (Src not reduced) was a control. TB1, TB3 and TB11 exhibited reduced sensitivity to estrogen and showed slow growth in BHPI (Figure 10b,c). In contrast, TB8 lost E_2 stimulation of cell proliferation, while BHPI slightly increased its proliferation (Figure 10b,c). This suggests TB8 cells with normal Src levels exhibit a different BHPI resistance mechanism than cells with reduced levels of Src. Compared to parental MCF-7 cells, MB5 and MB7 cells showed slightly reduced E2-stimulated cell proliferation and 1 μM BHPI had minimal effects on their proliferation (Figure 9b,c). Since T47D and MCF-7 cells display different sensitivity to growth inhibition and killing by BHPI (Figure 9c and 10c), data obtained from the two sets of BHPI-resistant cell lines should be broadly applicable.

We then compared UPR activation in parental cells and BHPI resistant clones. BHPI-resistant T47D and MCF-7 clones exhibited minimal BHPI induction of sp-XBP1 (Figure 11a and 9d). To test whether reactive UPR responses were impaired in the resistant clones, we compared sp-XBP1 expression in parental cells and in resistant clones treated with the classic UPR activators TUN and thapsigargin (THG). Consistent with an intact reactive UPR pathway in the BHPI resistant clones, sp-XBP1 mRNA induction by the UPR activators was nearly identical in parental and BHPI-resistant clones (Figure 11b and 9e). In 100 nM BHPI, which blocks growth and kills wild type T47D cells (Figure 10a), activation of the PERK-p-eIF2α arm of the UPR and inhibition of protein synthesis were nearly abolished in the resistant clones (Figure 11c,d). While increasing BHPI to 1 μM

restored strong BHPI inhibition of protein synthesis, these cells still grow slowly (Figures 10c and 11d). Notably, while 100 nM and 1 μM BHPI strongly reduced ATP levels in wild-type T47D and MCF-7 cells, in the BHPI-resistant clones, BHPI lost the ability to reduce ATP levels (Figure 9f and 11e) and therefore failed to induce necrotic cell death (Figure 5f) and HMGB1 release (Figure 11g). Since BHPI resistance arose from impaired activation of the anticipatory UPR pathway, and Src, which triggers activation of the pathway, was reduced in several of the clones, we explored whether restoring Src levels could re-sensitize resistant clones to BHPI.

Overexpressing Src re-sensitizes resistant breast cancer cells to BHPI-stimulated UPR hyperactivation

To test whether down-regulation of Src was critical for acquisition of BHPI resistance and was rate-limiting for UPR hyperactivation, we used transduction with a Src lentivirus and a control luciferase lentivirus. Although the Src lentivirus increased Src levels in T47D cells, it did not alter levels of the other components of the complex, ERα and PLCγ (Figure 12a). Consistent with a saturating and rate-limiting level of Src in wild type T47D cells, increasing Src levels did not increase BHPI-induced cell death, while several-fold Src knockdown reduced cell death. Moreover, the higher Src level in T47D cells transduced with Src lentivirus greatly attenuated the effect of Src knockdown on BHPI-induced cell death (Figure 13a). Restoration of Src in BHPI-resistant cells was complicated by the surprising finding that BHPI treatment elicited rapid turnover of Src protein in the BHPI-resistant clones, but not in parental T47D cells. 100 nM BHPI for 1 hour did not reduce Src levels in T47D cells or in the TB8 clone (WT Src level), but reduced Src levels in TB1, TB3 and TB11 cells (Figure 12b). Moreover, 1-hour treatment with 1 μM BHPI, but not

100 nM BHPI, significantly reduced Src expression in MB5 cells. Surprisingly, Src depletion was not blocked by the proteasome-inhibitor MG132 (Figure 12c,d). Thus, viral transduction may only partially restore Src levels and function in the BHPI-resistant clones. While restoration of Src protein in BHPI-resistant TB1 cells did not significantly increase ATP depletion (Figure 12e), it increased phosphorylation of eIF2α, partially restored BHPI inhibition of protein synthesis and partially restored BHPI inhibition of cell proliferation (Figure 13b-d). These data show restoring the level of Src oncogene in BHPI-resistant cancer cells partially re-sensitizes the cells to BHPI-mediated UPR hyperactivation and cell death.

Consistent with our observations in T47D cells, 1 μM BHPI nearly eliminated expression of Src protein in MCF-7-derived MB5 cells and viral transduction partially restored Src expression (Figure 13e). Restoring Src expression in MB5 cells increased BHPI-mediated ATP depletion and inhibition of protein synthesis (Figure 13f,g). Notably, while 1 μM BHPI did not inhibit proliferation in MB5 cells transduced with control luciferase virus, it significantly inhibited cell proliferation in cells transduced with Src virus (Figure 13h). These data show restoring the level of Src oncogene in BHPI-resistant cells re-sensitizes them to BHPI-mediated UPR hyperactivation and cell death.

DISCUSSION

How signals from hormones and biomodulators bound to steroid receptors elicit phosphorylation of PLCγ and activation of the anticipatory UPR was unknown. We show that a single activating kinase, Src, triggers both types of anticipatory UPR activation: the mild and transient tumor protective mode and the strong and sustained cancer-targeting

lethal mode (Figure 1). Although Src is abundant in ERα$^+$ breast cancer cells, and was known to activate multiple pro-growth signaling pathways (26, 27), its key role in activation of the hormone-mediated anticipatory UPR unveils a previously unexplored oncogenic mechanism. Src's role in rapid activation of the anticipatory UPR in cancer cells plays an enabling role in facilitating the diverse mitogenic activities of Src. In ERα$^+$ breast cancer cells, acting through the anticipatory UPR, Src level and activity serve as a molecular rheostat integrating diverse signals. Activation of the UPR at diagnosis is strongly correlated with tumor recurrence, tamoxifen resistance and a poor prognosis (3). Consistent with our finding that constitutively active ERα mutations that are partially tamoxifen resistant elicit weak long-term activation of the anticipatory UPR (20, 22), in tamoxifen resistant MCF-7 cells, sustained and gradually increasing Src activation is observed (27).

While there have been several studies reported that Src activates PLCγ (28-30), in the absence of a downstream PLCγ activated pathway, these studies did not attract a great deal of interest. Our finding that Src is a rate-limiting controller of the anticipatory UPR provides a framework and context that integrates these seemingly diverse observations. For example, vitamin D receptor, in rat colonocytes stimulates PLCγ activation through Src-mediated tyrosine phosphorylation (29). Notably, the insect hormone ecdysone binding to ecdysone receptor (EcR) activated PLCγ in a Src-dependent manner and calcium in the cell increased (31, 32). This activity was shown to be essential for ecdysone-mediated insect development, but was not linked to the UPR. Our work makes it highly likely that ecdysone-EcR are acting through the Src-PLCγ pathway to provide an essential authorizing signal through activation of the anticipatory UPR. Conservation of

the Src-regulated anticipatory UPR from insects to humans demonstrates its importance. Similarly, the observation that unconjugated bile acids act through Src and result in death of esophageal cancer cells raises the possibility that bile acids, perhaps acting through bile acid receptors, are inducing lethal activation of the anticipatory UPR (33). In some systems, such as direct activation of Src and PLCγ by sphingolipids (34), Src activation may result from perturbation of its membrane environment and likely does not require an activating hormone receptor.

Usually resistance to an anticancer drug involves either mutation of its target, as is seen with aromatase inhibitors and ERα mutations in breast cancer (35, 36), or overexpression of the target protein as is seen with antiandrogens and androgen receptor (AR) in prostate cancer (37). Unexpectedly we found that clonal cell lines identified in unbiased long-term selection for resistance to BHPI often exhibited down-regulation of pro-growth Src. Since UPR activation by classical UPR activators tunicamycin and thapsigargin was unaffected, it is likely that down-regulation of Src was the key event in acquisition of BHPI resistance. Notably, down-regulation of Src was more common than down-regulation of ERα, the direct target of BHPI. Moreover, Src overexpression re-sensitized resistant clones to BHPI-stimulated UPR hyperactivation.

In normal cells, activated Src undergoes reversible protein dephosphorylation and ubiquitin-mediated protein degradation (38, 39). Therapeutic HSP90 inhibitors enhance Src degradation in cancer cells (40, 41). Consistent with a regulatory role for degradation controlling Src level and ultimately activity, in several BHPI-resistant breast cancer cell lines, Src was rapidly degraded through a proteasome-independent mechanism (Figure 12b,c,e).

Our findings that moderate down-regulation of Src leads to BHPI resistance in long-term culture and that 3-4 fold knockdown of Src is sufficient to strongly inhibit BHPI-induced cell death are surprising in light of the overexpression and abundance of Src in ERα$^+$ breast cancer cells. Only a small fraction of ERα is extranuclear near the plasma membrane, and much of the extranuclear ERα is devoted to activating ERK and other signaling pathways. Therefore, total Src is in large excess over what is required to complex with ERα and PLCγ and activate the anticipatory UPR. Partitioning of limiting Src between the ERα- and PLCγ-regulated anticipatory UPR and other signal transduction pathways likely provides a novel mechanism for coordinating activity of the UPR and the growth-stimulating signaling pathways. While this type of limiting availability due to competition between different complexes is well studied in the context of transcription factors, such as CBP (42), it has been less widely considered in the control of UPR activation.

Taken together our findings that Src is down-regulated in BHPI-resistant clones, that 3-4 fold down-regulation of Src attenuates both the protective activation of the anticipatory UPR, and BHPI-induced lethal hyperactivation of the anticipatory UPR, strongly suggests elevated levels and activity of Src in breast cancer play a major role in key life-death decisions that surround activation of the anticipatory UPR (Figure 14).

FIGURES

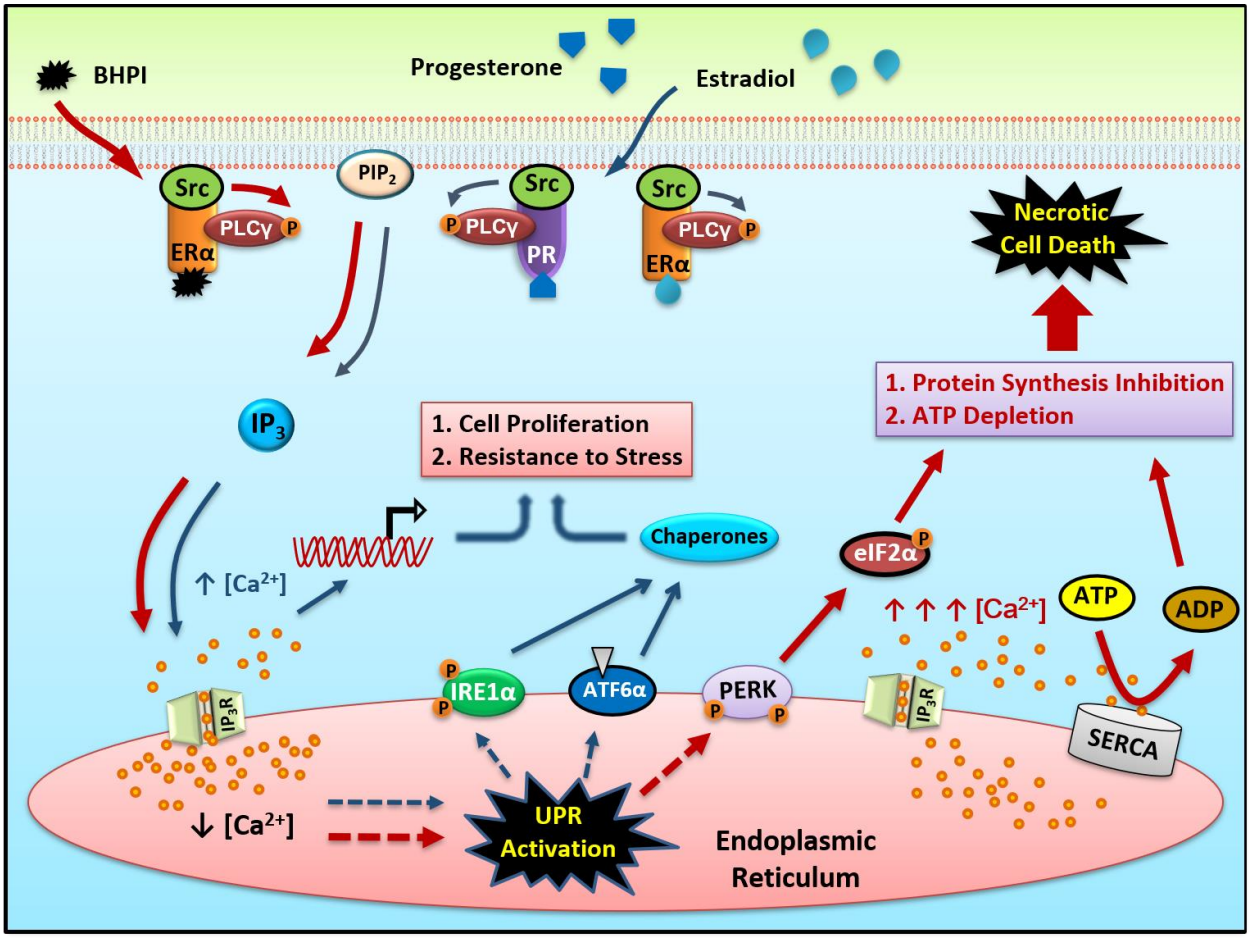

Figure 4.1 Schematic model of moderate and strong anticipatory UPR activation.

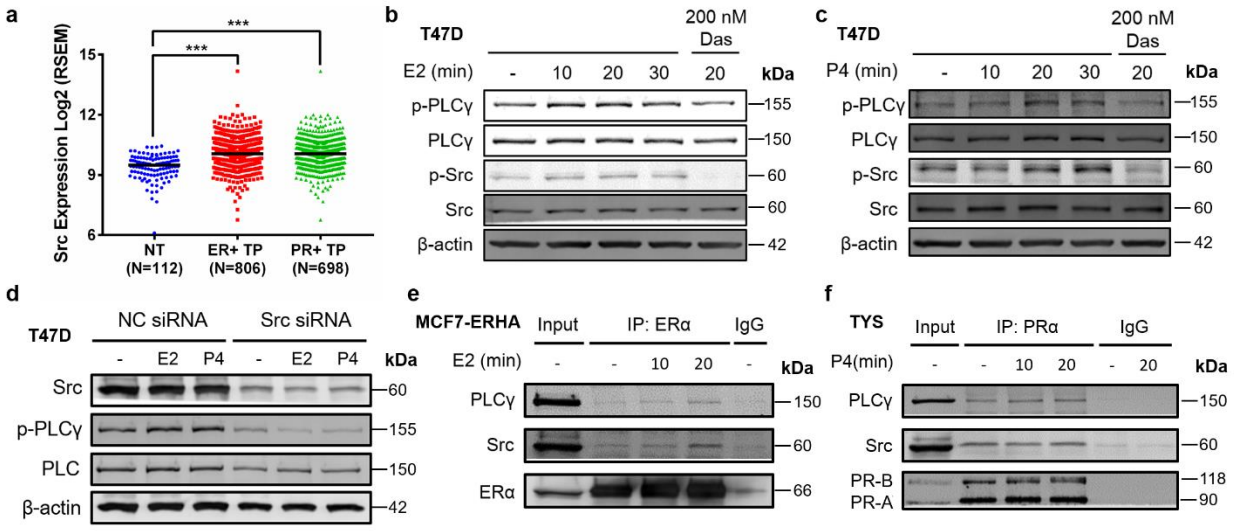

Figure 4.2 Src mediates steroid hormone-stimulated PLCγ phosphorylation. (**a**) *Src* gene expression in normal tissues (NT), ERα$^+$ primary breast cancer (ER+ TP) and PR$^+$ primary breast cancer (PR+ TP). * indicates a significant difference among groups using one-way ANOVA followed by Tukey's *post hoc* test. *** $P < 0.001$. (**b,c**) Western blotting analysis of phosphorylated PLCγ (p-PLCγ, tyrosine 783), total PLCγ, phosphorylated Src (p-Src), total Src and β-actin in ERα$^+$ T47D cells treated with vehicle control or dasatinib (Das) for 5 min., followed by treatment with 10 nM E_2 (**b**) or 10 nM progesterone (P_4) (**c**). (**d**) Western blotting analysis of Src, p-PLCγ, PLCγ and β-actin protein levels following treatment of T47D cells with either 100 nM non-coding (NC) or Src siRNA SMARTpool, followed by treatment with vehicle, E_2 or P_4 for 30 min. (**e**) Co-immunoprecipitation and western blotting analysis of ERα, Src and PLCγ interactions in MCF7-ERαHA cells. Using magnetic beads, cell lysates were immunoprecipitated with ERα or mouse IgG antibodies. The immunoprecipitates were blotted with PLCγ, Src and ERα antibodies. (**f**) Co-immunoprecipitation and western blot analyses of PR, Src and PLCγ interactions in T47D-ERαY537S (TYS) cells. Cell lysates were immunoprecipitated with PR or mouse IgG antibodies. The immunoprecipitates were blotted with PLCγ, Src and PR antibodies.

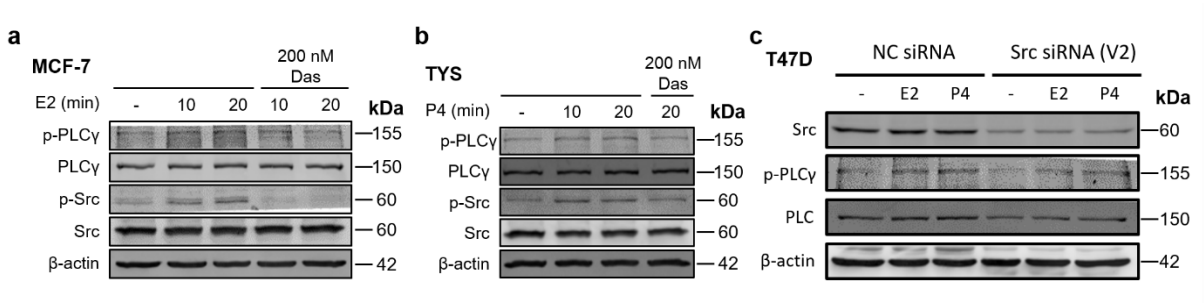

Figure 4.3 Src mediates steroid hormones-stimulated PLCγ phosphorylation. (**a**) Western blot analysis of phosphorylated PLCγ (p-PLCγ, tyrosine 783), total PLCγ, phosphorylated Src (p-Src), total Src and β-actin in ER^+ MCF-7 cells treated with a vehicle control or dasatinib (Das) for 5 min, followed by treatment with 10 nM E_2 for the indicated time. (**b**) Western blot analysis of p-PLCγ, total PLCγ, p-Src, total Src and β-actin in TYS (T47D-ERαY537S) cells treated with vehicle or dasatinib for 5 min, followed by treatment with 10nM progesterone (P_4) for the indicated time. (**c**) Western blot analysis of Src, p-PLCγ, PLCγ and β-actin protein levels following treatment of T47D cells with either 100 nM non-coding (NC) or Src siRNA SMARTpool (version 2), followed by treatment with vehicle, E_2 or P_4 for 30 min.

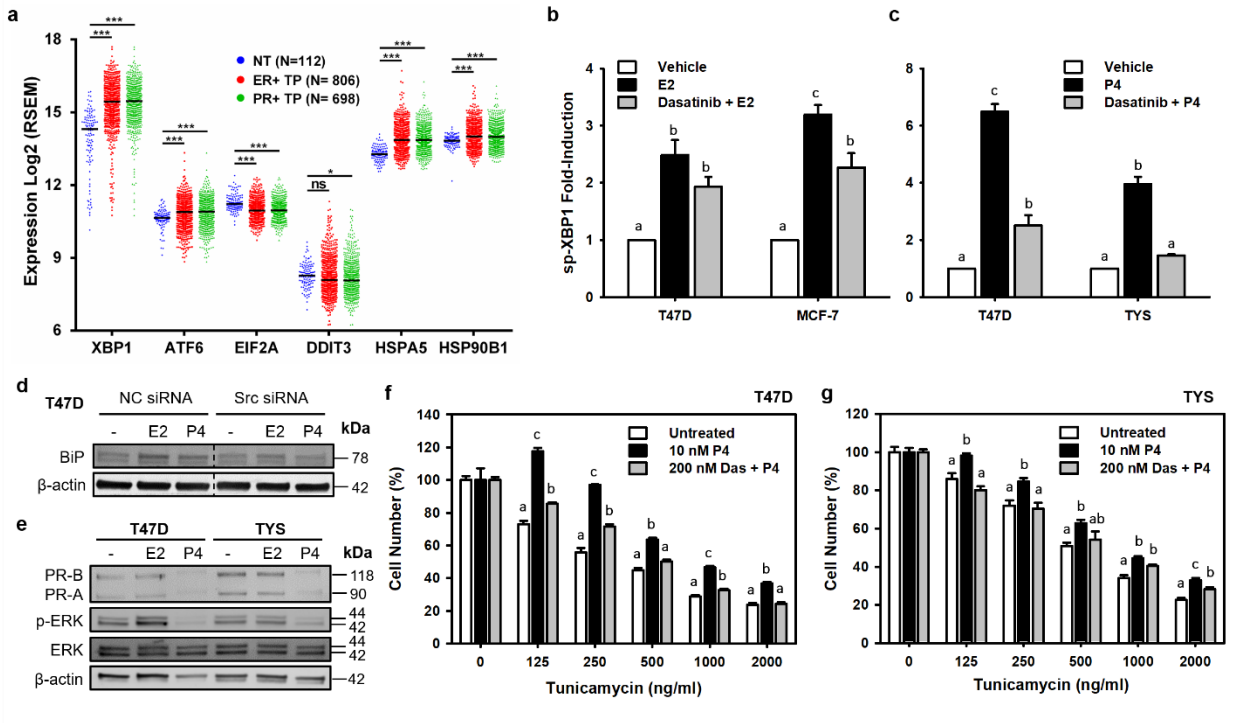

Figure 4.4 Estrogen and progesterone activate the protective anticipatory unfolded protein response through Src. (**a**) UPR marker gene expression in normal breast tissues (NT), ERα positive primary breast cancer (ER+ TP) and PR positive primary breast cancer (PR+ TP). * indicates a significant difference among groups using one-way ANOVA followed by Tukey's post hoc test. * $P < 0.05$, *** $P < 0.001$. (**b,c**) qRT-PCR analysis of spliced XBP1 (*sp-XBP1*) mRNA level in T47D cells treated for 15 min. with vehicle, or with 200 nM dasatinib, followed by treatment with vehicle, 10 nM E_2 (**b**) or P_4 (**c**) for 4 hr. Different letters indicate a significant difference among groups ($P<0.05$) using one-way ANOVA followed by Tukey's *post hoc* test (mean ± s.e.m., n = 3). (**d**) Western blotting analysis of BiP and β-actin protein levels following treatment of T47D cells with either 100 nM non-coding (NC) or Src siRNA SMARTpool, followed by treatment with vehicle, E_2 or P_4 for 4 hr. (**e**) Western blot analysis of PR, phosphorylated ERK (p-ERK), total ERK and β-actin protein levels in T47D cells and TYS cells treated with vehicle, 10 nM E_2 or 10 nM P_4 for 24 hr. (**f,g**) Weak dasatinib-sensitive anticipatory activation of UPR with progesterone protects cells against subsequent tunicamycin-induced cell death. T47D (**f**) and TYS (**g**) cells were maintained in medium with ethanol-vehicle (Untreated), 10 nM P_4 or P_4 plus 200 nM dasatinib for 48 hr. Vehicle control, P_4 and dasatinib were

Figure 4.4 (cont.) removed from medium and cells were then treated with the indicated concentrations of tunicamycin (TUN) for 96 hr. Different letters indicate a significant difference among groups ($P<0.05$) using one-way ANOVA followed by Tukey's *post hoc* test (mean ± s.e.m., n = 6).

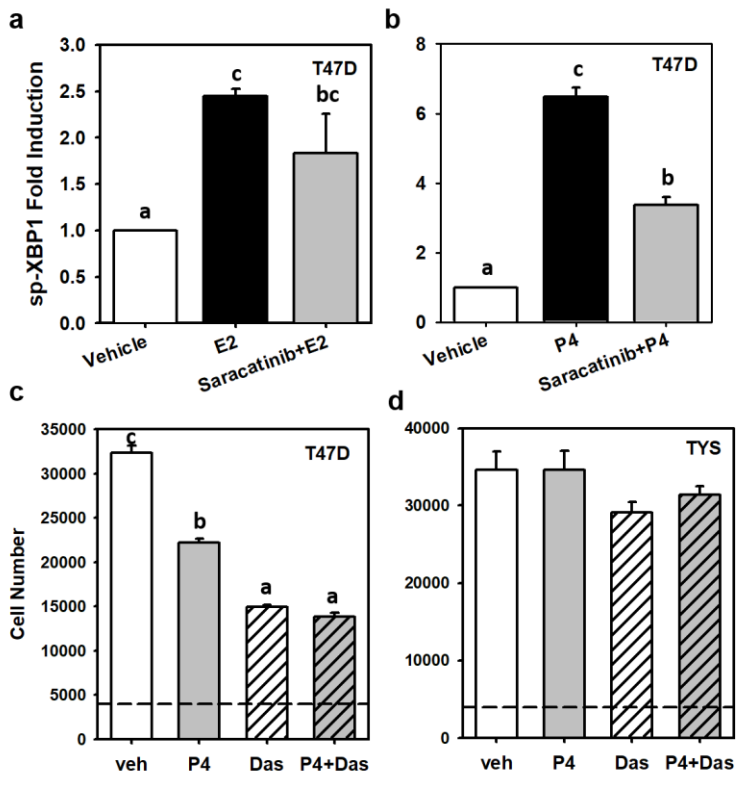

Figure 4.5 Steroid hormones activate anticipatory UPR through Src. (**a,b**) qRT-PCR analysis of spliced XBP1 (*sp-XBP1*) gene expression in T47D cells treated with vehicle or 100 nM saracatinib for 15 min, followed by treatment with vehicle, 10 nM E_2 (**a**) or P_4 (**b**) for 4 hr. Different letters indicate a significant difference among groups (P<0.05) using one-way ANOVA followed by Tukey's *post hoc* test (mean ± s.e.m., n = 3). (**c,d**) MTS assay of T47D (**c**) and TYS cells (**d**) treated with vehicle, 10 nM P_4, 200 nM dasatinib (Das) and P_4 + Das for 96 hr. (**d**) Different letters indicate a significant difference among groups (P < 0.05) using one-way ANOVA followed by Tukey's *post hoc* test (mean ± s.e.m., n = 6).

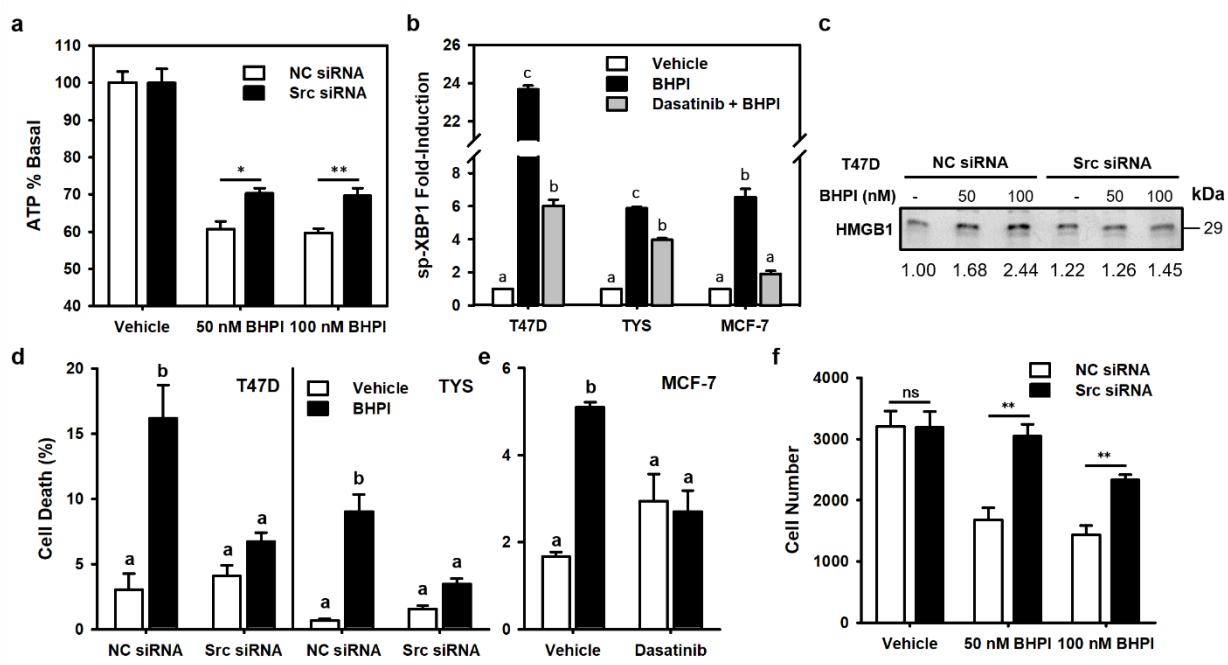

Figure 4.6 BHPI kills ERα positive breast cancer cells by hyperactivating the UPR through Src. (**a**) Src knockdown blocks cytotoxic BHPI-mediated ATP depletion. ATP level analysis following treatment of T47D cells with either 100 nM NC siRNA or Src siRNA SMARTpool, followed by treatment for 24 hr. with vehicle or the indicated concentration of BHPI. * indicates a significant difference among groups using Student's t-test. * P< 0.05, ** P < 0.005 (mean ± s.e.m., n = 6). (**b**) qRT-PCR analysis of sp-XBP1 gene expression in T47D, TYS and MCF-7 cells treated with vehicle or 200 nM dasatinib for 15 min., followed by treatment with vehicle or 100 nM BHPI. Different letters indicate a significant difference among groups (P<0.05) using one-way ANOVA followed by Tukey's *post hoc* test (mean ± s.e.m., n = 3). (**c**) Western blot analysis of BHPI-stimulated HMGB1 release into the cell culture medium at 50 or 100 nM BHPI following treatment of T47D cells with either 100 nM NC or Src siRNA SMARTpool. (**d**) Src knockdown blocks BHPI-induced cell death. T47D and TYS cells were treated with 100 nM NC or Src siRNA followed by treatment with 100 nM BHPI for 24 (T47D) or 1 hr (TYS). (**e**) Inhibiting Src activity blocks BHPI-induced cell death. MCF-7 cells were treated with 2 hr. treatment with vehicle, 100 nM BHPI, 200 nM dasatinib or dasatinib + BHPI. (**d,e**) Cell death was monitored by an automated trypan blue assay. Different letters indicate a significant difference among groups (P<0.05) using one-way ANOVA followed by Tukey's *post hoc*

Figure 4.6 (cont.) test (mean ± s.e.m., n = 3). (**f**) MTS assay following treatment of T47D cells with either 100 nM NC or Src siRNA SMARTpool, followed by treatment with vehicle or indicated concentration of BHPI for 72 hr. * indicates a significant difference among groups using Student's t-test. ** $P < 0.005$, ns not significant (mean ± s.e.m., n = 6).

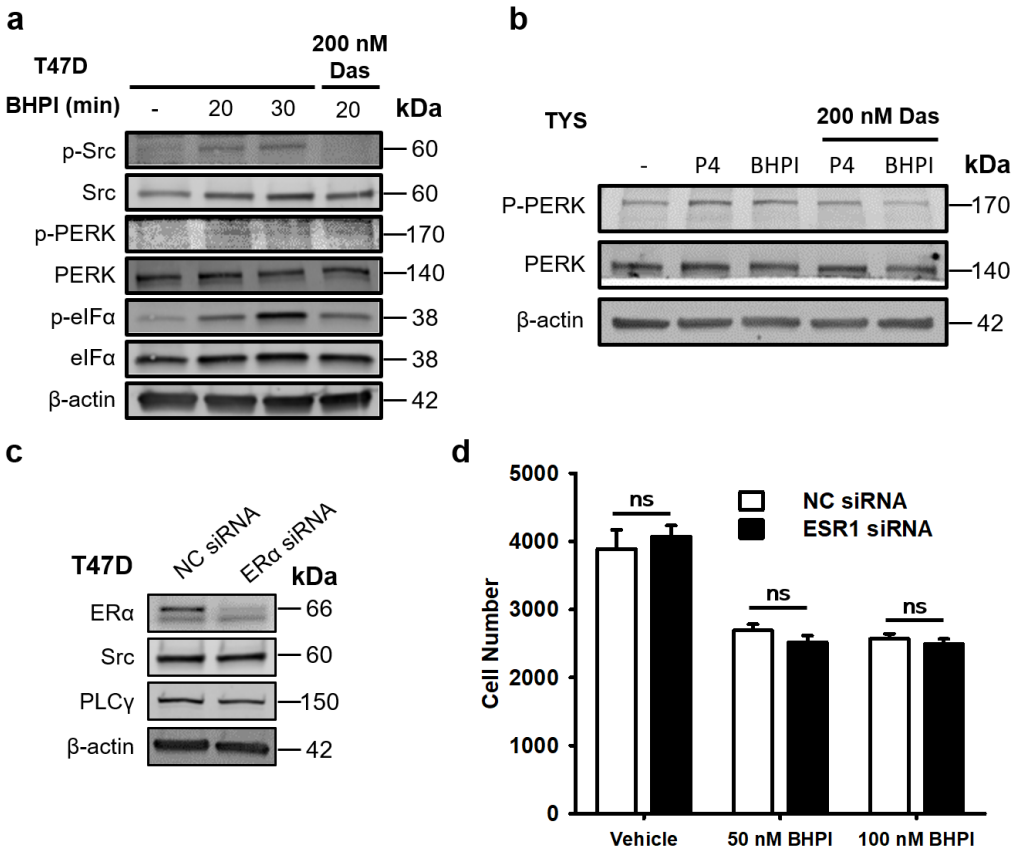

Figure 4.7 BHPI hyperactivates UPR through Src kinase. (**a**) Western blot of p-Src, total Src, phosphorylated PERK (p-PERK), total PERK, phosphorylated eIF2α (p-eIF2α), total eIF2α and β-actin in T47D cells treated with a vehicle control or dasatinib for 5 min, followed by treatment with 100nM BHPI for the indicated time. (**b**) Western blot of p-PERK, total PERK and β-actin in TYS cells treated with a vehicle control or dasatinib for 5 min, followed by treatment with 10 nM P_4 or 100nM BHPI for 20 min. (**c**) Western blot of ERα, Src, PLCγ and β-actin following treatment of T47D cells with either 100 nM NC or ERα siRNA SMARTpool. (**d**) MTS assay following treatment of T47D cells with either 100 nM NC or ERα siRNA SMARTpool, followed by treatment with vehicle or the indicated concentration of BHPI for 48 hr. ns not significant (mean ± s.e.m., n = 6).

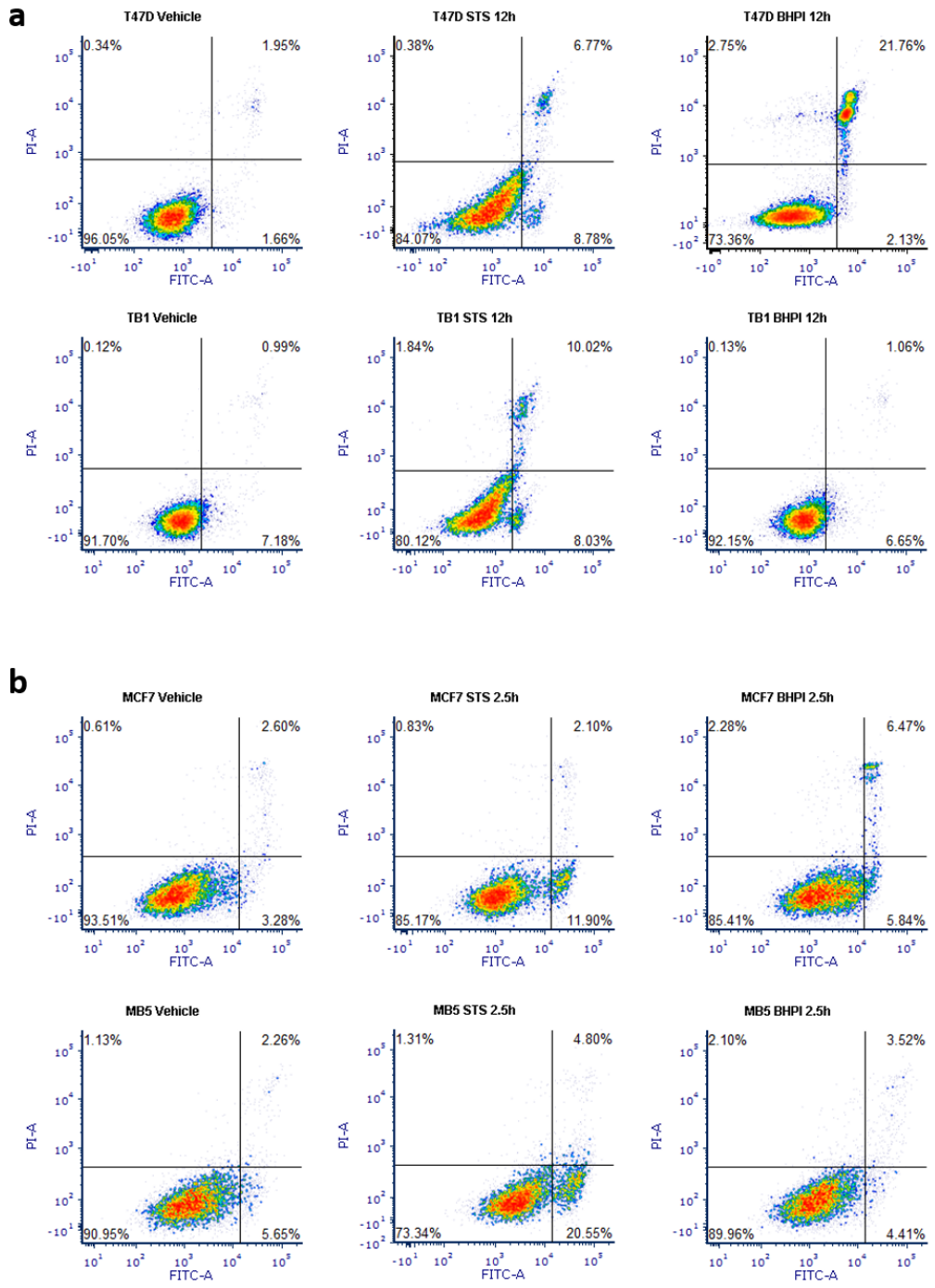

Figure 4.8 BHPI resistant cells remain sensitive to an apoptosis inducer. (**a**) Flow cytometry histograms of annexin V-FITC (FITC-A) and propidium iodide (PI) staining of T47D and TB1 cells after treatment with 1 μM staurosporine (STS) or 1 μM BHPI for 12 hr. (**b**) Flow cytometry histograms of annexin V-FITC and PI staining of MCF-7 and MB5 cells after treatment with 1 μM STS or 1 μM BHPI for 2.5 hr.

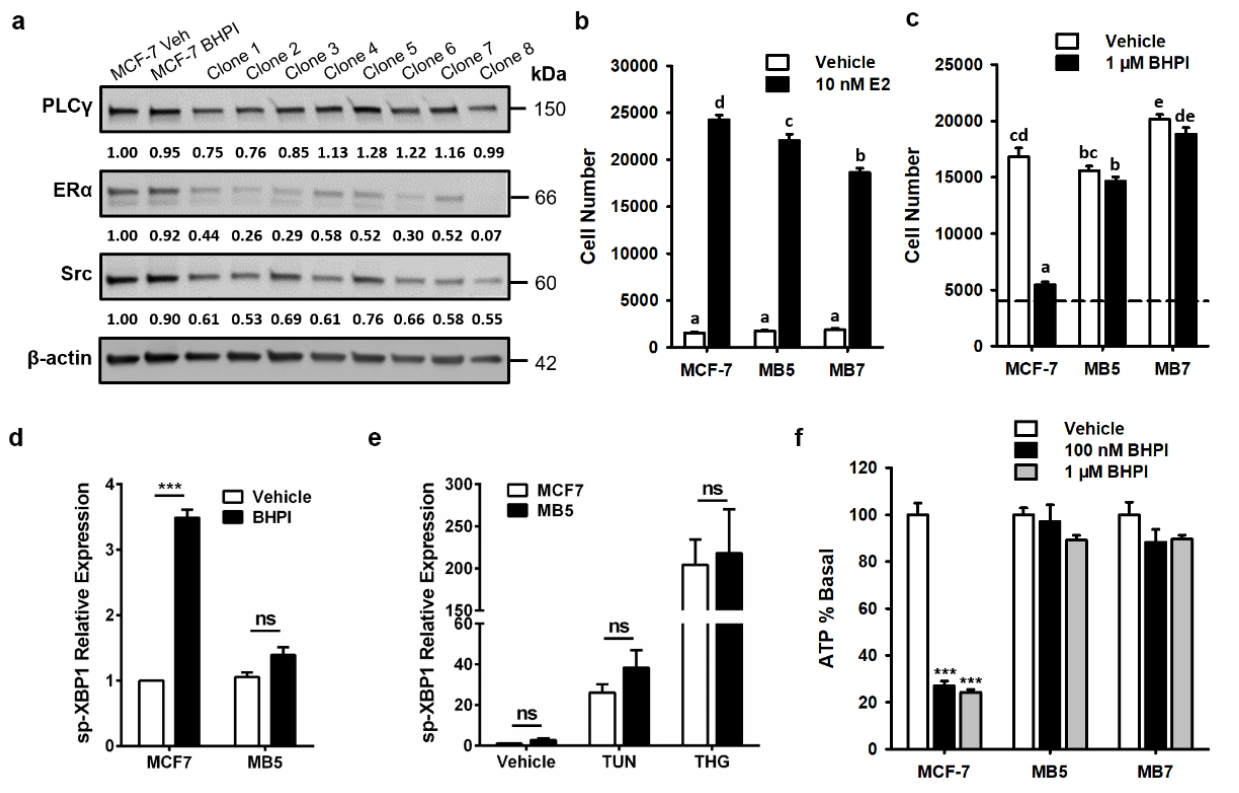

Figure 4.9 Identification and characterization of the BHPI-resistant MCF-7 clones. (**a**) Western blot analysis of PLCγ, ERα, Src and β-actin in MCF-7 parental cells and BHPI resistant clones treated with vehicle or 5 μM BHPI. All BHPI resistant clones were cultured in medium containing 5 μM BHPI. (**b,c**) Proliferation of MCF-7 and resistant clones treated with vehicle, 10 nM E_2 (**b**) and 1 μM BHPI (**c**) for 96 hr. Different letters indicate a significant difference among groups ($P<0.05$) using one-way ANOVA followed by Tukey's *post hoc* test (mean ± s.e.m., n = 6). (**d, e**) qRT-PCR analysis of sp-XBP1 gene expression in MCF-7 and BHPI resistant clone MB5 treated for with either vehicle, or 1 μM BHPI for 4 hr (**d**), or 10 μg/ml tunicamycin (TUN) or 1 μM thapsigargin (THG) for 2 hr (**e**). * indicates a significant difference among groups using one-way ANOVA followed by Tukey's *post hoc* test. *** $P < 0.001$ (mean ± s.e.m., n = 3). (**f**) ATP levels in MCF-7 and BHPI-resistant clones treated with vehicle or indicated concentrations of BHPI for 24 hr. * indicates a significant difference among groups using Student's t-test. *** $P < 0.001$ (mean ± s.e.m., n = 4).

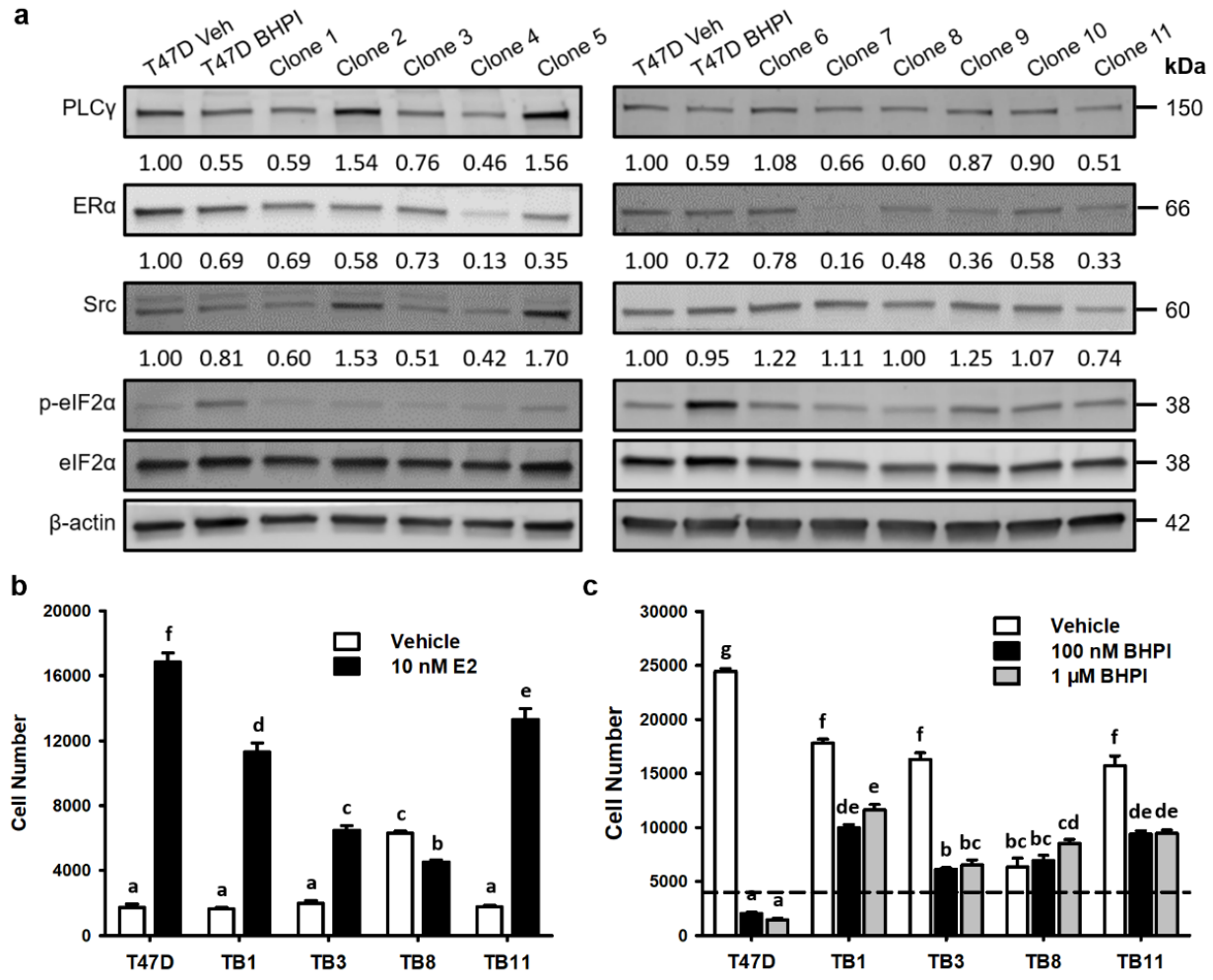

Figure 4.10 Identification and characterization of the BHPI-resistant clones. (**a**) Western blot of PLCγ, ERα, Src, phosphorylated eIF2α (p-eIF2α), eIF2α and β-actin in T47D parental cells and BHPI resistant clones treated with vehicle or 1 μM BHPI. All BHPI resistant clones were cultured in medium containing 1 μM BHPI. (**b**) Proliferation of T47D and resistant clones treated with vehicle, 10 nM E_2 and indicated concentrations of BHPI (**c**) for 96 hr. (**b,c**) Different letters indicate a significant difference among groups ($P < 0.05$) using one-way ANOVA followed by Tukey's *post hoc* test (mean ± s.e.m., n = 6).

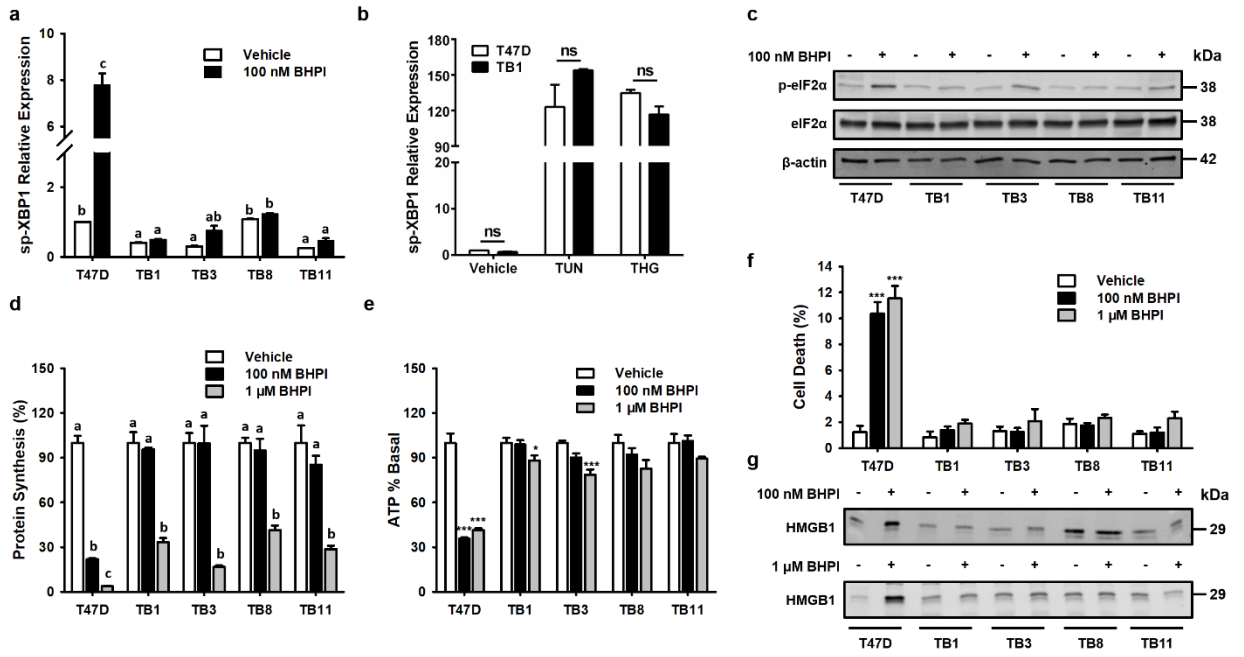

Figure 4.11 Src downregulation confers BHPI resistance on breast cancer cells. (**a, b**) qRT-PCR analysis of sp-XBP1 gene expression in wild type T47D and in BHPI-resistant clones treated with vehicle or 100 nM BHPI for 4 hr (**a**), 10 μg/ml tunicamycin (TUN) or 1 μM thapsigargin (THG) for 2 hr (**b**). Different letters (**a**) or * (**b**) indicate a significant difference among groups ($P < 0.05$) using one-way ANOVA followed by Tukey's *post hoc* test. *** $P < 0.001$ (mean ± s.e.m., n = 3). (**c**) Western blot of p-eIF2α, total eIF2α and β-actin protein levels in T47D and BHPI-resistant clones treated with vehicle or 100 nM BHPI for 1 hr. (**d**) Protein synthesis assay in T47D and BHPI-resistant clones treated with vehicle, 100 nM BHPI and 1 μM BHPI for 1 hr (mean ± s.e.m., n=4). (**e**) ATP levels in T47D cells and BHPI-resistant clones treated with vehicle or the indicated concentrations of BHPI for 24 hr. * indicates a significant difference among groups using Student's t-test. * $P< 0.05$, *** $P < 0.001$ (mean ± s.e.m., n = 6). (**f**) Trypan blue exclusion assay for cell death in T47D and BHPI-resistant clones after 24 hr. treatment with vehicle, 100 nM BHPI or 1 μM BHPI. * indicates a significant difference among groups using one-way ANOVA followed by Tukey's *post hoc* test. *** $P < 0.001$ (mean ± s.e.m., n = 3). (**g**) Western blot showing HMGB1 release into the cell culture medium in 100 nM and 1 μM of BHPI.

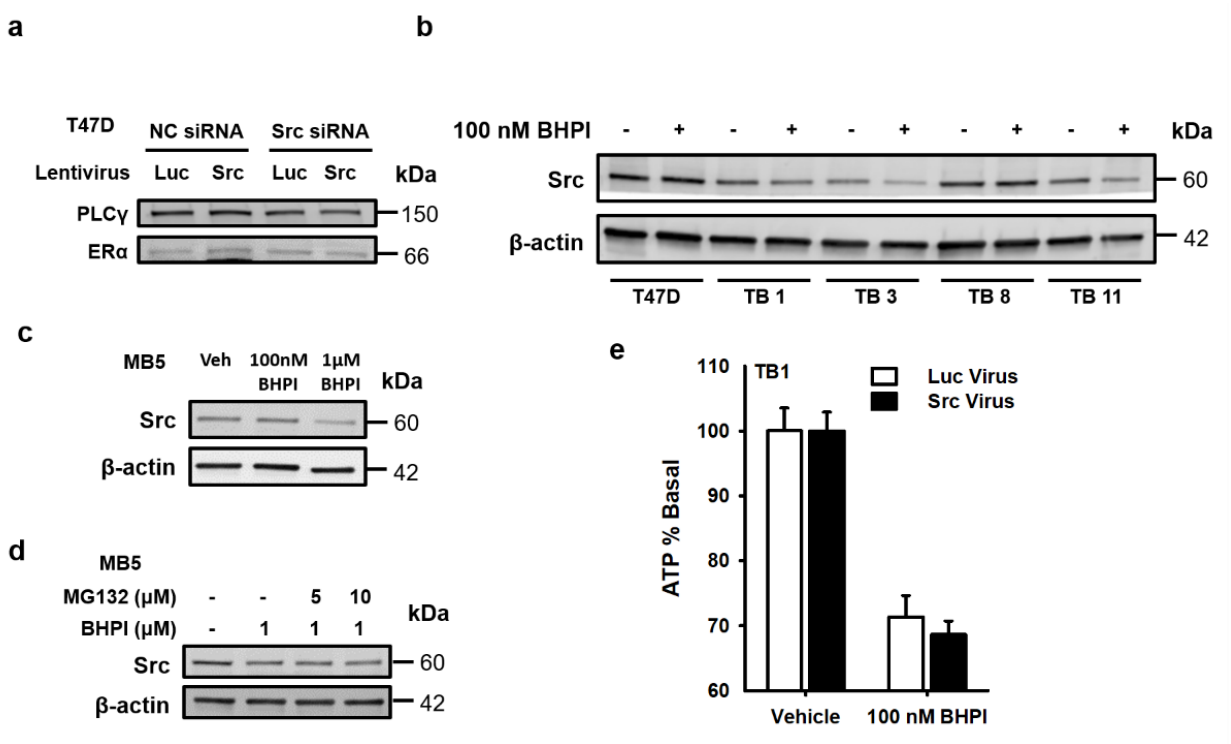

Figure 4.12 BHPI rapidly downregulates Src expression in BHPI resistant breast cancer cells. (**a**) Western blot of PLCγ and ERα of T47D cells transduced with luciferase-expressing virus or Src-expressing virus following knockdown with either 100 nM NC or Src siRNA SMARTpool. All cells were treated with 100 nM BHPI for 24 hr. (**b**) Western blot analysis of Src and β-actin protein levels in T47D and BHPI resistant clones treated with vehicle or 100nM BHPI for 1 hr. (**c**) Western blot analysis of Src and β-actin protein levels in MB 5 treated with vehicle, 100 nM and 1 μM BHPI for 1 hr. (**d**) Western blot of Src and β-actin protein levels in MB5 cells treated with vehicle, 5 μM or 10 μM MG132 for 15 min. followed treatment with vehicle or 1 μM BHPI for 1 hr. (**e**) ATP levels in TB1 cells treated with vehicle or 100 nM BHPI for 1 hr. following viral transduction with control virus or Src-expressing virus. (mean ± s.e.m., n = 4).

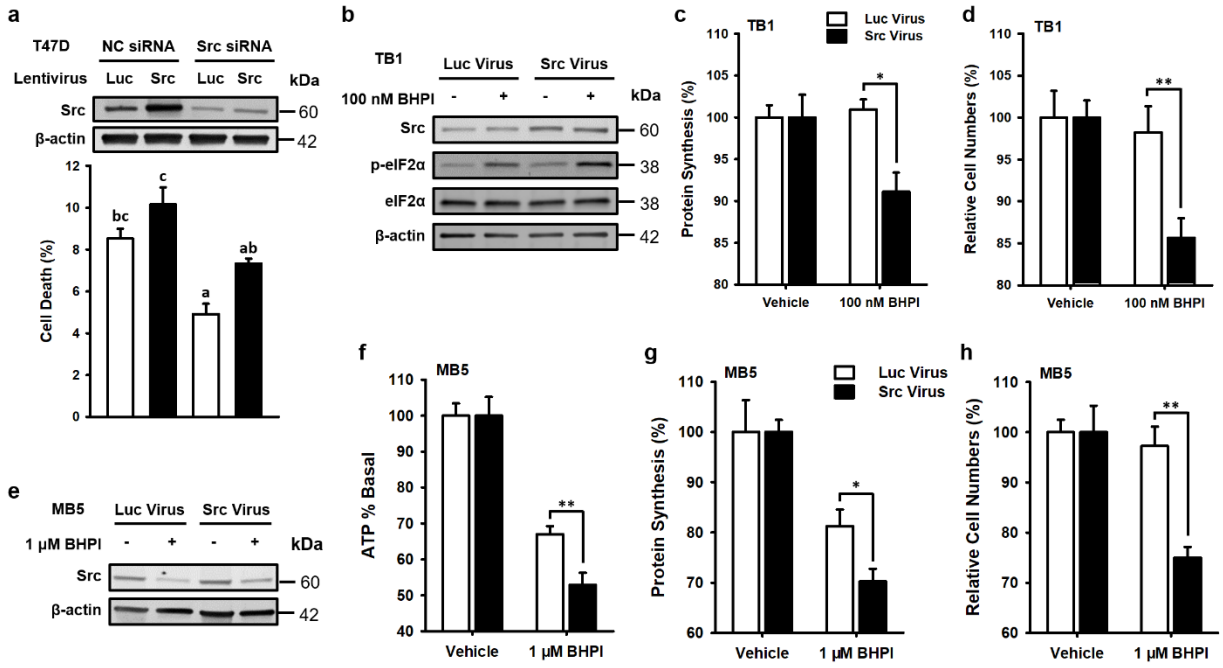

Figure 4.13 Src overexpression partially restores sensitivity to BHPI in BHPI resistant cells. (**a-h**) For all virus transduction experiments, cells were cultured in medium containing virus for 24 hr., then kept in virus-free medium for 24 hr. to allow protein overexpression. (**a**) Western blot of Src and β-actin and trypan blue exclusion viability assay of T47D cells transduced with luciferase-expressing virus or Src-expressing virus following knockdown with either 100 nM NC or Src siRNA SMARTpool. All cells were treated with 100 nM BHPI for 24 hours. Different letters indicate a significant difference among groups ($P < 0.05$) using one-way ANOVA followed by Tukey's *post hoc* test (mean ± s.e.m., n = 3). (**b**) Western blot of Src, p-eIF2α, total eIF2α and β-actin protein levels in TB1 cells treated with vehicle or 100 nM BHPI for 1 hr. following viral transduction with control virus or Src-expressing virus. (**c**) Protein synthesis in TB1 cells treated with vehicle or 100 nM BHPI for 1 hr. following viral transduction with control virus or Src-expressing virus (mean ± s.e.m., n = 4). (**d**) MTS assay of TB1 cells treated with vehicle or 100 nM BHPI for 96 hr. following viral transduction with control virus or Src-expressing virus. (mean ± s.e.m., n = 6). (**e**) Western blot of Src and β-actin in MB5 cells treated with vehicle or 1 μM BHPI for 8 hr. following viral transduction with luciferase-expressing virus or Src-expressing virus. (**f**) ATP level in MB5 cells treated with vehicle or 1 μM BHPI for 1 hr. following viral transduction with control virus or Src-expressing

Figure 4.13 (cont.) virus (mean ± s.e.m., n = 4). (**g**) Protein synthesis in MB5 cells treated with vehicle or 1 μM BHPI for 1 hr. following viral transduction with control virus or Src-expressing virus (mean ± s.e.m., n = 4). (**h**) MTS assay of MB5 cells treated with vehicle or 1 μM BHPI for 72 hr. following viral transduction with control virus or Src-expressing virus (mean ± s.e.m., n = 6). (**c,d,f,g,h**) * indicates a significant difference among groups using Student's t-test. * $P < 0.05$, ** $P < 0.005$.

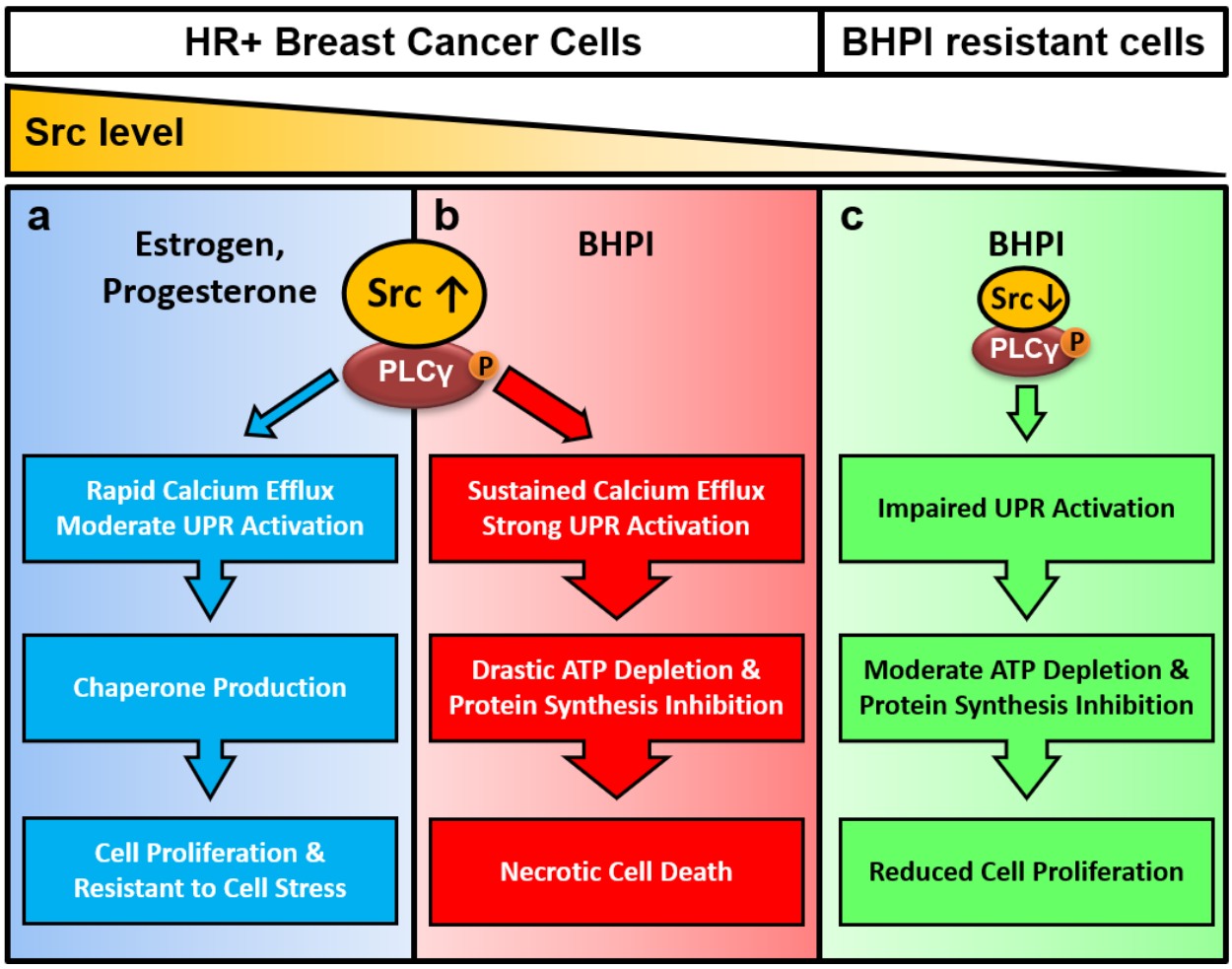

Figure 4.14 Graphic summary depicting correlation between Src level and anticipatory UPR activation. (**a**) Elevated Src expression in steroid hormone receptor positive (HR+) breast cancer cells facilitates E_2- or P_4-stimulated UPR activation and protects cells from accumulated UPR stress. (**b**) BHPI takes advantage of Src overexpression, hyperactivates the anticipatory UPR and tips the scale from protective to lethal. (**c**) In BHPI-resistant cells, reduced Src expression disrupts UPR activation, therefore allows breast cancer cells to survive under otherwise lethal concentrations of BHPI.

REFERENCES

1. Walter P, Ron D. The unfolded protein response: from stress pathway to homeostatic regulation. Science. 2011;334(6059):1081-6.

2. Gass JN, Gifford NM, Brewer JW. Activation of an unfolded protein response during differentiation of antibody-secreting B cells. J Biol Chem. 2002;277(50):49047-54.

3. Andruska N, Zheng X, Yang X, Helferich WG, Shapiro DJ. Anticipatory estrogen activation of the unfolded protein response is linked to cell proliferation and poor survival in estrogen receptor alpha-positive breast cancer. Oncogene. 2015;34(29):3760-9.

4. Yu L, Andruska N, Zheng X, Shapiro DJ. Anticipatory Activation of the Unfolded Protein Response by Epidermal Growth Factor is Required for Immediate Early Gene Expression and Cell Proliferation. Mol Cell Endocrinol. 2016;422:31-41.

5. Karali E, Bellou S, Stellas D, Klinakis A, Murphy C, Fotsis T. VEGF Signals through ATF6 and PERK to Promote Endothelial Cell Survival and Angiogenesis in the Absence of ER Stress. Mol Cell. 2014;54(4):559-72.

6. Shapiro DJ, Livezey M, Yu L, Zheng X, Andruska N. Anticipatory UPR activation: A protective pathway and target in cancer. Trends in Endocrinology & Metabolism. 2016;27(10):731-41.

7. Zheng X, Andruska N, Yu L, Mao C, Kim JE, Livezey M, et al. Interplay between steroid hormone activation of the unfolded protein response and nuclear receptor action. Steroids. 2016;114:2-6.

8. Yeatman TJ. A renaissance for SRC. Nat Rev Cancer. 2004;4(6):470.

9. Zhang S, Yu D. Targeting Src family kinases in anti-cancer therapies: turning promise into triumph. Trends Pharmacol Sci. 2012;33(3):122-8.

10. Frame MC. Src in cancer: deregulation and consequences for cell behaviour. Biochimica et Biophysica Acta (BBA)-Reviews on Cancer. 2002;1602(2):114-30.

11. Migliaccio A, Piccolo D, Castoria G, Di Domenico M, Bilancio A, Lombardi M, et al. Activation of the Src/p21ras/Erk pathway by progesterone receptor via cross-talk with estrogen receptor. The EMBO journal. 1998;17(7):2008-18.

12. Song RX, Zhang Z, Santen RJ. Estrogen rapid action via protein complex formation involving ERα and Src. Trends in Endocrinology & Metabolism. 2005;16(8):347-53.

13. Barletta F, Wong C-W, McNally C, Komm BS, Katzenellenbogen B, Cheskis BJ. Characterization of the interactions of estrogen receptor and MNAR in the activation of cSrc. Mol Endocrinol. 2004;18(5):1096-108.

14. Boonyaratanakornkit V, Scott MP, Ribon V, Sherman L, Anderson SM, Maller JL, et al. Progesterone receptor contains a proline-rich motif that directly interacts with SH3 domains and activates c-Src family tyrosine kinases. Mol Cell. 2001;8(2):269-80.

15. Malhotra JD, Kaufman RJ. Endoplasmic reticulum stress and oxidative stress: a vicious cycle or a double-edged sword? Antioxidants & redox signaling. 2007;9(12):2277-94.

16. Verfaillie T, Garg AD, Agostinis P. Targeting ER stress induced apoptosis and inflammation in cancer. Cancer Lett. 2013;332(2):249-64.

17. Breckenridge DG, Stojanovic M, Marcellus RC, Shore GC. Caspase cleavage product of BAP31 induces mitochondrial fission through endoplasmic reticulum calcium signals, enhancing cytochrome c release to the cytosol. The Journal of cell biology. 2003;160(7):1115-27.

18. Livezey M, Huang R, Hergenrother PJ, Shapiro DJ. Strong and sustained activation of the anticipatory unfolded protein response induces necrotic cell death. Cell Death & Differentiation. 2018;25(10):1796–807.

19. Andruska ND, Zheng X, Yang X, Mao C, Cherian MM, Mahapatra L, et al. Estrogen receptor α inhibitor activates the unfolded protein response, blocks protein synthesis, and induces tumor regression. Proc Natl Acad Sci. 2015;112(15):4737-42.

20. Mao C, Livezey M, Kim JE, Shapiro DJ. Antiestrogen Resistant Cell Lines Expressing Estrogen Receptor alpha Mutations Upregulate the Unfolded Protein Response and are Killed by BHPI. Sci Rep. 2016;6:34753.

21. Zheng X, Andruska N, Lambrecht MJ, He S, Parissenti A, Hergenrother PJ, et al. Targeting multidrug-resistant ovarian cancer through estrogen receptor α dependent ATP depletion caused by hyperactivation of the unfolded protein response. Oncotarget. 2018;9(19):14741.

22. Yu L, Wang L, Mao C, Duraki D, Kim JE, Huang R, et al. Estrogen-Independent Myc Overexpression Confers Endocrine Therapy Resistance on Breast Cancer Cells Expressing ERαY537S and ERαD538G Mutations. Cancer Lett. 2019;442:373-82.

23. Levin ER, Hammes SR. Nuclear receptors outside the nucleus: extranuclear signalling by steroid receptors. Nature reviews Molecular cell biology. 2016;17(12):783-97.

24. Dong D, Ni M, Li J, Xiong S, Ye W, Virrey JJ, et al. Critical role of the stress chaperone GRP78/BiP in tumor proliferation, survival, and tumor angiogenesis in transgene-induced mammary tumor development. Cancer Res. 2008;68(2):498-505.

25. Yoshida H, Matsui T, Yamamoto A, Okada T, Mori K. XBP1 mRNA is induced by ATF6 and spliced by IRE1 in response to ER stress to produce a highly active transcription factor. Cell. 2001;107(7):881-91.

26. Roskoski Jr R. Src protein-tyrosine kinase structure, mechanism, and small molecule inhibitors. Pharmacol Res. 2015;94:9-25.

27. Fan P, Griffith OL, Agboke FA, Anur P, Zou X, McDaniel RE, et al. c-Src modulates estrogen-induced stress and apoptosis in estrogen-deprived breast cancer cells. Cancer Res. 2013;73(14):4510-20.

28. Nakanishi O, Shibasaki F, Hidaka M, Homma Y, Takenawa T. Phospholipase C-gamma 1 associates with viral and cellular src kinases. J Biol Chem. 1993;268(15):10754-9.

29. Khare S, Bolt M, Wali R, Skarosi S, Roy H, Niedziela S, et al. 1, 25 dihydroxyvitamin D3 stimulates phospholipase C-gamma in rat colonocytes: role of c-Src in PLC-gamma activation. J Clin Invest. 1997;99(8):1831.

30. Dong D-J, Jing Y-P, Liu W, Wang J-X, Zhao X-F. The steroid hormone 20-hydroxyecdysone upregulates Ste-20 family serine/threonine kinase Hippo to induce programmed cell death. J Biol Chem. 2015:jbc. M115. 643783.

31. Jing Y-P, Liu W, Wang J-X, Zhao X-F. The steroid hormone 20-hydroxyecdysone via non-genomic pathway activates Ca2+/calmodulin-dependent protein kinase II to regulate gene expression. J Biol Chem. 2015:jbc. M114. 622696.

32. Liu W, Cai M-J, Zheng C-C, Wang J-X, Zhao X-F. Phospholipase C gamma 1 connects the cell membrane pathway to the nuclear receptor pathway in insect steroid hormone signaling. J Biol Chem. 2014:jbc. M113. 547018.

33. Sharma R, Quilty F, Gilmer JF, Long A, Byrne A-M. Unconjugated secondary bile acids activate the unfolded protein response and induce golgi fragmentation via a src-kinase-dependant mechanism. Oncotarget. 2017;8(1):967.

34. Ng MM, Chang F, Burgess DR. Movement of membrane domains and requirement of membrane signaling molecules for cytokinesis. Dev Cell. 2005;9(6):781-90.

35. Robinson DR, Wu Y-M, Vats P, Su F, Lonigro RJ, Cao X, et al. Activating ESR1 mutations in hormone-resistant metastatic breast cancer. Nat Genet. 2013;45(12):1446-51.

36. Toy W, Shen Y, Won H, Green B, Sakr RA, Will M, et al. ESR1 ligand-binding domain mutations in hormone-resistant breast cancer. Nat Genet. 2013;45(12):1439-45.

37. Watson PA, Arora VK, Sawyers CL. Emerging mechanisms of resistance to androgen receptor inhibitors in prostate cancer. Nat Rev Cancer. 2015;15(12):701.

38. Harris KF, Shoji I, Cooper EM, Kumar S, Oda H, Howley PM. Ubiquitin-mediated degradation of active Src tyrosine kinase. Proc Natl Acad Sci. 1999;96(24):13738-43.

39. Roskoski R. Src kinase regulation by phosphorylation and dephosphorylation. Biochem Biophys Res Commun. 2005;331(1):1-14.

40. Taipale M, Krykbaeva I, Koeva M, Kayatekin C, Westover KD, Karras GI, et al. Quantitative analysis of HSP90-client interactions reveals principles of substrate recognition. Cell. 2012;150(5):987-1001.

41. An WG, Schulte TW, Neckers LM. The heat shock protein 90 antagonist geldanamycin alters chaperone association with p210bcr-abl and v-src proteins before their degradation by the proteasome. Cell Growth and Differentiation-Publication American Association for Cancer Research. 2000;11(7):355-60.

42. Kamei Y, Xu L, Heinzel T, Torchia J, Kurokawa R, Gloss B, et al. A CBP integrator complex mediates transcriptional activation and AP-1 inhibition by nuclear receptors. Cell. 1996;85(3):403-14.

CHAPTER 5

DISCUSSION

Estrogen (E_2), acting through estrogen receptor α (ERα), stimulates breast cancers proliferation and metastasis. Endocrine therapies using aromatase inhibitors, selective ER modulators (SERMs) and selective ER degraders (SERDs), inhibit E_2:ERα activities, and are mainstays in treatment of ERα positive breast cancers (1). Even though these endocrine therapies are effective initially, selection and outgrowth of breast cancer cells resistant to endocrine therapy is common (2-4). The mechanisms underlying endocrine resistance are complex, however, with the advent of powerful DNA sequencing techniques, clustered mutations in the ERα LBD were identified in 20-40% of ERα positive metastatic breast cancers (3, 5-8). While all metastatic ERα positive breast cancers display resistance to endocrine therapy and ultimately to standard chemotherapy, patients with tumors harboring the common ERαY537S and ERαD538G mutations exhibit 1-year and 6-month shorter median survival than patients whose metastatic tumors contain wild type ERα (9). To explore roles of these mutations, viral transduction, CRISPR/Cas9 and long-term-estrogen-deprivation were used to express ERα LBD mutations in breast cancer cells (10-13).

Studies on breast cancer cells bearing ESR1 mutations are limited and were either restricted to a single mutation (10), or lacked extensive functional analysis (13). We, using RNA sequencing, compared T47D cells harboring ERαY537S and ERαD538G mutations and parental cells at two time points and confirmed several key observations with the MCF-7 dataset. Surprisingly, multidimensional scaling (MDS) analysis show that the

mutations are not simply constitutively active ERα, and instead exhibit unique gene expression patterns. Moreover, we demonstrated that Y537S and D538G ESR1 mutations are sufficient to confer on breast cancer cells partial resistance to antiestrogens and estrogen-independent cell proliferation. Compared to cells expressing ERαD538G, we and others, observe increased antiestrogen resistance in cell lines expressing ERαY537S (11, 13).

Previous studies focused almost entirely on proliferation-related properties of ESR1 mutations. However, ESR1 mutations were detected at higher allele frequency in metastases than in the primary breast cancers (8, 14). To probe the role of ESR1 mutations in metastasis-related properties we improved the wildly used trans-well assay (15) which over simplified the complicated process of metastasis. To better quantify cell numbers, we replaced traditional crystal violet staining with luciferase-expressing lentivirus transduction, or luciferase gene transfection. Our modified invasion-dissociation-rebinding (IDR) assay quantitates both the number of invaded cells and the number of invaded cells that then dissociate from the underside of the membrane and rebind on the bottom of the well. In the *in vitro* invasion-dissociation-rebinding assay, ERα mutations significantly increase both T47D cell invasion and dissociation-rebinding. Moreover, the dramatic increase in lung metastasis of TYS tumors compared to TDG tumors was not predicted by the conventional Matrigel and collagen invasion assays, but was better correlated with the dissociation-rebinding properties seen in the IDR assay. Our data shows that, compared to the traditional Matrigel invasion assay, our simple *in vitro* IDR assay explores cell properties that correlate with *in vivo* metastatic frequency and provides a useful *in vitro* model for investigation of metastasis-related properties.

To identify pathways contributing to these aggressive phenotypes of ERα mutant cells, we performed Gene Set Enrichment Analysis (GSEA) using T47D and MCF-7 RNAseq datasets. Using GSEA, we identified Myc target genes as one of the highly enriched pathway in ERα mutant cells; other upregulated pathways like “E2F targets” and “G2M checkpoint” are tightly correlated with Myc expression. Myc directly induces expression of cell cycle regulators, including Cyclin D, Cyclin E and E2Fs (16-18) and promotes cell cycle progression by regulating CDK phosphorylation and antagonizing cell cycle inhibitor expression (19, 20). Myc knockdown demonstrated that Myc is necessary for E_2-independent proliferation of the ERα mutant cells. Constitutive Myc expression in E_2-deprived parental cells was sufficient to induce moderate E_2-independent proliferation. Myc overexpression in tumors has been correlated with cancer stemness, which leads to reduced responsiveness to anticancer drugs and increased metastatic potential (21, 22). In breast cancer cells, overexpression of Myc and its downstream targets Cyclin E1 and Cyclin D1 results in decreased sensitivity to antiestrogens (23, 24). An analysis of Myc in 399 patients with ERα positive breast cancer showed that higher levels of Myc expression were associated with shorter relapse free survival (24). Notably, while these studies and our data demonstrate an important role for Myc in proliferation-related phenotypes and therapy resistance, Myc expression in T47D cells had no effect on metastasis-related invasion, dissociation and rebinding.

In addition to Myc upregulation, the ERα mutant breast cancer cells exhibit alterations in protective pathways associated with resistance to cell death. The unfolded protein response (UPR) was upregulated in E_2-treated T47D and MCF7 cells and in ERαY537S and ERαD538G mutants. UPR upregulation is consistent with our recent work

demonstrating E2-activation of the anticipatory UPR in ERα containing T47D and MCF-7 breast cancer cells (25), in PEO4 ovarian cancer cells (26), and estrogen-independent UPR activation in TYS and TDG cells (12). This pathway is unlike conventional reactive UPR activation in which cells respond to stress by activating a protective moderate UPR pathway (27, 28). In our study, we describe a fundamentally different type of very rapid UPR activation that anticipates future needs and occurs in the absence of cell stress or accumulation of unfolded proteins. In less than 2 minutes, mitogenic hormones trigger PLCγ-mediated production of inositol triphosphate (IP_3). IP_3 binds to and opens the endoplasmic reticulum IP_3R calcium channels releasing Ca^{2+} stored in the lumen of endoplasmic reticulum into the cytosol. This increase in cytosol Ca^{2+} stimulates activation of all three arms of the UPR. This anticipatory activation of the UPR is a newly identified pathway shared by several mitogenic hormones. We suggest this newly unveiled pathway is used by many, but not all, mitogenic hormones to prepare cells for the increased protein folding capacity that may company subsequent hormone-stimulated cell proliferation. Although this pathway is conserved from peptide hormones to steroid hormones, there are important differences in the activation mechanisms. VEGF induced UPR activation is not inhibited by blocking the ER calcium signal (29). However, EGF mediated activation of the UPR is totally dependent on IP_3 mediated calcium release from the endoplasmic reticulum.

Since a key feature of rapid anticipatory activation of the UPR is an increase in cytosolic calcium, we explored the effect of blocking calcium increase on well-characterized actions of EGF-EGFR. The mitogenic action of EGF is mediated in part by regulation of immediate early gene expression. Two major EGF-induced immediate early

genes, *c-fos* and *egr1* encode transcription factors important for cell cycle progression (30, 31). Rapid EGF:EGFR activation of the ERK signaling pathway is essential for induction of immediate early genes (32). Cytosolic calcium levels play an important role in regulating ERK activation (33, 34). However, blocking the transient and moderate increase in cytosol Ca^{2+} induced by EGF:EGFR activation had no effect on inhibiting EGF:EGFR stimulated ERK or AKT activation. Since blocking the EGF-induced increase in cytosol Ca^{2+} abolished induction and repression of gene expression by EGF, the anticipatory UPR pathway is not regulating immediate early gene expression through the ERK pathway. Transient calcium increase in the cytosol and ERK activation are two independent pathways regulated by EGF:EGFR that converge at the level of immediate early gene expression regulation.

These results indicate that the EGF induced anticipatory UPR pathway facilitates EGF stimulated cell proliferation in at least two ways. First, it increases UPR chaperone production, which contributes to EGF stimulated cell proliferation. Second, it releases calcium from lumen of the endoplasmic reticulum and cooperates with the ERK signaling pathway to regulate immediate early gene expression.

Previous studies suggested the G protein-coupled estrogen receptor, GPR30, could activate PLC and induce calcium mobilization (35). Our data showed that a GPR30 agonist has no effect on the anticipatory UPR activation (25). The non-receptor tyrosine kinase, c-Src, on the other hand has been shown to associate with and activate PLCγ (36). Other members of the steroid receptor superfamily, vitamin D receptor, in rat colonocytes stimulates PLCγ activation through Src mediated tyrosine phosphorylation (37). In human breast tumors, c-Src expression is highly elevated compared to normal

breast epithelium and this overexpression leads to increased tyrosine kinase activity (38). These data suggest Src may play a critical role in steroid hormones induced PLCγ activation. In this study, we showed that estrogen and progesterone rapidly induced Src phosphorylation, which then activated PLCγ in breast cancer cells.

Only approximately 5% of the total ERα protein population localizes at the membrane and can interact with other membrane proteins (39). Although less well characterized, progesterone receptor (PR) was known to translocate to the plasma membrane and mediate kinase signals (40). Multiple mechanisms by which the steroid hormone receptors interact with and activate Src have been described. ERα interacts directly with the SH2 domain of Src protein through its phosphorylated Y537 residue with the help of scaffold proteins including MNAR, Shc and PELP1 (41-43). Androgen receptor (AR) forms binary complexes with ERα interacts with and activates Src (44). Using co-immunoprecipitation we showed that ERα and PRs form protein complexes with Src and PLCγ through two different mechanisms. Estrogen stimulated PLCγ via enhancing the association of ERα with Src and PLCγ, while progesterone induced activation of PLCγ through a pre-exist protein complex involving PRs, Src and PLCγ.

In breast cancers, Src is a crucial protein in a complex interaction network. Crosstalk between Src, EGFR and ERα contributes to tamoxifen resistance in breast cancer cells and in patients (45, 46). A very recent study revealed that loss of C-terminal Src kinase (CSK), a suppressor of Src family kinases, confers endocrine therapy resistance in ER+ breast cancer cells (47). Given the importance of Src in ER+ breast cancer cells, ongoing clinical trials are exploring combination of Src inhibitors dasatinib and bosutinib with endocrine therapies (48). By targeting ERα-Src complex, BHPI distorts the anticipatory

UPR pathway and tips the scales from cytoprotective to cytotoxic (49). Instead of blocking ERα function, BHPI hyperactivates ERα-Src mediated UPR, induces sustained increase of cytosol calcium, toxic protein synthesis inhibition and drastic ATP depletion, leading to necrotic cell death.

Our work demonstrated that c-Src is the key protein tyrosine kinase mediating steroid hormones stimulated UPR activation. In breast cancer cells, overexpressed Src facilitates the estrogen and progesterone activated moderate anticipatory UPR which protects cells from EnR stress induced apoptosis. BHPI hijacks the ERα-Src-PLCγ protein complex and causes strong and sustained UPR activation, resulting in necrotic cell death. To survive under lethal hyperactivation of UPR, BHPI resistant cells downregulate Src expression and diminish UPR activation. Thus, Src plays a previously undescribed pivotal role in activation of the tumor protective anticipatory UPR, thereby increasing the resilience of breast cancer cells. This is a new role for Src and the UPR in the pathology of breast cancer.

REFERENCES

1. Clarke R, Tyson JJ, Dixon JM. Endocrine resistance in breast cancer - An overview and update. Mol Cell Endocrinol. 2015.

2. Osborne CK, Shou J, Massarweh S, Schiff R. Crosstalk between estrogen receptor and growth factor receptor pathways as a cause for endocrine therapy resistance in breast cancer. Clin Cancer Res. 2005;11(2):865s-70s.

3. Li S, Shen D, Shao J, Crowder R, Liu W, Prat A, et al. Endocrine-therapy-resistant ESR1 variants revealed by genomic characterization of breast-cancer-derived xenografts. Cell reports. 2013;4(6):1116-30.

4. Karnik PS, Kulkarni S, Liu X-P, Budd GT, Bukowski RM. Estrogen receptor mutations in tamoxifen-resistant breast cancer. Cancer Res. 1994;54(2):349-53.

5. Toy W, Shen Y, Won H, Green B, Sakr RA, Will M, et al. ESR1 ligand-binding domain mutations in hormone-resistant breast cancer. Nat Genet. 2013;45(12):1439-45.

6. Robinson DR, Wu Y-M, Vats P, Su F, Lonigro RJ, Cao X, et al. Activating ESR1 mutations in hormone-resistant metastatic breast cancer. Nat Genet. 2013;45(12):1446-51.

7. Jeselsohn R, Buchwalter G, De Angelis C, Brown M, Schiff R. ESR1 mutations—a mechanism for acquired endocrine resistance in breast cancer. Nature reviews Clinical oncology. 2015;12(10):573.

8. Takeshita T, Yamamoto Y, Yamamoto-Ibusuki M, Inao T, Sueta A, Fujiwara S, et al. Droplet digital polymerase chain reaction assay for screening of ESR1 mutations in 325 breast cancer specimens. Transl Res. 2015;166(6):540-53. e2.

9. Chandarlapaty S, Chen D, He W, Sung P, Samoila A, You D, et al. Prevalence of ESR1 mutations in cell-free DNA and outcomes in metastatic breast cancer: a secondary analysis of the BOLERO-2 clinical trial. JAMA oncology. 2016;2(10):1310-5.

10. Harrod A, Fulton J, Nguyen VTM, Periyasamy M, Ramos-Garcia L, Lai CF, et al. Genomic modelling of the ESR1 Y537S mutation for evaluating function and new therapeutic approaches for metastatic breast cancer. Oncogene. 2017;36(16):2286-96.

11. Martin L-A, Ribas R, Simigdala N, Schuster E, Pancholi S, Tenev T, et al. Discovery of naturally occurring ESR1 mutations in breast cancer cell lines modelling endocrine resistance. Nat Commun. 2017;8:1865.

12. Mao C, Livezey M, Kim JE, Shapiro DJ. Antiestrogen Resistant Cell Lines Expressing Estrogen Receptor alpha Mutations Upregulate the Unfolded Protein Response and are Killed by BHPI. Sci Rep. 2016;6:34753.

13. Bahreini A, Li Z, Wang P, Levine KM, Tasdemir N, Cao L, et al. Mutation site and context dependent effects of ESR1 mutation in genome-edited breast cancer cell models. Breast Cancer Res. 2017;19(1):60.

14. Wang P, Bahreini A, Gyanchandani R, Lucas PC, Hartmaier RJ, Watters RJ, et al. Sensitive detection of mono-and polyclonal ESR1 mutations in primary tumors, metastatic lesions, and cell-free DNA of breast cancer patients. Clin Cancer Res. 2016;22(5):1130-7.

15. Platet N, Garcia M. A new bioassay using transient transfection for invasion-related gene analysis. Invasion and Metastasis. 1998;18(4):198-208.

16. Pérez-Roger I, Solomon DL, Sewing A, Land H. Myc activation of cyclin E/Cdk2 kinase involves induction of cyclin E gene transcription and inhibition of p27 Kip1 binding to newly formed complexes. Oncogene. 1997;14(20).

17. Bretones G, Delgado MD, León J. Myc and cell cycle control. Biochim Biophys Acta. 2015;1849(5):506-16.

18. Wu S, Cetinkaya C, Munoz-Alonso MJ, Von Der Lehr N, Bahram F, Beuger V, et al. Myc represses differentiation-induced p21CIP1 expression via Miz-1-dependent interaction with the p21 core promoter. Oncogene. 2003;22(3):351-60.

19. Mukherjee S, Conrad SE. c-Myc suppresses p21WAF1/CIP1 expression during estrogen signaling and antiestrogen resistance in human breast cancer cells. J Biol Chem. 2005;280(18):17617-25.

20. Seoane J, Le H-V, Massague J. Myc suppression of the p21Cip1 Cdk inhibitor influences the outcome of the p53 response to DNA damage. Nature. 2002;419(6908):729-34.

21. Malta TM, Sokolov A, Gentles AJ, Burzykowski T, Poisson L, Weinstein JN, et al. Machine learning identifies stemness features associated with oncogenic dedifferentiation. Cell. 2018;173(2):338-54. e15.

22. Li L, Osdal T, Ho Y, Chun S, McDonald T, Agarwal P, et al. SIRT1 activation by a c-MYC oncogenic network promotes the maintenance and drug resistance of human FLT3-ITD acute Myeloid Leukemia stem cells. Cell stem cell. 2014;15(4):431-46.

23. Venditti M, Iwasiow B, Orr FW, Shiu RP. C-myc gene expression alone is sufficient to confer resistance to antiestrogen in human breast cancer cells. Int J Cancer. 2002;99(1):35-42.

24. Miller TW, Balko JM, Ghazoui Z, Dunbier A, Anderson H, Dowsett M, et al. A gene expression signature from human breast cancer cells with acquired hormone independence identifies MYC as a mediator of antiestrogen resistance. Clin Cancer Res. 2011;17(7):2024-34.

25. Andruska N, Zheng X, Yang X, Helferich WG, Shapiro DJ. Anticipatory estrogen activation of the unfolded protein response is linked to cell proliferation and poor survival in estrogen receptor alpha-positive breast cancer. Oncogene. 2015;34(29):3760-9.

26. Zheng X, Andruska N, Lambrecht MJ, He S, Parissenti A, Hergenrother PJ, et al. Targeting multidrug-resistant ovarian cancer through estrogen receptor α dependent ATP depletion caused by hyperactivation of the unfolded protein response. Oncotarget. 2018;9(19):14741.

27. Tsai YC, Weissman AM. The unfolded protein response, degradation from the endoplasmic reticulum, and cancer. Genes & cancer. 2010;1(7):764-78.

28. Brewer JW, Hendershot LM, Sherr CJ, Diehl JA. Mammalian unfolded protein response inhibits cyclin D1 translation and cell-cycle progression. Proc Natl Acad Sci. 1999;96(15):8505-10.

29. Karali E, Bellou S, Stellas D, Klinakis A, Murphy C, Fotsis T. VEGF Signals through ATF6 and PERK to Promote Endothelial Cell Survival and Angiogenesis in the Absence of ER Stress. Mol Cell. 2014;54(4):559-72.

30. Gurland G, Ashcom G, Cochran BH, Schwartz J. Rapid events in growth hormone action. Induction of c-fos and c-jun transcription in 3T3-F442A preadipocytes. Endocrinology. 1990;127(6):3187-95.

31. Zwang Y, Oren M, Yarden Y. Consistency test of the cell cycle: roles for p53 and EGR1. Cancer Res. 2012;72(5):1051-4.

32. Gille H, Kortenjann M, Thomae O, Moomaw C, Slaughter C, Cobb MH, et al. ERK phosphorylation potentiates Elk-1-mediated ternary complex formation and transactivation. The EMBO journal. 1995;14(5):951.

33. Schmitt JM, Wayman GA, Nozaki N, Soderling TR. Calcium activation of ERK mediated by calmodulin kinase I. J Biol Chem. 2004;279(23):24064-72.

34. Xia Z, Dudek H, Miranti CK, Greenberg ME. Calcium influx via the NMDA receptor induces immediate early gene transcription by a MAP kinase/ERK-dependent mechanism. The Journal of neuroscience. 1996;16(17):5425-36.

35. Prossnitz ER, Arterburn JB, Smith HO, Oprea TI, Sklar LA, Hathaway HJ. Estrogen signaling through the transmembrane G protein-coupled receptor GPR30. Annu Rev Physiol. 2008;70:165-90.

36. Nakanishi O, Shibasaki F, Hidaka M, Homma Y, Takenawa T. Phospholipase C-gamma 1 associates with viral and cellular src kinases. J Biol Chem. 1993;268(15):10754-9.

37. Khare S, Bolt M, Wali R, Skarosi S, Roy H, Niedziela S, et al. 1, 25 dihydroxyvitamin D3 stimulates phospholipase C-gamma in rat colonocytes: role of c-Src in PLC-gamma activation. J Clin Invest. 1997;99(8):1831.

38. Summy JM, Gallick GE. Treatment for advanced tumors: SRC reclaims center stage. Clin Cancer Res. 2006;12(5):1398-401.

39. Levin ER, Hammes SR. Nuclear receptors outside the nucleus: extranuclear signalling by steroid receptors. Nature reviews Molecular cell biology. 2016;17(12):783.

40. Boonyaratanakornkit V, Scott MP, Ribon V, Sherman L, Anderson SM, Maller JL, et al. Progesterone receptor contains a proline-rich motif that directly interacts with SH3 domains and activates c-Src family tyrosine kinases. Mol Cell. 2001;8(2):269-80.

41. Vallabhaneni S, Nair BC, Cortez V, Challa R, Chakravarty D, Tekmal RR, et al. Significance of ER–Src axis in hormonal therapy resistance. Breast cancer research and treatment. 2011;130(2):377-85.

42. Cheskis BJ, Greger J, Cooch N, McNally C, Mclarney S, Lam H-S, et al. MNAR plays an important role in ERa activation of Src/MAPK and PI3K/Akt signaling pathways. Steroids. 2008;73(9-10):901-5.

43. Liu L, Damen JE, Hughes MR, Babic I, Jirik FR, Krystal G. The Src homology 2 (SH2) domain of SH2-containing inositol phosphatase (SHIP) is essential for tyrosine phosphorylation of SHIP, its association with Shc, and its induction of apoptosis. J Biol Chem. 1997;272(14):8983-8.

44. Migliaccio A, Castoria G, Di Domenico M, de Falco A, Bilancio A, Lombardi M, et al. Steroid-induced androgen receptor–oestradiol receptor β–Src complex triggers prostate cancer cell proliferation. The EMBO journal. 2000;19(20):5406-17.

45. Riggins RB, Schrecengost RS, Guerrero MS, Bouton AH. Pathways to tamoxifen resistance. Cancer Lett. 2007;256(1):1-24.

46. Zhang S, Yu D. Targeting Src family kinases in anti-cancer therapies: turning promise into triumph. Trends Pharmacol Sci. 2012;33(3):122-8.

47. Xiao T, Li W, Wang X, Xu H, Yang J, Wu Q, et al. Estrogen-regulated feedback loop limits the efficacy of estrogen receptor–targeted breast cancer therapy. Proc Natl Acad Sci. 2018;115(31):7869-78.

48. Mayer EL, Krop IE. Advances in targeting SRC in the treatment of breast cancer and other solid malignancies. Clin Cancer Res. 2010;16(14):3526-32.

49. Shapiro DJ, Livezey M, Yu L, Zheng X, Andruska N. Anticipatory UPR activation: a protective pathway and target in cancer. Trends in Endocrinology & Metabolism. 2016;27(10):731-41.